



**Addis Ababa University
Addis Ababa Institute of Technology
School of Chemical and Bio Engineering**

Integration of Fenton oxidation and biological process with sequencing batch
reactor for the treatment of textile wastewater

Desta Solomon

PhD Dissertation

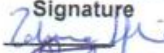
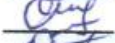


**In partial fulfillment of the requirements for the attainment of the
degree of Doctor of Philosophy in Chemical Engineering
(Environmental Engineering)**

Submitted to: School of Chemical and Bio Engineering

**Addis Ababa University
Addis Ababa, Ethiopia
February, 2020**

**Addis Ababa University
Addis Ababa Institute of Technology
School of Chemical and Bio Engineering**

This is to certify that the PhD dissertation prepared by Desta Solomon Damte, entitled: **“Integration of Fenton oxidation and biological process with sequencing batch reactor for the treatment of textile wastewater”** and submitted in partial fulfilment of the requirements for degree of Doctor of Philosophy in Chemical Engineering (Environmental Engineering stream) compiles with the regulation of the university and meets the accepted standards with respect to originality and quality.

Name and Signature of Members of the Examining Board			
Name		Signature	Date
1. <u>Dr. Ing. Zebene Kiflie</u>	(Advisor)		<u>14 / 07 / 2021</u>
2. <u>Dr. Nigus Gabbive</u>	(Internal Examiner)		<u>14 / 07 / 2021</u>
3. <u>Prof. Temesegn Garoma</u>	(External Examiner)		<u>14 / 07 / 2021</u>
4. <u>Dr. Eng. Abubeker Yimam</u>	(Dean, SCBE)		<u>14 / 07 / 2021</u>

ABSTRACT

The study was mainly aimed to investigate the treatment efficiency of the integrated system of biological oxidation and homo catalytic advanced oxidation process for the treatment of textile wastewater. Mineralization of a methyl orange dyes using artificial solar Fenton oxidation, degradation of a Basic Blue 41 dyes and real textile waste water with conventional Fenton oxidation were examined at laboratory scale in batch experiments using Box–Behnken statistical experiment design. Dyestuff, hydrogen peroxide (H_2O_2) and ferrous ion dose (Fe^{2+}) concentrations were selected as potential independent factors for simulated dye aqueous solutions while for real wastewater Fenton reagents (H_2O_2 and Fe^{2+}) and pH were selected as independent potential factors. Besides, color and total organic carbon (TOC) removal were measured as desired response functions for artificial solar Fenton oxidation while color and chemical oxygen demand (COD) were selected as desired response for conventional Fenton oxidation processes. The total time of irradiation used in the case of artificial solar Fenton oxidation for all the experimental runs were 20 minutes while the total reaction time for conventional Fenton oxidation processes was 1hour. Perturbation plots showed that iron dosage was the key process factor on the responses for both solar and conventional Fenton processes. At constant dye stuff dose, color, TOC and COD removal increased with increasing H_2O_2 and Fe^{2+} concentrations up to a certain level. High concentrations of H_2O_2 and Fe^{2+} for a constant dye stuff dose did not result in better removal of color, TOC and COD. The optimum ratio of $Fe^{2+} / H_2O_2 /$ dyestuff which gives a complete color removal and 96% TOC removal for the highest level of dye dose for artificial solar Fenton was found to be 72 /1386 / 255 (mg/L). In this regard, Percent color removal was higher than TOC removal.

During degradation of Basic Blue 41 dye, the optimum ratio of $\text{H}_2\text{O}_2/\text{Fe}^{2+}/\text{dyestuff}$ which gives a complete color removal and 95% COD removal was found to be 1195mg/L /90mg/L /255mg/L while in the case of real wastewater degradation, the optimum ratio of that gives 87% color removal and 79% COD removal were $\text{Fe}^{2+}/\text{H}_2\text{O}_2/\text{pH}$ (500.4mg/L/5187.6mg/L/2.9). In this regard,, Fenton oxidation using optimum Fenton reagents at a pH of 2.9 is effective for the treatment of acrylic fiber processing textile wastewater.

Subsequently, real textile wastewater was taken and treated with a sequencing batch reactor (SBR) using a biomass taken from domestic wastewater treatment plant. Cycle period, air flowrate and sludge retention time (SRT) were initially optimized using the response surface methodology (RSM). The optimum ratio of cycle period/ air flowrate/SRT which indicated 57% COD removal and 54% color removal was found to be 25 h /15L/h /16d. Two types of wastewater substrate concentrations and various hydraulic retention time (HRT) were used at optimized conditions. COD removal, color removal, sludge volume index (SVI) and mixed liquor suspended solid (MLSS) were measured. The maximum COD removal (73%) and color removal (65.8%) were obtained at an organic loading rate of 0.078 kg COD/m³d. SVI at the optimized condition was found to be 90-92 mL/g. A first order kinetic model was used to represent the degradation of textile wastewater.

Finally, the removal of COD and color studied on a real textile wastewater using a single stage of Fenton oxidation, (SBR) and also with the combination of SBR with Fenton oxidation. Optimum amount of chemical reagents and SBR process factors were used. The effluent obtained from SBR at steady state conditions indicated a maximum COD and color removal of 74.1% and 64.6% respectively. The effluent obtained from Fenton followed by SBR (Fenton +SBR) at steady state conditions indicated a maximum COD and color removal

efficiency of 86.3% and 84% respectively. while SBR followed by Fenton (SBR+ Fenton) for three Fenton oxidation experimental runs indicated a maximum COD and color removal of 80.2% and 73.6% respectively.

ACKNOWLEDGEMENTS

First and foremost, I would like to thank the almighty God for all the blessings during this research work. I would also like to express my deep and sincere gratitude to my main advisor Dr. Ing. Zebene Kiflie for his supervision, insightful guidance, valuable comments, follow-up and encouragement throughout this Ph.D. work. I would like to extend my heartfelt gratitude to my co-advisor Prof. Dr. Ir. Stijn Van Hulle, for his useful guidance, constructive comments and follow up throughout this research work.

I am extremely grateful to my mother for her prayer for my welfare. I am also thankful to all my three sisters. Furthermore, I am very much thankful to Ms. Semegne Assefa for her sisterly continuous help whenever I faced critical administration challenges in various circumstances at AAU.

My gratitude to Prof. Dr. Santiago Esplugas and Ms. Nuria Lopez and their advanced oxidation research group members in Spain, Barcelona University, Department of Analytical Chemistry and Chemical Engineering for their assistance during my laboratory work.

Last but not least, I would like to express my gratitude to the staffs of school of Chemical and Bio Engineering of Addis Ababa Institute of Technology, Finally, I would like to say thanks to all people who have supported me directly or indirectly for the accomplishment of this study.

TABLE OF CONTENTS

ABSTRACT.....	i
ACKNOWLEDGEMENTS.....	iv
TABLE OF CONTENTS.....	v
LIST OF FIGURES.....	x
LIST OF TABLES.....	xii
LIST OF PUBLICATIONS.....	xiv
ACRONYMS and CHEMICAL FORMULAS.....	xv
1 Introduction.....	1
1.1 Background of the study.....	1
1.2 Scope of the study.....	3
1.3 Statements of the problem.....	3
1.4 Research Objectives.....	5
1.4.1 General objective.....	5
1.4.2 Specific Objectives.....	6
2 Literature review.....	7
2.1 Dyes.....	7
2.2 Textile industry processes.....	9
2.2.1 Sizing and desizing.....	10
2.2.2 Bleaching.....	10
2.2.3 Mercerization.....	10
2.2.4 Dyeing and printing.....	11
2.2.5 Finishing.....	13

2.3	Characteristics of textile wastewater.....	14
2.4	Environmental impact of textile wastewater	14
2.5	The textile industry standards for water pollutants	15
2.6	Treatment processes for textile wastewater	16
2.6.1	Physical methods.....	17
2.6.2	Oxidation methods	21
2.6.3	Fenton process	22
2.6.4	The integration of Advanced oxidation processes with biological processes	33
2.7	Statistical design of experiments.....	36
3	Materials and Methods.....	38
3.1	Mineralization of a methyl orange dye using artificial solar Fenton process	38
3.1.1	Chemicals used in the mineralization of methyl orange dye	38
3.1.2	Artificial solar irradiation: Solar box (SB)	39
3.1.3	Techniques and analytical instrument used in the mineralization of methyl orange dyes ..	40
3.1.4	Experimental design, analysis and statistical validation during treatment of methyl orange dyes with artificial Fenton oxidation	40
3.2	Degradation of a Basic Blue 41 dyes using Fenton reagent	42
3.2.1	Chemicals used during degradation of a Basic Blue 41 dye aqueous solution	42
3.2.2	Fenton oxidation during degradation of Basic Blue 41 dye aqueous solution	42
3.2.3	Analytical procedures during degradation of Basic Blue 41 dyes.....	43
3.2.4	Experimental design, analysis and statistical validation during degradation of Basic Blue 41 dyes with conventional Fenton oxidation.....	43
3.3	Degradation of textile Industry Wastewater by Fenton Oxidation.....	44
3.3.1	Wastewater collection.....	44
3.3.2	Chemicals used during degradation of real textile wastewater	45
3.3.3	Fenton oxidation during treatment of real textile wastewater.....	45

3.3.4	Analytical procedures during treatment of real textile wastewater with conventional Fenton oxidation	45
3.3.5	Experimental design, analysis and statistical validation during degradation of real textile wastewater with conventional Fenton oxidation	46
3.4	Sequencing batch reactor (SBR)	46
3.4.1	Experimental procedure of SBR	47
3.4.2	Experimental design, analysis and statistical validation during treatment of textile wastewater with SBR	49
3.5	Integration of sequencing batch reactor with Fenton oxidation	49
3.5.1	Experimental procedure of SBR in the integrated system	49
3.5.2	Fenton oxidation after optimization for the combined process with SBR	50
3.5.3	Fenton oxidation before optimization in the integrated system	51
3.5.4	Fenton oxidation after optimization for the combined process with SBR	51
3.5.5	Fenton followed by SBR (Fenton stage+ SBR)	52
3.5.6	SBR followed by Fenton (SBR stage +Fenton)	52
4	Results and Discussion	53
4.1	Mineralization of methyl orange dyes	53
4.1.1	RSM modelling in the mineralization of methyl orange dyes	53
4.1.2	Assessment of the model adequacy for responses during mineralization of dye aqueous solution	55
4.1.3	Decolorization of methyl orange dye aqueous solution	57
4.1.4	Total organic carbon (TOC) removal of dye stuff	60
4.1.5	Perturbation plots during mineralization of methyl orange dye	64
4.1.6	Optimization of Artificial Soar Fenton treated simulated dye aqueous solution for color and TOC removal	64
4.2	Degradation of Basic blue 41 dye aqueous solution with conventional Fenton oxidation	65
4.2.1	Regression model and statistical testing in the degradation of a Basic Blue 41 dyes	65

4.2.2	Evaluation of the model adequacy for responses during degradation of Basic Blue 41 dye aqueous solution	68
4.2.3	Color removal in for Basic Blue 41 dyes	69
4.2.4	Chemical oxygen demand (COD) removal of Basic Blue 41 dye stuff.....	72
4.2.5	Perturbation plots during degradation of Basic Blue 41 dye aqueous solution.....	75
4.2.6	Optimization of Fenton treated Basic blue 41 dye solution for color and COD removal...	76
4.3	Degradation of real textile wastewater with conventional Fenton oxidation.....	77
4.3.1	RSM modeling for Fenton oxidation stage in the degradation of real textile wastewater ..	77
4.3.2	Effect of iron doses on color and COD removal for real wastewater treatment with Fenton oxidation	80
4.3.3	Effect of hydrogen peroxide doses on color and COD removal in the Fenton oxidation stage	81
4.3.4	Effect of pH on color and COD removal Efficiency in the Fenton oxidation stage.....	82
4.3.5	Perturbation plots during degradation of real wastewater with conventional Fenton oxidation	84
4.3.6	Optimization during treatment of real textile wastewater with conventional Fenton oxidation	85
4.4	Treatment of textile wastewater with SBR.....	86
4.4.1	Regression model and statistical testing for degradation of textile wastewater with SBR .	86
4.4.2	Effect of process variables on treatment of textile wastewater in SBR	89
4.4.3	Optimization of process factors of SBR treated textile waste water for color and COD removal	94
4.4.4	Optimum condition Performance of SBR at various OLR	95
4.4.5	Kinetic study in SBR	99
4.5	Treatment of textile wastewater with the integration Fenton with SBR.....	101
4.5.1	Single Fenton oxidation stage at optimum conditions at various reaction time	101
4.5.2	Single SBR stage treatment for integrated system	102

4.5.3	Fenton followed by SBR (Fenton + SBR)	104
4.5.4	SBR followed by Fenton (SBR stage +Fenton)	107
4.5.5	Comparison of treatment efficiencies of single Fenton stage, single SBR stage, Fenton+ SBR and SBR+ Fenton	108
5	Conclusions and Recommendations	110
5.1	Conclusions.....	110
5.2	Recommendation.....	112
6	References	113

LIST OF FIGURES

Figure 2-1 Schematic representation for acrylic fiber dyeing processes at KK textile factories, Ethiopia	13
Figure 2-2. Classification of Fenton process.....	26
Figure 2-3 Reaction pathways of the Photo-Fenton process.....	27
Figure 2-4 Schematic representation for the choice of appropriate treatment processes for various industrial wastewaters based on their biodegradability levels.	35
Figure 3-1 Experimental set up of artificial solar photo-Fenton	40
Figure 3-2 Schematic representation of the SBR system.....	48
Figure 4-1 The variation between observed and predicted values for a. Color removal, b. TOC removal	56
Figure 4-2 Normal probability plot of residual of linear model for a color removal , b TOC removal.....	57
Figure 4-3 3D plot for the effect of ferrous ion and dye dose on color removal during artificial solar Fenton oxidation.....	59
Figure 4-4 3D plots for the effect of hydrogen peroxide and dye dose on color removal during artificial solar Fenton oxidation.	60
Figure 4-5 Difference between rate of decolorization and TOC removal.....	62
Figure 4-6 3D plot for the effect of ferrous ion and dye dose on TOC removal.....	63
Figure 4-7 The effect of Hydrogen peroxide dose and dye dose on TOC removal.....	63
Figure 4-8 Perturbation plot for a, color removal, b TOC removal.....	65
Figure 4-9 Predicted versus actual plot for a Color removal , b COD removal during treatment of Basic Blue 41 dyes with conventional Fenton oxidation	68
Figure 4-10 Normal probability plot of residual of linear model for a color removal , b COD removal during treatment of Basic Blue 41 dyes with conventional Fenton oxidation	69
Figure 4-11 3D plot for the effect of hydrogen peroxide and dye dose on color removal during treatment of Basic Blue 41 dyes with conventional Fenton oxidation.....	71
Figure 4-12 The effect of iron and dye dose on color removal during treatment of Basic Blue 41 dyes with conventional Fenton oxidation.....	71
Figure 4-13 3D plot for the effect of Hydrogen peroxide and dye dose on COD removal during treatment of Basic Blue 41 dyes with conventional Fenton oxidation.....	74
Figure 4-14 3D plot for the effect of ferrous ion and dye dose on COD removal during treatment of Basic Blue 41 dyes with conventional Fenton oxidation	75
Figure 4-15 Perturbation plot for a color removal , b COD removal during treatment of Basic Blue 41 dyes with conventional Fenton oxidation	76

Figure 4-16 3D plot that shows effect of iron and hydrogen peroxide doses on color removal during treatment of real wastewater with conventional Fenton oxidation.....	82
Figure 4-17 3D plot that shows effect of iron and hydrogen peroxide doses on color removal COD removal during treatment of real wastewater with conventional Fenton oxidation	83
Figure 4-18 3D plot that shows effect of pH on color removal.....	83
Figure 4-19 3D plot that shows effect of pH on COD removal	84
Figure 4-20 Perturbation plot for a) color removal and b) COD removal during treatment of real wastewater with conventional Fenton oxidation	85
Figure 4-21 Effect of air flowrate, sludge retention time and cycle period on COD removal.	93
Figure 4-22 Effect of air flowrate, sludge retention time and cycle period on color removal.	94
Figure 4-23 Effect of air flowrate, sludge retention time and cycle period on SVI.	94
Figure 4-24 (a) COD removal and (b) decolorization of textile wastewater at optimum conditions using various OLR and HRT.....	97
Figure 4-25 MLSS and SVI of textile wastewater at optimum conditions using various OLR and HRT.	99
Figure 4-26 Kinetic plot for the treatment of textile wastewater in SBR.....	100
Figure 4-27 Treatment of textile wastewater using SBR.....	103
Figure 4-28 Treatment of textile wastewater using Fenton followed by SBR.....	105
Figure 4-29 Treatment of textile wastewater using SBR followed by Fenton.....	107

LIST OF TABLES

Table 2-1: Classification of dyes based on chemical structure	8
Table 2-2 Classification of dyes based on method of application	9
Table 2-3 Major dye classes and substrate fibers	12
Table 2-4 Limit values of textile wastewater to discharge to water bodies	16
Table 2-5 Comparison among various wastewater treatment technologies	18
Table 2-6 Advantages and disadvantages among different wastewater treatment technologies	19
Table 2-7 Classification of conventional AOP's	22
Table 3-1 General characteristic of methyl orange dye	38
Table 3-2 Coded levels and independent variables used for solar Fenton oxidation with BBD	39
Table 3-3 General characteristic of Basic Blue 41	42
Table 3-4 Coded levels and independent variables used for conventional Fenton oxidation with BBD....	44
Table 3-5 Characteristics of KK Textile wastewater	44
Table 3-6 Coded level and independent variables used with BBD for real wastewater treatment.....	46
Table 3-7 Coded level and independent variables used in BBD by SBR biological system for KK textile wastewater.	48
Table 3-8 Experimental conditions of SBR at optimized conditions for single SBR stage treatment.	49
Table 3-9 Experimental conditions of SBR at optimized condition for integrated treatment system	50
Table 4-1 Box–Behnken design matrix along with experimental and predicted values during treatment of methyl orange dyes with artificial solar Fenton oxidation.....	54
Table 4-2 Regression coefficients and model performance indicators during treatment of Methyl orange dye with artificial solar Fenton oxidation	55
Table 4-3 Comparison between rate of mineralization and color removal.	61
Table 4-4 Box–Behnken design matrix along with experimental and predicted values during degradation of Basic Blue 41 dyes with conventional Fenton oxidation.....	66
Table 4-5 Regression coefficients and model performance indicators for RSM modeling of color removal and COD reduction when treating Basic-Blue 41 dyes with Fenton oxidation.....	67
Table 4-6 Box–Behnken Design matrix along with experimental and predicted values during real wastewater treatment with conventional Fenton oxidation.....	78

Table 4-7 Model performance indicators for color removal and COD reduction during treatment of real wastewater with conventional Fenton oxidation	79
Table 4-8 Experimental and predicted values for COD removal, color removal and SVI during single stage SBR stage treatment.	88
Table 4-9 Response surface quadratic model for color removal during single SBR treatment stage.....	90
Table 4-10 Response surface quadratic model for COD reduction during single SBR treatment stage.....	91
Table 4-11 Response surface quadratic model for SVI during single SBR treatment stage.	92
Table 4-12 COD removal and decolorization of textile wastewater at optimum conditions at various OLR and HRT.	97
Table 4-13 Values of rate constant (K) and the determination coefficient (R^2) at various OLR and HRT.	100
Table 4-14 COD removal and decolorization of textile wastewater using SBR at optimum conditions at various OLR and HRT.....	103
Table 4-15 Treatment of textile wastewater using Fenton followed by SBR	106
Table 4-16 Treatment of textile wastewater using SBR followed by Fenton (SBR +Fenton).....	108
Table 4-17 Summary of treatment of textile waste water by different treatment schemes.....	109

LIST OF PUBLICATIONS

1.Solomon D, Kiflie Z, Hulle S Van, Kinetic investigation and optimization of a sequencing batch reactor for the treatment of textile wastewater. Nanotechnol.,2019 ; Environ Eng 4:15.

<https://doi.org/10.1007/s41204-019-0062-6>

2. Solomon D, Kiflie Z, Hulle S Van, Using Box–Behnken experimental design to optimize the degradation of Basic Blue 41 dye by Fenton reaction. Int. J Ind Chem., 2020 , Int J Ind Chem 11:43-53

<https://doi.org/10.1007/s40090-020-00201-5>

3. Solomon D, Kiflie Z, Hulle S Van, Integration of sequencing batch reactor and homo catalytic advanced oxidation processes for the treatment of textile wastewater. Nanotechnol.,2020 ; Environ Eng 5:7 .

<https://doi.org/10.1007/s41204-020-0070-6>

ACRONYMS and CHEMICAL FORMULAS

AOP	Advanced oxidation Process
BOD	Biological oxygen demand
BBD	Box-Behnken design
COD	Chemical oxygen demand
Fe^{2+}	Ferrous ion
Fe^{3+}	Ferric ion
$\text{FeSO}_4 \cdot 7\text{H}_2\text{O}$	Hydrated ferrous sulfate
H_2SO_4	Sulfuric acid
HRT	Hydraulic retention time
H_2O_2	Hydrogen Peroxide
HO.	Hydroxyl radical
HO ₂ .	Per hydroxyl radical
mg	Milligram
mg/L	Milligram per liter
MLSS	Mixed liquor suspended solid
O_2^{-1}	Superoxide ion
O_3	Ozone
OLR	Organic loading rate
NaOH	Sodium hydroxide
RSM	Response Surface Methodology
SBR	Sequencing Batch Reactor
SRT	Sludge Retention Time
SVI	Sludge Volume Index
TSS	Total Suspended Solid
TOC	Total Organic Carbon
UV	Ultraviolet

1 Introduction

1.1 Background of the study

Aquatic medium can be polluted through various anthropogenic activities. Some of these activities are: discharging of partially treated or untreated domestic and industrial wastewater in to water bodies and water bodies can be also polluted indirectly through the use of various synthetic chemicals to increase agricultural products, such as biocides and fertilizers. In this regard, very water-soluble substances can be transported and dispersed at faster rate in the water cycle [1]. Moreover, negligent enforcement of the rules, illegal use and inappropriate application of substances are also causes for the discharge of such polluted effluent in to the environment [1].

Textile industry plays a key role in the economy of many countries. This industry consumes different types of chemicals and considerable amount of water in its various stages of production. Consequently, the effluent produced during this processes discharges considerable concentrations of dyes, various inorganic and organic chemicals and trace metals [2]. Subsequently, untreated or incompletely treated textile effluent adversely affect the environment and human health .

Even though Ethiopia's textile industry has been recognized as a key growth industry since 1995, its activity was uninspiring until the implementation of the growth and transformation policy (GTP) in 2015. However, after the declaration of development policy, various industrial zone have been constructed, and this leads to the improvement of foreign investment policy. Consequently, currently Ethiopia textile industry is competitive sector across the world along with other known countries in this sector like China and Bangladesh [3]. Today, Ethiopia has more than 115 textile and garment factories. In this regard, half of these firms are small and medium sized enterprise and the rest of these are foreign owned and most are administered under Indian, Chinese and

Turkish investors. Besides, most of these industries has no appropriate wastewater treatment plant and they discharge their untreated or partially treated effluent to nearby water bodies and canals [4].

Physical, chemical and biological treatment technologies can be implemented during treatment process of textile effluent. Although, physical and chemical treatment methods are efficient in the removal of color from textile effluent, however, these treatment methods has some limitations due to they produced excess sludge and these consequently would increase the cost of treatment to discard the excess sludge produced [5]. Moreover, such type of wastewater is not effectively treated by single stage biological treatment due to such effluent is non-biodegradable and toxic [1]. In this regard, Advanced oxidation processes (AOP's) can be the best alternative technology to degrade such type of wastewater [6]. In this sense, various previous research reported that AOP's is effective treatment technology for such non-biodegradable wastewater due to the processes can generate hydroxyl radical ($\text{OH}\cdot$). Consequently, this process has sufficient capacity to entirely mineralize recalcitrant organic compounds in to H_2O and CO_2 [5].

However, treatment of effluent with single AOP's is expensive due to this process consumed considerable amount of chemical reagents and energy [1]. In this sense, AOP's can be used along with biological treatment technologies. Accordingly, AOP's can initially increase the biodegradability of the effluent and consequently biological treatment can be used as a polishing step with the lowest cost [7].

Therefore, the integration of AOP's along with biological process has attracted many researchers in the treatment of various types of wastewater [1]. However, most studies in this field did not report about optimization of the process parameters in each stage of the treatment, they were not

also reported about effect of chemically pretreated effluent up on the subsequent biological stage and their reports were not also incorporated economic analysis of this hybrid method. Thus, such hybrid method was not still widely implemented at industrial scale [1]. Therefore, this study mainly focuses in the analysis of treatment efficiency of single stage Fenton process, biological process along with hybrid treatment system of biological and Fenton process for the treatment of textile wastewater.

1.2 Scope of the study

The study covers comparison and selection of the best treatment technologies at laboratory scale among various single and integrated wastewater treatment approaches using homo catalytic advanced oxidation processes and biological sequencing batch reactor combinations.

1.3 Statements of the problem

Various human activities in urban areas and different processing industries eventually discharge their wastewater to the land or aquatic environment. In this regard, there should be a monitoring activity in the identification of harmful constituents in both quality and quantity before they released in to the environment. Furthermore, the mechanism of identification and controlling of such contaminants in these effluent required investigation of local situations, proper application of scientific principles and also required appropriate engineering solutions based on previous trends and consideration of local and federal regulations.

Most textile processing industries in Ethiopia do not usually properly treated their wastewater according to local environmental regulation and standards. For instance, Dadi, et. al, 2016 [4] reported about environmental and health impacts of effluents from four different textile and garment plants in the town of Gelan and Dukem in Oromia regional states, Ethiopia. Accordingly,

they studied physiochemical and bacteriological composition of four textile factories and they concluded that the concentrations of these pollutants were higher than the permissible limit given by the Federal Environmental Protection Authority (FEPA).

Furthermore, KK acrylic fiber dyeing processing textile industries at Akaki Kalty sub city, Addis Ababa, Ethiopia has conventional biological activated sludge wastewater treatment plant and its daily flow rate after dyeing process is 750m³. However, this industry discharges highly visible color containing effluent at the end of this treatment. Therefore, applied research should be carried out in order to solve such severe environmental pollution.

Environmental engineers currently faced difficulties to obtain suitable treatment technologies as to fulfill the stringent discharge limit of textile effluent. Most available conventional wastewater technologies do not completely treat such waste water according to the discharge limit. In this regard, treatment processes such as coagulation, precipitation, adsorption with local available or purchased adsorbent and air stripping can transfer pollutants from the aqueous phase to a second phase, but the pollutant would not be removed [8].

Furthermore, biological processes are the cheapest among other alternative treatment technologies and has the ability to decrease the organic constituent and decolorize the textile wastewater. However, this treatment is not efficient in the complete mineralization of such effluent [9].

Besides, AOP's are competitive wastewater treatment technology for those effluent which are not effectively treated by conventional treatment methods. However, treatment of wastewater with single AOP's is expensive [10]. Therefore, there is no single treatment technology which can effectively treat wastewater. In this regard, among various potential hybrid treatment technologies, the biological hybrid technology is more preferable than any other alternatives [7].

Previous researches drawbacks in the study of wastewater treatment methods with the application of the integration of chemical and biological processes lacks optimization in each process stage and also the absence of biodegradability assessments in the pre oxidation stage [11].

In this regard, chemicals used in the pre-treatment stage should not be neither excess nor deficient [11]. Besides, optimization of both treatment stages should be considered to properly design the integrated treatment system [7]. In this sense, previous researchers were not considered the optimization of biological stage during treatment of textile wastewater using the combination of Fenton oxidation with SBR [8, 12–15]. Therefore, in this study we optimized all the potential selected process factors which were used both in the biological treatment stages and also in the chemical oxidation stage. Furthermore, the total cycle period was optimized during the SBR process stage. Therefore, this study can be useful to show an alternative approach in the minimization of the residence time of the SBR processes and this can further enhance the overall treatment efficiency of integrated treatment system.

1.4 Research Objectives

1.4.1 General objective

The general objective of the study was to investigate the treatment efficiency of the integrated system of biological oxidation and homo catalytic advanced oxidation process for the treatment of textile wastewater.

1.4.2 Specific Objectives

The specific objectives of the study were:

- To analyze the efficiency of artificial solar Fenton in the mineralization of dye containing synthetic wastewater and optimizing the process variables.
- To observe the efficiency of conventional Fenton oxidation process in the degradation of dye containing synthetic wastewater and optimizing the process variables.
- To explore the efficiency of conventional Fenton oxidation on the degradation of real textile waste water and optimizing the process variables.
- To examine the treatment efficiency of biological process with sequencing reactor during degradation of real textile wastewater and optimizing the process variables.
- To investigate the treatment efficiency of the integrated system of sequencing batch reactor and conventional Fenton oxidation then to select the best sequence of integrated treatment system for the degradation of real textile wastewater.

2 Literature review

2.1 Dyes

Dye molecules have two basic constituents: chromophores, which determine the color and the auxochromes which are responsible for increasing the affinity to be attracted toward the fiber and cause the molecule to be slightly soluble in water [10]. The chromophore group is a radical configuration consisting of conjugated double bonds which comprises delocalized electrons. The chromogen, which has an aromatic structure normally contain benzene, naphthalene, or anthracene rings. The most essential chromophores are azo ($-N=N-$), carbonyl ($-C=O$), methine ($-CH=$), nitro ($-NO_2$) and quinoid groups. The most significant auxochromes are amine ($-NH_2$), carboxyl ($-COOH$), sulfonate (SO_3H) and hydroxyl ($-OH$) [16].

The classification of dyes can be broadly viewed in two categories. Accordingly, the chemist classify based on their common parent chemical structure. Such type of classification of dyes is indicated in table 2.1 [10]. On the other hand, dyes can be classified according to their method of application to the fiber as indicated in Table 2.2 [10]. Furthermore, dyes which are used in textile industries can be generally categorized in to the following three major classes: (a) nonionic (dispersed dyes) (b) anionic (direct, acid, and reactive dyes), (c) cationic (all basic dyes) [10].

Various process industries such as plastics, printing, leather, paper and textiles use dyes to give desired color to their products. Consequently, wastewater from these industries contains different concentrations of these dye stuffs [17]. There are more than hundred thousand dye available and 7×10^5 t are produced every year [18]. Moreover, about 40,000 pigments and dyes are registered, they have more than 7,000 distinct chemical structure [19]. However, only 10-15% of these dyes discharged in to the environment as liquid waste [20].

Table 2-1: Classification of dyes based on chemical structure [10]

No.	Dye type	Characteristics	Examples
1.	Polynitro derivatives of phenols containing at least nitro group ortho or para to the hydroxyl group. Nitro dyes	Polynitro derivatives of phenols containing at least nitro group ortho or para to the hydroxyl group.	Picric acid, Maritus yellow and Naphthol yellow S
2.	Azo dyes	The azo dyes represent the largest and the most important group of dyes. They are characterized by the presence of one or more azo groups ($-N=N-$), which form bridges between two or more aromatic rings.	Aniline yellow, Butter yellow, Chrysoidine, Methyl Orange, Orange II, Para Red, Resorcin Yellow, Disperse Red 1 and Congo Red.
3.	Diphenylmethane dyes		Auramine O
4.	Triphenylmethane dyes	Central carbon atom is joined to two benzene rings and to p-quinoid group. Triphenylmethane dyes are not fast to light or washing, however, except when applied to acrylic fibers. They are used in large quantities for coloring paper, and typewriter ribbons where fastness to light is not so important.	Malachite Green, Pararosanine, Rosanine and Crystal Violet
5.	Xanthene dyes	Obtained by condensing phenols with phthalic anhydride in the presence of zinc chloride, sulphuric acid, or anhydrous oxalic acid.	Fluorescein, eosin, and Rhodamine B
6.	Phthaeleins	Phthaeleins are related to xanthene dyes	Phenolphthalein
7.	Indigoid and Thioindigoid dyes	Indigoid is the parent compound of indigoid dyes.	Tyrian Purple and Thioindigo
8.	Anthraquinoid dyes	A p-quinoid group is fused to two other benzene rings.	Alizarin

Table 2-2 Classification of dyes based on method of application [10]

No.	Dye type	Characteristics	Examples
1.	Direct dyes	These contain acidic or basic groups and combine with polar groups in the fiber. Such dyes color a fabric directly when the fiber is immersed in a hot aqueous solution of the dye.	Naphthol Yellow S and Martius Yellow
2.	Mordant dyes	This class of dyes requires a pretreatment of the fiber with a mordant material designed to bind the dye. The mordant becomes attached to the fiber and then combines with the dye to form an insoluble colored complex. This complex is called a lake. Commonly used mordant are the oxides of aluminum, iron and chromium.	Alizarin
3.	Vat dyes	These dyes are insoluble in water, but on reduction with sodium hydrosulphite yield alkali soluble forms (Leuco-compounds) which may be colorless. It is in this form they are introduced into the fabric. The reducing operation was carried out in wooden vats, giving rise to the name 'Vat Dyes'. After the reduced dye has been absorbed in the fiber, the original insoluble colored dye is reformed by oxidation with air or chemicals.	Indigo
4.	Ingrain dyes	These dyes are synthesized within the fabric, and may be applied to any type of fiber.	Azo dyes
5.	Disperse dyes	These are insoluble in water, but are capable of dissolving certain synthetic fibers. Disperse dyes are usually applied in the form of a dispersion of finely divided dye in a soap solution in the presence of some solubilizing agent such as phenol, cresol, or benzoic acid. The absorption into the fiber is carried out at high temperatures and pressures.	Celliton Fast Pink B and Celliton Fast Blue B

2.2 Textile industry processes

Textile process industries commonly manufactured fibers. Consequently, these fibers can be further processed and changed in to yarn. Subsequently, the yarn can be further processed in to fabrics [2]. Finally, the fabrics can be undergoes through various wet processing stages. Furthermore, all these stages are discussed in detail in the following paragraphs [2].

2.2.1 Sizing and desizing

The processes of dyeing and printing can be influenced by the type of sizing agents used. In this regard, water-insoluble starches are used as sizing agent for natural fibers and this usually hindered the spreading of dye molecule in to the fabric. Therefore, the starch should be removed before the stage of dyeing and printing. Such sizing substances can be removed by using either enzymatic or mineral acid hydrolysis desizing agents. Furthermore, such oxidation or hydrolysis processes can convert starch in to water soluble smaller substances [21]. Subsequently, the biological oxygen demand (BOD) of the effluent after desizing process is about 300 to 450 ppm and the pH is usually in the range of 4-5 [22]. Besides, enzymes can convert the starch in to ethanol and ethanol can be further recovered with distillation processes. Consequently, this ethanol can be used as fuel and this processes also simultaneously reduce the BOD concentrations of the raw effluent [23].

2.2.2 Bleaching

Bleaching process can remove natural color of the fabric. In this regard, hypochlorite was widely used as a bleaching agent in the past. However, peracetic acid and hydrogen peroxide currently substituted hypochlorite. Besides, peracetic acid is the most preferable bleaching agent than others due to it gives better shininess and little damage to the processed fabric [24].

2.2.3 Mercerization

Dye uptake rate and lustrous properties of a fiber can be enhanced with the process of mercerization. In this sense, this process can be carried out with high concentration of alkali solutions (sodium hydroxide) [21]. During spread of this solution along the cotton fabric, the fabric undergoes longitudinal shrinkage. The extra sodium hydroxide used should be removed with washing after 1-3 minutes along with elongating the fiber under high pressure. Consequently, dye

uptake rate and lustrous properties of a fiber can be improved. Furthermore, sodium hydroxide during washing can be recovered by using membrane techniques [21].

2.2.4 Dyeing and printing

Color can be added to fabrics, fibers and yarns through the process of dyeing. This process can be carried out in the presence of dye solution and auxiliary chemicals. Chromophores and auxochrome are responsible to give color during this process [25]. Printing and dyeing process under go similar procedures. However, in the case of dyeing, the dye is added in the form of solution while in printing dye added in the form of thick paste as to prevent fast spreading of dyes [26]. Therefore, waste composition of printing is similar to dyeing [26]. Furthermore, at the end of this dyeing process, some additional processes such as reduction clearing at 800 °C , soaping process at 70 °C , cold and hot wash, neutralization and anti-static finishing treatment at 500 °C [27]. Consequently, colored fiber un loaded from the carrier and extra liquid would be squeezed from the fiber with hydro- extraction. Finally, this dewatered fiber would be transferred to hot air blower so as to dry the fiber to desired level [27]. Table 2-3 shows different types of dye-stuff and their corresponding fibers [27].

2.2.4.1 Polyester Fiber Dyeing

Initially, some amount of fiber would be precisely measured and loaded to the carrier with manual pressing and water. Consequently, this loaded carrier would be transported to high temperature high pressure (HTHP) dyeing apparatus [27]. In this regard, precisely measured amount of water is filled in distinct container along with a homogenous mixture of leveling agent, acetic acid and precise amount of dispersed dyes are pumped in to this dyeing equipment. Subsequently, steam used to raise the temperature of these dye bath homogenous mixtures to 132°C and mixing process were simultaneously carried out with internal recycling. Finally, at the end of dying process, the

temperature of this dyeing equipment decreases to 70-80⁰C and the dye bath solutions removed [27]. Furthermore, at the end of this dyeing process, some additional process such as reduction clearing at 80⁰c, soaping process at 70⁰c, cold and hot wash, neutralization and anti-static finishing treatment at 50⁰c [27]. Consequently, colored fiber unloaded from the carrier and extra liquid is squeezed from this fiber with the process of hydro-extraction. Finally, this dewatered fiber is transferred to hot air blower so as to dry this fiber to the desired level [27].

Table 2-3 Major dye classes and substrate fibers [27]

Dye Classes	Fibers
Acid	Wool ,silk and nylon
Azoic	Cotton and cellulose
Basic	Acrylic, certain polyesters
Chrome	Wool, silk and nylon
Direct	Cotton, rayon and other cellulosic
Disperse	Polyester, acetate and other synthetic
Fiber Reactive	Cotton and other cellulosic, wool
Naphtol (azoic)	Cotton, rayon, other cellulosic
Mordant (absolute)	Natural fiber(pretreated with metals)
Pigment	All (requires binders)
Solvent	Synthetic(rarely used in commerce)
Sulfur	Cotton and other cellulosic
Vat	Cotton and other cellulosic

2.2.4.2 Acrylic Fiber Dyeing

The dyeing mechanism of acrylic and polyester fiber are almost similar. However, the slight difference in the dyeing process between theses fibers is due to during polyester fiber dyeing process, dispersed dyes and leveling agent are used while during acrylic fiber dyeing process, basic dye stuff and retarder used [27]. Besides, reduction clearing procedure is commonly used during polyester fiber dyeing while acrylic fiber dyeing process does not use this procedure. Furthermore, the schematic process flow diagram for acrylic fiber dyeing process at KK textile factory, Addis Ababa, Ethiopia is shown in Figure 2-1.

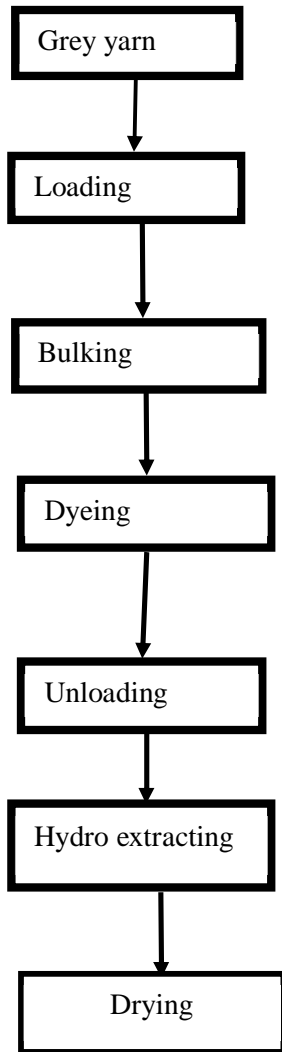


Figure 2-1 Schematic representation for acrylic fiber dyeing processes at KK textile factories, Ethiopia

2.2.5 Finishing

Finishing processes can improve definite properties of a fabric. In this regard, particular properties of the fabric such as water proofing, softening, UV and antibacterial protection can be enhanced with this processes [28]. However, pollution of wastewater with various contaminants can be also caused by this processes [28].

2.3 Characteristics of textile wastewater

Enormous amount of water is commonly consumed by textile industry. In this regard, water used in various stages of the process and also it is used for cleaning purpose [1]. Textile wastewater usually contains various chemicals and dyestuffs and the chemical composition of such waste water is the main cause for the pollution of the environment. Dyes, soluble substances, suspended solids, recalcitrant substances are the main constituents of textile wastewater [1].

Textile industry required 80-100m³ water to produce one ton of finished products and consequently 115-175 Kg COD containing effluent discharges during the production of 1 ton of textile product. Consequently, the effluent is highly saline, has intense color and has low biodegradable organic constituents [29].

Textile industries used a variety of chemicals and these chemicals varied with the variation of the nature of raw materials used and the desired product [30]. Consequently, the composition of each effluent obtained from these processes differ in composition due to variations in process, fabrics and machinery [31]. Accordingly, the characteristics of various types of textile wastewaters have been reported by several previous researchers. Accordingly, a typical textile effluent has a COD value which ranges from 150-12000 and also has a BOD value which ranges from 80-6000 (mg/L) [1]. Accordingly, this wastewater has a BOD/COD ratio of 0.25 and such value usually indicates that textile effluent is non-biodegradable [32, 33].

2.4 Environmental impact of textile wastewater

Water bodies comprising even little concentration of dyes is usually easily observable and aesthetically not attractive [34]. In addition, dyes are harmful to aquatic organisms due to they comprise halides, metals, etc. [10]. Moreover, most of them can cause cancer and are mutagenic

and toxic. Furthermore, they can be a cause for the destruction of aquatic fauna and flora [35] and are also non-biodegradable due to their xenobiotic nature and complex structure [36]. Therefore, effluent containing dyes are difficult to be treated with aerobic digestion and they do not easily reacted with oxidizing agents, light and heat [37]. Moreover, un treated textile effluent can contains significant amount of suspended solids. In this regard, oxygen transfer process in the air-water boundary can be also hindered by such suspended solid when they released directly in to aquatic medium [38].

Besides, textile effluent containing soluble inorganic salts which directly discharges in to the water bodies would not be further useful for various human activities and it is also toxic to aquatic organisms. Moreover, various inorganic acids and bases that are present in textile effluent can be directly inter in to aquatic medium, and these have adverse effect in the overall marine life [38].

2.5 The textile industry standards for water pollutants

Textile wastewater that are untreated or partially treated has devastating effect to the societies and the aquatic environment. Therefore, such effluent required stringent discharge standard to all the parameters under consideration. The discharge limit of such effluent vary from one industry to the other due to different textile industries used different types of dyes and machineries [2].

In addition, regarding discharge limit of textile effluent, dyes and metal ions is the main concern due to they have adverse effect to the societies and environment [2]. Research on technologies which can be implemented for the treatment of textile effluent should not only focus on the removal of color but they should also give emphasis on the complete mineralization of organic compounds, attempt to recover salts, investigate methods to recover dyes and should search for treatment technologies that do not produce excess sludge [2]. In this regard, Table 2-4 shows limit values to

discharge different textile industry pollutants to water bodies. This values was established by the Environmental protection authority of Addis Ababa city government, Ethiopia [39].

Table 2-4 Limit values of textile wastewater to discharge to water bodies [39]

Parameters	Limit values
Temperature	40 °C
pH	6-9
BOD ₅ at 20 °C	90% removal or 50 mg/l, whichever is less
Total nitrogen (as N)	80% removal or 40 mg/l, whichever is less
COD (mg O ₂ /l)	80% removal or 150 mg/L, whichever is less
Total phosphorous (as P)	80% removal or 10mg/L, whichever is less
Suspended solids	30mg/L
Total ammonia (as N)	20mg/L
Oil, fats and grease	20mg/L
Phenols	1mg/L
Mercury (as Hg)	0.001mg/L
Nickel (as Ni)	2mg/L
Cobalt (as Co)	1mg/L
Lead (as Pb)	0.5mg/L
Antimony (as Sb)	2mg/L
Tin (as Sn)	5mg/L
Chromium (as Cr VI)	0.1mg/L
Chromium (as total Cr)	1mg/L
Arsenic (as As)	0.25mg/L
Cadmium (as Cd)	1mg/L
Zinc (as Zn)	5mg/L
Copper (as Cu)	2mg/L
Mineral oils (Interceptors)	20mg/L
Benzene, toluene and xylene (combined)	1mg/L
Mineral oils (Biological Treatment)	5mg/L
Organochlorine pesticides (as Cl)	0.03mg/L
Mothproofing agents (as Cl)	0.003
Organo phosphorous pesticides (as P)	0.003mg/L
Adsorbable organic halogen compounds (AOX)	5mg/L
Sulfides (as S)	2mg/L

2.6 Treatment processes for textile wastewater

Raw textile effluent mainly contains various inorganic compounds, color and high COD concentration. In this regard, aquatic organisms which are living in colored wastewater cannot

obtain sun light due to light cannot easily penetrate in such wastewater. Therefore, this effluent should be effectively treated with appropriate treatment technologies in order to entirely remove such undesirable color.

Discharging of untreated/ partially treated textile wastewater into river cause adverse effect to the aquatic environment However, whenever such effluent effectively treated, the receiving water bodies would be safe from pollution and can also further used for various human activities [40]. In this regard, various treatment processes including physical, chemical, biochemical, hybrid treatment processes have been developed to treat such wastewater with technically and economically feasible alternative treatment technologies [40].

2.6.1 Physical methods

Effluent which contains disperse dyes can be effectively decolorized with coagulation-flocculation based physical methods [41]. However, these treatment methods has low color removal efficiency for effluent containing vat and reactive dyes. Besides, these treatment has limitation due to generation of huge amount of sludge and less decolorization efficiency for most kind of dyes [41]. On the other hand, adsorption process has high decolorization efficiency for all kinds of dyes. Besides, the treatment efficiency of adsorption is determined based on its ability to adsorb the target contaminants and also on its regeneration capacity [42].

Among various adsorption processes, activated carbon is an effective adsorbent for a wide range of dyes [2]. However, this treatment technology was not applied for the decolorization of textile effluent due to it is expensive and also difficult to regenerate [43]. In this regard, some researchers used low cost adsorbent materials such as peat, bentonite clay, fly ash and polymeric resins [2].

Furthermore, Table 2-5 and Table 2-6 summarizes in detail about the advantages and disadvantages of the various wastewater treatment methods [10].

Table 2-5 Comparison among various wastewater treatment technologies [10]

Technology	Advantages	Disadvantages
Coagulation flocculation	Simple, economically feasible	Causes extra pollution due to the undesired reactions in treated water and produces large amounts of sludge
Ozonation	No change in effluent volume	High production cost of ozone and the low ozone utilization due to poor mass transfer rate of ozone and short half-life
Photochemical	No sludge generation Rapid process and good sorption capacity for dyes	Formation of byproducts .High energy costs
Biodegradation	Economically attractive, publicly acceptable treatment	Slow process, necessary to create an optimal favorable environment, maintenance and nutrition requirements.
Adsorption on activated carbon	High adsorption capacity and no chemical degradation it can handle fairly large flow rates, producing a high quality of water without producing notorious sludge, residual contaminants, etc.	Relatively high operation costs, which hamper its large-scale application. Ineffective against disperse and vat dyes, the regeneration is expensive and results in loss of the adsorbent, non-destructive process
Electrochemical	Additional chemical is not required, easy implementation and the high removal rates nonhazardous end products	High cost of electric energy
Ion - exchange	No loss of sorbent on regeneration, effective	Economic constraints, not effective for disperse dyes. Less efficient for column or flow adsorption systems.
Membrane filtration	Environmentally friendly removes all dye types, produce a high-quality treated effluent	Concentrated sludge production. High pressures, expensive, incapable of treating large volumes

Table 2-6 Advantages and disadvantages among different wastewater treatment technologies [10]

Technology	Advantage	Disadvantage
Oxidation	Rapid and efficient process	Produces some very toxic compounds
Advanced oxidation process	Neither transfer pollutants from one phase to the other nor produce massive amounts of hazardous sludge Little or no consumption of chemicals, and efficiency for recalcitrant dyes), and organic contaminants are commonly oxidized to CO ₂ .	Operation is quite expensive. Treatment efficiency is inadequate because of the large variability of the composition of textile wastewaters.
Adsorption/biosorption	Easy operation, insensitivity to toxic substances, ability to treat concentrated forms of the dyes, and the possibility of reusing the spent adsorbent via regeneration. Fast, inexpensive, ecofriendly and recycling of waste materials.	
Electrocoagulation	High efficiency at low capital and operation costs, simplicity and compactness of the equipment required and easiness of process control that result in robustness. Eliminates or reduces the need for additional chemicals, and decrease drastically sludge production in comparison to coagulation. No sensitivity to toxicity. Low operating cost, good efficiency and selectivity, no toxic effect on microorganisms	High water conductivity is required to reduce power requirements. Lack of general design of batch or continuous electrocoagulation reactors. Complexity of the mechanisms involved in pollution abatement.
Biomass	Low operating cost, good efficiency and selectivity, no toxic effect on microorganisms.	Slow process, performance depends on some external factors (pH, salts).
Sonolysis	No Extra sludge production.	Requires a lot of dissolved oxygen, high cost.

Furthermore, others researchers were also used low cost biotic resources like wheat residue, treated ginger waster, ground nut shell charcoal, date stones and potato plant waste for the decolorization of textile wastewater [2].

However, all the low cost adsorbent were also has several problems such as their regeneration capacity and generation of excess sludge [44]. Furthermore, in order to select adsorbents as an alternative treatment technology, the adsorbent should be cheap, it should be easily regenerated and the effluent to be treated with this technology should also have low concentrations of pollutants [2].

Water can be recovered and reused with filtration technology such as nanofiltration (NF), ultrafiltration (UF) and reverse osmosis. The permeability capacity of a filter during separation process depends on the composition and temperature of the textile effluent. Besides, hydrolyzed reactive dyes and auxiliaries which are used for dyeing process can be recycled with membrane technology. Consequently, biological oxygen demand (BOD), color and chemical oxygen demand (COD) of the textile effluent can also be decreased [45]. However, some of the limitation of this technology are: its initial investment is high, fouling of membrane, generation of starch and water insoluble dyes [46].

Furthermore, there are numerous physicochemical techniques used like photocatalysis and photocatalytic oxidation [47], chemical coagulation [48], ozonation [49] and chemical precipitation [50] which have been reviewed for treatment of textile wastewater. Although, these treatment techniques are powerful in color removal but they caused for the transfer of pollutant from phase to other and this consequently causes for the increment of additional treatment cost and disposal task [5]. Besides, most of the organic matter present in textile wastewater are non-

biodegradable and toxic. Therefore, it is impossible to completely degrade such pollutant with single biological process [9]. In this regard, oxidation processes are more preferable to degrade such kinds of wastewater than any other kind of wastewater treatment technologies [1].

2.6.2 Oxidation methods

Bio refractory compounds can be degraded with direct oxidation treatment method. Accordingly, this method has the highest degradation potential for several substances. In this regard, the selection of most appropriate direct oxidation method for a degradation of target substance depends on several factors such as: operating conditions, process load and process limitation [51]. However, the operation cost of this method is high due to the method required specific operating conditions [52, 53].

On the other hand, AOP's are other better alternative treatment technology, it has high tendency to degrade several bio refractory organic compounds. In addition, the energy required for AOP's is by far less than direct oxidation. Moreover, wastewater treatment process can be carried out with AOP's with ambient temperature and pressure. Beside, hydroxyl radical can be formed during the process of AOP's [54]. In this regard, this radical are extremely reactive species and able to react efficiently with most organic compounds [54].

The hydroxyl radical react with most organic compounds with a rate of $10^6 - 10^9$ L/mol s [55]. AOP's are widely used in the treatment of various wastewater due to all kinds of this process commonly produce $\text{OH}\cdot$ and able to achieve required discharge limit for most type of wastewater. Furthermore, this radical is known oxidizing substance and also its reaction kinetics can be $10^6 - 10^{12}$ times quicker than ozone depending on the type of substance to be degraded [51].

The classification of AOP's depend on the method of OH· generation and also on the type of reaction phase. In this sense, the reaction phase can be (homogenous and heterogenous) and OH· radical generation mechanism can be (chemical, sono-chemical, photochemical and electro-chemical) [51].The classification of conventional AOPs based on the sources used for the generation of hydroxyl radicals is indicated in Table 2-7. Furthermore, the non-conventional AOP's which are not indicated in Table 2-7 include micro wave, plasma techniques and ionizing radiation [56].

Table 2-7 Classification of conventional AOP's [51]

	Examples
Homogenous	Fenton based processes
	Fenton: $H_2O_2 + Fe^{2+}$
	Fenton like: $H_2O_2 + Fe^{3+}/ m^{n+}$
	Sono-Fenton: US/ H_2O_2 / Fe^{2+}
	Photo-Fenton: UV/ $H_2O_2 + Fe^{2+}$
	Electro-Fenton
	Sono- Electro-Fenton
	Photo- Electro-Fenton
	Sono-photo -Fenton
	O ₃ based processes
	O ₃
	O ₃ + UV
	O ₃ + UV
	O ₃ + H ₂ O ₂
	O ₃ + UV+ H ₂ O ₂
Heterogenous	$H_2O_2 + Fe^{2+}/ Fe^{3+}/ m^{n+}$ -solid
	TiO ₂ / ZnO / CdS +UV
	$H_2O_2 + Fe^0 / Fe$ (nano-zero valent iron)
	$H_2O_2 +$ immobilized nano-zero valent iron

2.6.3 Fenton process

Advanced oxidation processes are competitive wastewater treatment technology and all types of this process commonly produced hydroxyl radical (OH·) [10]. Besides, this radical is the second most known oxidizing agent following fluorine [2, 10, 51]. Moreover, this radical is not selective,

it attacks several organic compounds and also it reacts at faster rates with most organic molecules [57]. In this regard, organic compounds degraded with this radical at approximately equal to their diffusion limited rates [58]. In addition, this radical can be degraded organic molecules either by extracting hydrogen atoms or giving hydrogen atom to the double bonds [59]. Subsequently, this radical has sufficient potential to produce lower molecular mass substance or complete mineralization of the target compounds to CO₂ and H₂O [59].

The Fenton oxidation can be carried out using the reaction between hydrogen peroxide (H₂O₂) oxidant and ferrous ion (Fe²⁺) catalyst in homogenous phase [60]. This process was first introduced by Fenton in 1884 G.C. during his activity on malic acid oxidation [10]. Furthermore, this reaction usually produce OH·. OH· has high electric potential value (E⁰) and also effective to mineralize organic molecules [61]. Fenton process can be carried out in four basic activities. These are: pH adjustment to acidic range, oxidation reaction, neutralization, and coagulation [62].

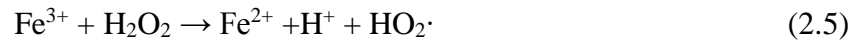
The first stage in Fenton reaction is lowering the pH of the effluent due to organic compounds degraded effectively at lower pH [63]. Besides, Fe²⁺ and H₂O₂ are more stable in this pH range [62]. In the process of Fenton oxidation, degradation can be achieved through both oxidation and coagulation processes and both ferric ion (Fe³⁺) and Fe²⁺ which are formed during the reaction are useful in the coagulation processes [64]. Previous researchers also reported about the degradation efficiency of Fenton oxidation for non-biodegradable industrial wastewater [65]. The degradation mechanism of organic pollutants by Fenton reaction is shown with equations 2.1 - 2.4 [66].



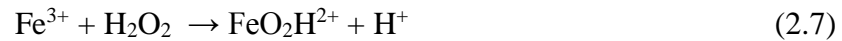
Where RH represents organic compounds



The reaction between H_2O_2 and Fe^{3+} gives Fe^{2+} as shown in equations 2.5 and 2.6 [64]. The benefit of these reactions is due to the regeneration of Fe^{2+} and subsequent formation of Fe^{2+} , this phenomenon is also important to maintain further Fenton reactions.



Fe^{3+} can be used in Fenton reaction as a substitute to Fe^{2+} . Consequently, there is a slow reaction between Fe^{3+} and H_2O_2 as indicated in equations 2.7 and 2.8 while there is fast reaction between Fe^{2+} and H_2O_2 . Subsequently, $OH\cdot$ is produced in each of these two separate reactions [67, 68].



Furthermore, Fenton reaction can be carried out with zero-valent iron (Fe^0). In this regard, Fe^0 is preferable suitable media due to it is efficient to degrade contaminants, its abundant availability and low cost [69]. Besides, Fe^0 at lower pH corrodes and produce Fe^{2+} and this cause for the continuation of further Fenton reaction as shown in equation 2.9 [70]. Consequently, Fe^{2+} react with available H_2O_2 in the usual conventional Fenton reaction [71]. H_2O_2 decomposition can be takes place with transition metal–ligand complexes and this result in the formation of reactive $OH\cdot$ [72]. Accordingly, Fenton based reaction with d block element such as copper (Cu) [73] is shown in equation 2.10.



Where, M is a d block element (transition metal).

The generation of ferrous ions in the $\text{Fe}^0 / \text{H}_2\text{O}_2$ system may be influenced by the addition of metal ions such as Fe^{3+} and Cu^{2+} [71]. Although, Fe^{3+} ions are generated by the Fenton reaction itself, an excess of these ions can also be the cause for the production of extra Fe^{2+} as expressed using equation 2.11 [71].



However, the efficiency of Fenton process can be hindered by the following reactions as indicated by equations 2.12-2.15. These reactions undesirably affect the efficiency of Fenton process [74–77].



Fenton process can be categorized as shown in Figure 2-2. Accordingly, this processes can be generally divided in two categories based on the requirement of external energy [10]. Fenton processes can use external energy such as electricity, ultrasound and light. In these sense, this external energy facilitate the removal efficiency. On the other hand, conventional Fenton process uses no kinds of external energies [10].

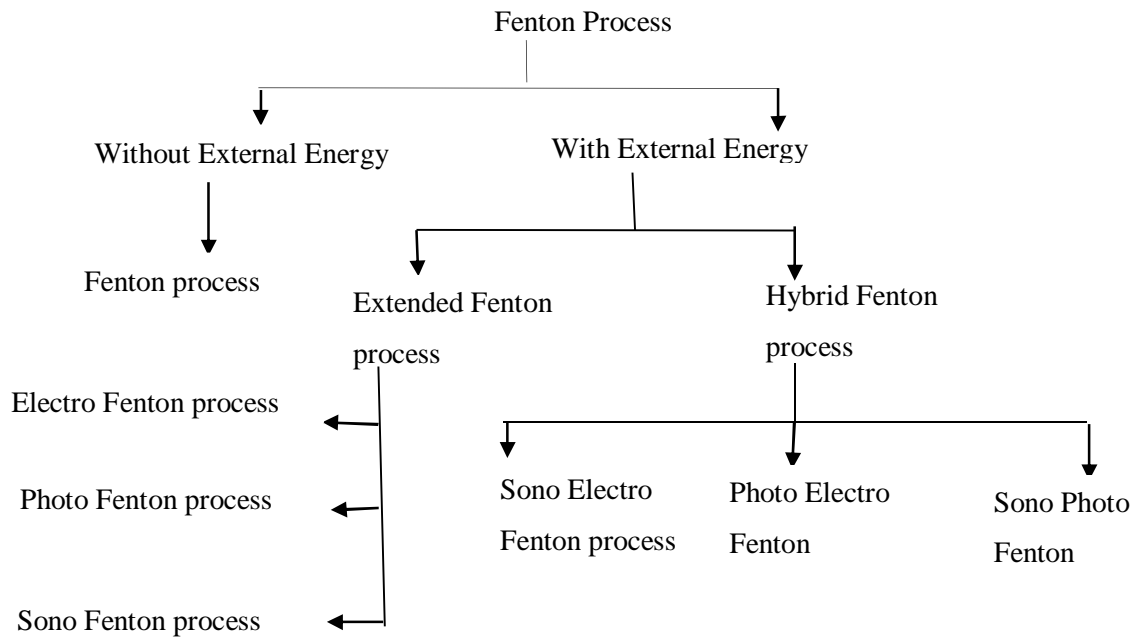


Figure 2-2. Classification of Fenton process

Besides, Fenton processes which uses external energy during the degradation processes can be classified as hybrid and extended Fenton reactions. Furthermore, hybrid Fenton process can be obtained by combining extended Fenton systems [10].

2.6.3.1 Photo-Fenton process

The integration of conventional Fenton process with UV radiation give photo-Fenton process. This process yields more $\text{OH}\cdot$ and its degradation capacity of organic substances is also better than conventional Fenton process [25]. Photo Fenton process mainly produce $\text{OH}\cdot$ at different reaction stages and this species is responsible for the removal of target organic pollutants [78]. The amount of excess sludge produced during conventional Fenton process can be reduced by using additional UV light [79]. The reaction path way that shows photo reduction of Fe^{3+} complexes to Fe^{2+} ions and the subsequent Fenton oxidation followed by degradation of organic compounds is shown by Figure 2-3 [80].

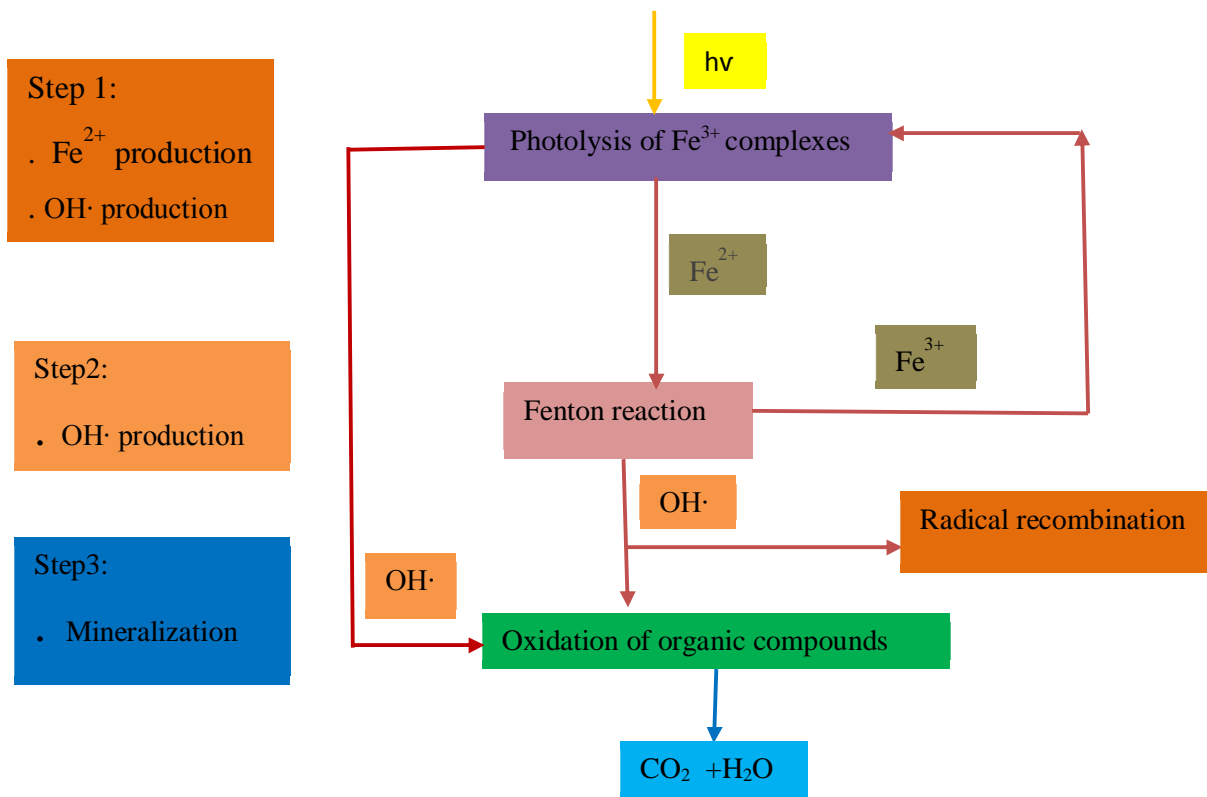
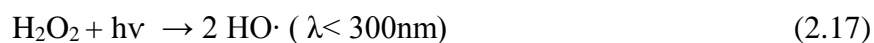
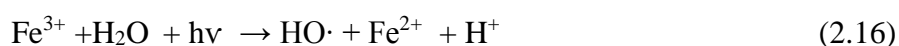
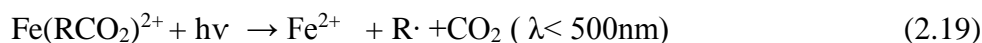
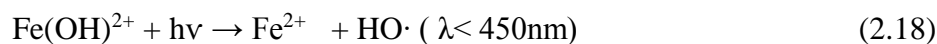


Figure 2-3 Reaction pathways of the Photo-Fenton process.

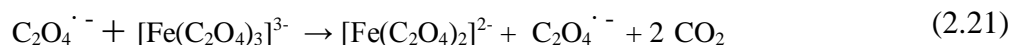
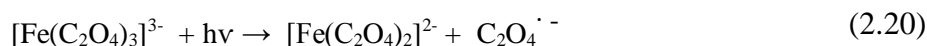
Furthermore, the extra OH· formed in the initial stage of this process also enhanced the oxidation process [81]. The cost of photo Fenton treatment process can be decreased by using solar energy (solar Fenton) and it can be appropriately applied for large scale industrial wastewater treatment [82]. During photo Fenton processes, OH· can be produced with various reaction steps along with its usual production with conventional Fenton oxidation process as indicated in equations 2.16 and 2.17 [83–85].



Ferric ion complexes ($\text{Fe}(\text{OH})^{2+}$ and $\text{Fe}(\text{RCO}_2)^{2+}$) at lower pH can absorb light in the photo Fenton process and this further gives extra ferrous ions as indicated in equations 2.18 and 2.19 [86]. Therefore, the production of this additional Fe^{2+} reagent improves the efficiency of Fenton process.



Ferrioxalate can be used as an intermediate compound to enhance the degradation of organic contaminant with photo Fenton process [87]. Accordingly, ferrioxalate at lower pH can generate CO_2 and Fe^{2+} complexes [87]. Subsequently, the formation of Fe^{2+} from ferrioxalate provides sufficient amount of catalyst for further Fenton process as indicated by equations 2.20 -2.22 [88].



In general, among various kinds Fenton process, conventional Fenton's process is preferably selected for the application of large scale non-biodegradable textile wastewater treatment due to this process does not required external energy, no special skills are required for operation, maintenance is relatively easy, It doesn't require special equipment and it is relatively cheap [89, 90]. On the other hand, some of the limitation of this method are the need of higher operational cost due to the use of chemical reagents and formation of a sludge containing large quantities of ferric ions [91, 92]. In this regard, these limitations can be improved by applying additional solar light to this process in order to increase the amount of hydroxyl radical producing and consequently

increases the removal efficiency. In addition to this, the solar Fenton process is more efficient than conventional Fenton process due to it generates few or no sludge along with better efficiency and also it is a good candidate wastewater treatment technology than extended Fenton process due to it utilizes relatively the cheapest source of energy [93].

Textile wastewater can be preferably treated effectively with Fenton process based AOP's . However, the use of this treatment technology requires substantial amount of operational cost for complete mineralization of this effluent due to this technology consumes considerable amount of chemical reagents and energy [94]. Therefore, the combination of this treatment technology with biological wastewater treatment processes can give better quality effluent with reasonable cost [1].

2.6.3.2 Biological systems and bioreactors

2.6.3.2.1 Attached growth systems

Biological process can be carried out with microbes which are attaching themselves within or on solid medium and such medium usually exist within the reactor in the form of support. The treated wastewater in this process is discharged after the end of removal process while the biomass remains attached to the surface [95]. The main types of bio reactors commonly used in such types of process are: rotating discs or fluidized beds and fixed bed [95]. In this regard, attached growth system can also have rotating discs configurations and such arrangement of bio reactor usually contains plastic discs which are immersed in the un treated effluent. Besides, this discs are populated by means of microorganisms. Moreover, other attached growth system can also include the expansion of the support with the vertical flow effluent is termed as fluidized bed reactor. Substances which are used as a support for this type of bio reactor includes metal oxides, activated carbon, sand, ion exchange beds and coal [96]. On the other hand, whenever the supports are stationery and do not move with the moving liquid, the bio reactor can be termed as fixed bed

reactor. Consequently, effluent flow through these supports and interact with attached biomass. Besides, some of the substances which are used as a support medium in this type of bioreactors are: redwood slats, rocks and plastic sheets [95]. Finally, some of the limitations of attached growth biological process as compared to suspended growth systems are: the requirement of considerable amount of energy during aeration and mass transfer problem for oxygen.

2.6.3.2.2 Suspended growth system

Biological process can also be takes place with a biomass which are suspended with in an effluent under treatment. Accordingly, in this process, the interaction between substrate and microorganisms are facilitated with appropriate mixing process. Besides, clarification process can remove biomass flocs after the end of this treatment. In this regard, the bioreactors in this type of biological process can be designed as either continuous or batch flow configuration. Arden and Lockett [97] in 1941 introduced aerobic activated sludge process, a continuous flow mode, which are used for the treatment of most domestic and industrial wastewater. In this regard, the wastewater is entered in to a tank which consist of suspended biomass with continuous aeration and mixing. After the end of this treatment, the biomass settled in a separate clarifier and some portion of this biomass recycled to the aeration tank and the rest of them also wasted accordingly. However, this technology has several operational limitations. Some of the limitations are: high biomass production, energy consumption and high operational cost [98]. On the other hand, due to strict environmental protection legislation and emergence of better technology causes for the substitution of conventional activated sludge process by high efficient and relatively cheap sequencing batch reactor (SBR) [98]. This treatment technology were introduced by R.L. Irvine [99] in 1971 which can be effectively applied for the treatment of both municipal and industrial wastewater [100].

2.6.3.2.2.1 The Sequencing Batch Reactor (SBR) technology

SBR is usually used for the removal of xenobiotic compounds in industrial and domestic wastewater. SBR has the following benefits at small scale: low construction and maintenance cost and flexibility in operation [101–103]. SBR usually use aerobic bacteria similar to conventional activated sludge process. It can degrade and convert the biodegradable portion of the organic matter in to new cells, gases and salts [13]. The SBR operates in five sequential stages (wastewater feeding, reaction, sedimentation, taking of the clarified effluent and idle stage) in discontinuous modes. This process has various advantage over conventional activated sludge process [98]. Some of the advantages are simplicity and flexibility, low cost, resistance to fluctuations in the influent and also process such as equalization, reaction and clarification occur in the same reactor [13, 98].

The SBR wastewater treatment process is more efficient than conventional activated sludge process with respect to economy and time. In this regard, 60% treatment costs can be saved [104] and also above 90% removal efficiency of biodegradable organic matter can be obtained [105] as compared to conventional activated sludge process. Furthermore, SBR are appropriate treatment technology which can be mainly applied especially for wastewater which has intermittent or low flow conditions [106].

2.6.3.2.2.1.1 Operational characteristics in SBR process

The SBR operates sequentially in a repeated cycles. A cycle is a group operations or phases comprising between the beginning (fill) and the end (draw and idle) of a waste water treatment. These cycles are defined by five phases: fill, react, settle, draw and idle. The total cycle time (t) is the sum of all these phase as presented in equation [107].

$$t_C = t_F + t_R + t_S + t_D + t_I \quad (2.23)$$

Where: t_c : total cycle time, h t_R : reaction time t_D : Draw time
 t_F : fill time ,h t_S : draw time t_I : Idle time

The number of cycle (N_C) per day is determined through the total cycle time (t_c)

$$N_C = 24/t_c \quad (2.24)$$

SBR usually operates with different volumes due to filling and draw phase. Hence, total reactor volume (V_T) defined as the maximum working volume and filling volume (V_f) defined as the volume of wastewater filled and discharged in every cycle. The difference between filling and total reactor volume is the minimum volume (V_{min}), i.e., volume that always inside the reactor [107].

$$V_{min} = V_T - V_F$$

Where: V_T : total reactor volume (L), V_F : filling volume (L) V_{min} : minimum volume (L)

Basic equations in SBR expressed in terms of equations commonly used with continuous stirred tank reactor system [107]. Accordingly, hydraulic retention time (HRT) expressed in equation 2.25

$$HRT = \frac{V_T}{Q} \quad (2.25)$$

Where HRT : Hydraulic retention time Q =daily wastewater flow rate ,L/d

Furthermore, the flow (Q) in SBR is defined by the product of filling volume (V_F) and number of cycle per day (N_C). Thus, HRT can be expressed as shown in equation 2.26 [107].

$$HRT = \frac{t_c}{V_F} \frac{1}{24} \quad (2.26)$$

Where: T_C : total cycle time, h V_F/V_T : exchange ratio

The solid retention time (SRT) determines the amount of biomass which remains in the bio reactor. Therefore, SRT can be expressed as the ratio of biomass concentrations inside the reactor to biomass leaving the reactor as expressed in equation 2.27 [107].

$$SRT = \frac{V_T \cdot X}{Q_W \cdot X_W} \quad (2.27)$$

Where, SRT: Solid retention time (d)

V_T : Total reactor volume

X_W : the solid biomass concentration (mg/L)

X : Biomass concentrations inside the reactor (mg/L)

Q_W : Waste flow rate (mg/L)

Even though biological treatment is the most economical alternative when compared with other physical and chemical processes, their application is often restricted because of technical constraints [108]. In this regard, previous researchers were reported about better removal efficiency of this treatment technology with the integration of Advanced oxidation processes [8, 12–15].

2.6.4 The integration of Advanced oxidation processes with biological processes

The selection of appropriate treatment technology for the treatment of a particular type of wastewater is extremely a difficult task. Besides, the selection of alternative effluent treatment technology also depends on cost of treatment and quality of effluent after treatment which is intended for certain use according to the discharge limit of a particular administration system.

In this regard, the use of biological treatment is attractive due to its low operating cost but the residence time is very high relative to that of other processes. On the other hand, the removal rate of advanced oxidation processes is relatively high while the operating cost is relatively expensive due to the use of reagents and irradiation sources. Capital and operating costs of biological treatment methods are 5-20 and 3-10 times cheaper than those of chemical methods, respectively [107–113]. Therefore, there is no single treatment technology which can be independently sufficient for the treatment of wastewater.

In this regard, the integration of various wastewater treatment techniques can help to develop economically and technically feasible alternative treatment technology [20]. Moreover, among various potential hybrid treatment technologies, the biological hybrid technology is more preferable than any other alternatives [7]. In addition, strategies for the choice of appropriate treatment technologies is shown in Figure 2-4. Accordingly, biological treatment process is not suitable for wastewater containing non-biodegradable pollutant due to the microorganism cannot degrade the part of organics while AOP's are suitable for the treatment of wastewater containing non-biodegradable and toxic pollutants [6].

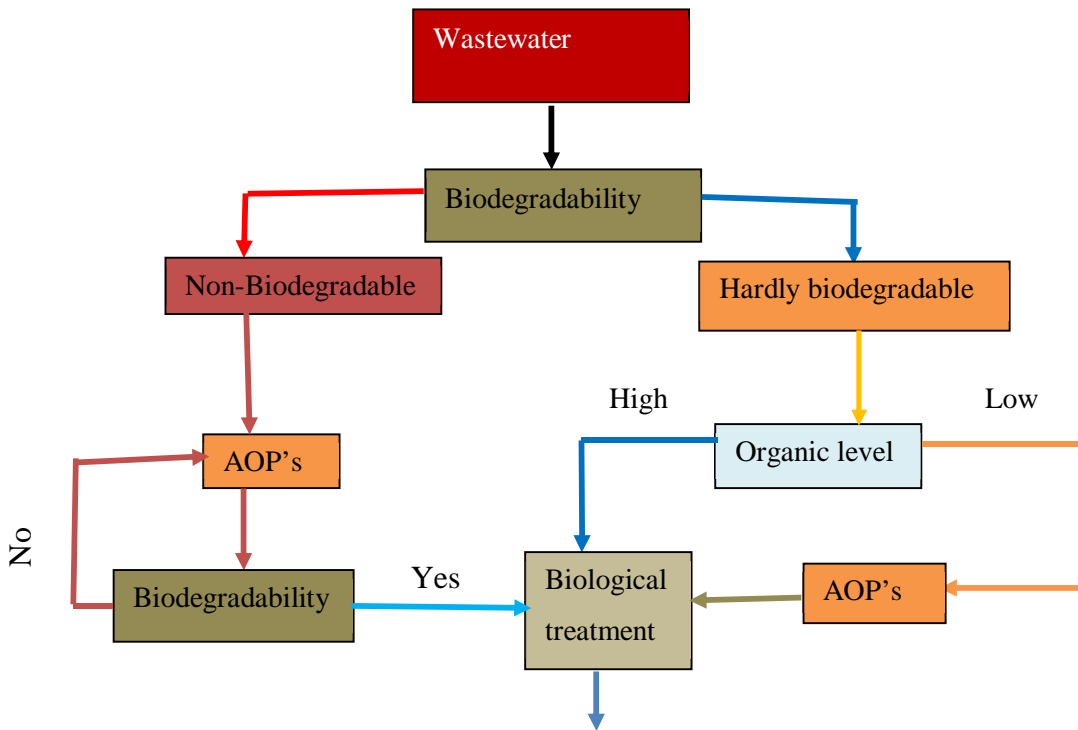


Figure 2-4 Schematic representation for the choice of appropriate treatment processes for various industrial wastewaters based on their biodegradability levels [6].

In the process of hybrid treatment system, whenever chemical oxidation used as a first stage treatment, the effluent obtained from this chemical oxidation may produce harmful intermediates than the initial un treated wastewater to the subsequent biological process due to the following reasons [1]:

- Production of stable and less biodegradable intermediates than the initial un treated effluent.
- Peroxidation with chemical method may not preferentially degrade bio refractory organic portion of the effluent
- Lack of selection of appropriate process conditions. For instance, the use of longer reaction time can cause for the shortage of sufficient available substrate concentrations for the microorganisms in the subsequent stage.

- Pre oxidation with excess catalyst and oxidant can create unfavorable condition for the microorganisms activity in the subsequent biological process.

In this regard, the treatment efficiency of the integration of AOP's with biological processes for industrial wastewater in various configuration were reported by [7]. Furthermore, few studies were also reported on the treatment of real or simulated textile wastewater with AOP's followed by biological oxidation [116]. Accordingly, they reported the treatment efficiency of the combination of SBR with Fenton oxidation for textile effluents [22,23] and also concerning degradation and decolorization of dyes from aqueous solution with the integration of SBR and Fenton oxidation [118, 119].

2.7 Statistical design of experiments

Whenever multiple responses and variables are considered in the case of studying of effect of variables, the conventional method of changing one variable at a time approach would not be suitable to properly observe the effects of process factors. In this regard, statistical design of experiments are appropriate to conduct the experiments in orderly manner, to properly study interactions among process factors and also to precisely optimize process variables based on the factors and levels selected. Consequently, Experimental design with response surface methodology (RSM) helps to examine the interaction between independent and dependent variables together with optimization of process parameters [120]. In this regard, RSM can restrict the number of experiments for recognition of optimal conditions for a targeted response and can be also used effectively in the optimization process [121]. In addition, RSM usually comprises the following basic steps: (1) choice of independent variables and their ranges, (2) the choice of experimental design (3) estimation of mathematical coefficients using linear regression analysis

technique and (4) evaluation of model adequacy followed by finding of optimal conditions [122]. Furthermore, there are different types of RSM designs, namely three level factorial design, central composite design (CCD), Box-Behnken design (BBD) and D-optimal design [123].

Furthermore, among the different kinds of RSM experimental designs, BBD is an independent, rotatable quadratic design with no embedded factorial points where the variables combinations are at the midpoints of the edge of the variables space and at the center. In addition, during the selection of appropriate experimental design, the ratio of number of experiments to number of coefficients in the quadratic model should be reasonable. In this regard, when this ratio is in the range of 1.5-2.6, it shows that the experimental design under consideration is reasonable. Accordingly, this ratio for BBD with three factors is commonly 1.6. In addition, in the comparison of different RSM design approaches, BBD and Doehlert matrix are slightly more efficient than CCD and more efficient than three level full factorial design [123]. Furthermore, BBD is usually very efficient and economically interesting due to the fewer number of experiments and also allows calculation of the response functions at intermediate levels and enables estimation of the system performance at any experimental point within the range studied [123]. In this context, BBD is widely used, easy and effective design tool [124]. Hence, it is widely applied for optimization of wastewater treatment processes [121].

3 Materials and Methods

3.1 Mineralization of a methyl orange dye using artificial solar Fenton process

3.1.1 Chemicals used in the mineralization of methyl orange dye

Methyl orange dye was obtained from research laboratory of analytical chemistry and chemical engineering, Barcelona University, Spain. It was used in the experimental studies since it is widely used in textile, printing, paper, pharmaceuticals, food industries and in research laboratories. Characteristics of methyl orange dye are presented in Table 3-1. An accurately weighted quantity of the dye was dissolved in miliQ water to prepare a stock solution (1000mg/l). Experimental solutions of the desired concentration were obtained by successive dilution.

All chemicals used in the study were of highest commercially available grade. Analytical grade of hydrogen peroxide (30w/w, from Merck), $\text{FeSO}_4 \cdot 7\text{H}_2\text{O}$ were (PA from panreac), NaHSO_3 (PAI from panreac) and reagents were used without further purification. The pH adjustment was done using reagent grade sulfuric acid (H_2SO_4 , 96% purity from panreac).

Table 3-1 General characteristic of methyl orange dye

Color index number	CI.13025
Chemical classification	Azo dye
Molecular weight	327.33 g/mol
λ_{max} (nm)	463.273
Molecular formula	$\text{C}_{14}\text{H}_{14}\text{N}_3\text{NaO}_3 \text{ S}$

All the required solutions were prepared in miliQ water (double deionized water). The detail information about experimental levels and ranges used in the 17 experimental runs for all the three process factors (Dye stuff dose, Fe^{2+} dose and H_2O_2 dose) was shown on Table 3-2

Table 3-2 Coded levels and independent variables used for solar Fenton oxidation with BBD

Factors	Units	Coded Levels		
		Low	medium	high
		-1	0	+1
Dye stuff dose	mg/L	15	135	255
Ferrous ion (Fe ²⁺) dose	mg/L	0	60	120
Hydrogen peroxide (H ₂ O ₂) dose	mg/L	105	1055	2005

3.1.2 Artificial solar irradiation: Solar box (SB)

As shown on Figure 3-1 a solar box (CO.FO.ME.GRA 220V 50 Hz) with a Xenon lamp (Phillips 1 kW) was used as a source of irradiation. The irradiation entering the photo reactor was 3.59J/s measured also by o-nitro benzaldehyde actinometry [125]. The tubular photo reactor (24 cm length, 2.11 cm diameter, Duran glass material) was placed at the bottom of the Solar box on the axis of a parabolic mirror made of reflective aluminum. A filter cutting off wavelengths under 280 nm was placed between the lamp and the reactor. The Dye solution of various levels (15mg/L, 135 mg/L and 255 mg/L) was prepared and feed in to a batch jacketed feeding tank (total volume 1L). Next Fe²⁺ and finally H₂O₂ were added.

The solution to be treated was pumped to solar box by peristaltic pump (Ecoline VC-280 II, Ismatec) from a stirred double jacket reservoir batch tank (total volume 1L) with a flow-rate of 0.71 L/min. The reservoir was connected to an ultra-thermostatic bath (HaaKe.K10) to assure constant temperature during the processes and all connections employed were made of teflon to avoid losses by adsorption. The total time of irradiation used for all experimental runs were 20 minutes. A preliminary sample was collected from each level of dye solution before irradiation to represent initial concentration at 0 min and no conversion was observed.

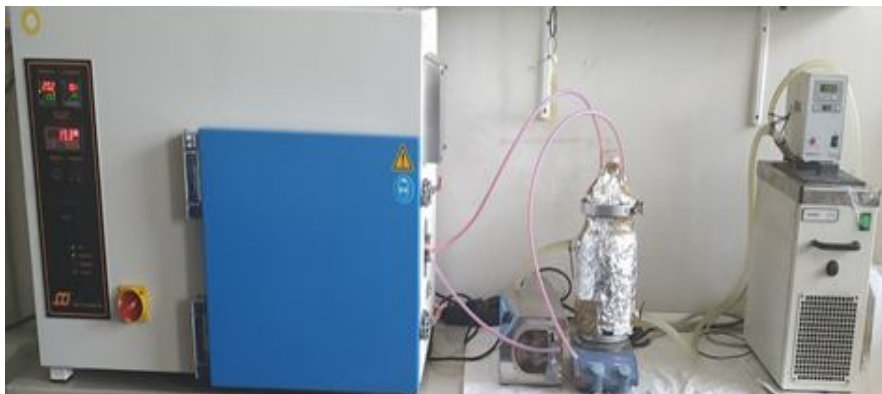


Figure 3-1 **Experimental set up of artificial solar photo-Fenton**

3.1.3 Techniques and analytical instrument used in the mineralization of methyl orange dyes

TOC was analyzed with a Shimadzu TOC-V CNS analyzer. Reproducible TOC values, with an accuracy of $\pm 1\%$, were obtained by injecting 50 μL samples into the analyzer. Samples were quenched with sodium hydrogen sulfite, or the same volume of methanol, to avoid further reactions depending on the analysis to be done. The iron (II) content was determined by o-phenontraleine standardized procedure (ISO 6332). The color of the samples was analyzed by measuring the absorbance of supernatant sample at wavelength corresponding to the maximum absorbance, i.e., 463 nm in DR 6000 (USA).

3.1.4 Experimental design, analysis and statistical validation during treatment of methyl orange dyes with artificial Fenton oxidation

Response surface methodology (RSM) was used for the optimization of experiments. In this research, BBD was used for optimization of COD and color removal efficiencies. Here, a 2^3 factorial design was used to identify the influence of 3 parameters including: dye dose (A), Fe^{2+} (B) and H_2O_2 (C) concentrations. These factors were chosen based on literature and preliminary experiments. From these preliminary experiments, the range of A, B and C were selected as shown in Table 2. A total of 17 experiments were conducted with 5 replicates at the central point, and the

designation of values was according to [126]. A second-order regression model was employed for analysis and proves to be a good estimation of response surface [127] and is expressed as shown in Equation 3.1.

$$Y = \beta_0 + \sum_{i=1}^k \beta_i X_i + \sum_{i=1}^k \beta_{ii} X_i^2 + \sum_{i=1}^{k-1} \sum_{j=i+1}^k \beta_{ij} X_i X_j \quad (3.1)$$

Where y = response; x_i and x_j = input variables; β_0 = intercept constant; β_i = first-order regression coefficient; β_{ii} = second-order regression coefficient representing quadratic effect of factor i ; and β_{ij} = coefficient of interaction between two factors i and j [128]. The analysis of variances (ANOVA) result was obtained using statistical software package Design-Expert® version 7.0.0 (Stat-Ease, Inc.) to study the results and to determine the implication of fitted quadratic model. The fitted model was illustrated in the form of 3D plots to know the interaction between the variables and responses.

The quality of model was checked [129] using several coefficients. In this regard, values of probability < 0.05 show that model terms are significant and values > 0.05 point out that model terms are not significant [121]. Besides, the co-relation coefficient R^2 , which evaluates the correlation between experimental data and predicted responses [130], the adjusted R^2 which takes the number of factors into account [131] and the predicted R^2 which indicates how much a regression model predicts responses for new observations. The adequate precision was used to describe the signal-to-noise ratio [132]. Moreover, the value of adequate precision should be higher than 4. Besides, smaller coefficient of variation factor also describes the repeatability and reproducibility of the models [121].

3.2 Degradation of a Basic Blue 41 dyes using Fenton reagent

3.2.1 Chemicals used during degradation of a Basic Blue 41 dye aqueous solution

Mono-azo dye Basic Blue 41 was purchased from Bezema Dyes and Chemicals NBE Plc, Switzerland. It was used in the experimental studies since it is widely used for dyeing purpose at KK acrylic fiber processing textile industry in Addis Ababa, Ethiopia. Characteristics of Basic Blue 41 are presented in Table 3-3. An accurately weighted quantity of the dye (Basic Blue 41) was dissolved in distilled water to prepare a stock solution (1000mg/l). Experimental solutions of the desired concentration were obtained by successive dilutions.

All chemicals used in the study were of highest commercially available grade. Analytical grade hydrogen peroxide (30%(w/v)) and $\text{FeSO}_4 \cdot 7\text{H}_2\text{O}$ were purchased from HIMEDIA Laboratories pvt. Ltd. India. The pH adjustment was done using reagent grade sulfuric acid and sodium hydroxide solutions. All the required solutions were prepared in distilled water.

Table 3-3 General characteristic of Basic Blue 41 [133]

Color index number	CI.11105
Chemical classification	Monoazo
Molecular weight	482.57g/mol
λ_{max} (nm)	617
Molecular formula	$\text{C}_{20}\text{H}_{26}\text{N}_4\text{O}_6\text{S}_2$

3.2.2 Fenton oxidation during degradation of Basic Blue 41 dye aqueous solution

Batch experiments of Fenton oxidation were carried out in glass beakers having 2 liter of operating capacity at room temperature (20-22°C). Initially, the pH of the sample was adjusted to 3.0 using 0.5 M H_2SO_4 . Consequently, a catalyst $\text{FeSO}_4 \cdot 7\text{H}_2\text{O}$ was added and reaction proceeded with

further addition of H_2O_2 for the formation of hydroxyl radicals. During reaction, the sample solution was continuously stirred using a magnetic stirrer at 150 rpm for 60 min. After 60 minutes, residual hydrogen peroxide was eliminated by addition of sodium sulfite. Consequently, pH of the solution increased above 7 with sodium hydroxide. Subsequently, settling of samples was carried out in Imhoff cone for 2 h. Finally, the supernatant was analyzed.

3.2.3 Analytical procedures during degradation of Basic Blue 41 dyes

The color of the samples was analyzed by measuring the absorbance of supernatant sample at wavelength corresponding to the maximum absorbance, i.e., 617 nm in Spectro UV-Vis UVD-3200 (USA). The COD concentration of the samples was measured using a COD digester -HI 839800 (Hungary) following standard methods [134]. The pH of the sample was determined using pH-meter Hanna HI 11310 (Rumania).

3.2.4 Experimental design, analysis and statistical validation during degradation of Basic Blue 41 dyes with conventional Fenton oxidation

Response surface methodology (RSM) was used for the optimization of experiments. In this research, BBD is used and RSM was employed for optimization of COD and color removal efficiencies. Here, a 2^3 factorial design was used to identify the influence of 3 parameters including: dye dose (A), H_2O_2 (B) and Fe^{2+} (C) concentrations. In addition, these factors were chosen based on literature and preliminary experiments. In this sense, the ranges of A, B and C were selected based on Table 3-4 . Besides, a total of 17 experiments were conducted with 5 replicates at the central point and the designation of these values was according to [126].

Table 3-4 Coded levels and independent variables used for conventional Fenton oxidation with BBD

Factors	Units	Coded Levels		
		Low	medium	high
		-1	0	+1
Dye stuff dose	mg/L	15	135	255
Hydrogen peroxide (H ₂ O ₂) dose	mg/L	105	1055	2005
Ferrous ion (Fe ²⁺) dose	mg/L	0	60	120

3.3 Degradation of textile Industry Wastewater by Fenton Oxidation

3.3.1 Wastewater collection

Raw textile wastewater sample was taken from KK acrylic fiber dyeing process textile factory located in Addis Ababa, capital city of Ethiopia. The samples were taken during dyeing process particularly at a time of dark shading just after screening of course particles. Sampling bottles were cleaned and rinsed with distilled water before a new sample were taken. Sample characterizations were done in-situ and in laboratories in order to check any change of the sample during transportation process. Samples were kept at 4°C until further use. The characteristics of real wastewater sample are given in Table 3-5 below.

Table 3-5 Characteristics of KK Textile wastewater

Serial numbers	parameters	Values
1	pH	8.35 ± 2.01
2	COD (mg/L)	1970 ± 70
3	Absorbance at 617nm	0.97 ± 0.01
4	BOD ₅ (mg/L)	207 ± 17

3.3.2 Chemicals used during degradation of real textile wastewater

All chemicals used in the study were of highest commercially available grade. Analytical grade of hydrogen peroxide (30w/w, from merck), $\text{FeSO}_4 \cdot 7\text{H}_2\text{O}$ were (PA from panreac), NaHSO_3 (PAI from panreac) and reagents were used without further purification. The pH adjustment was done using reagent grade sulfuric acid (H_2SO_4 , 96% purity from panreac). All the required solutions were prepared in distilled water.

3.3.3 Fenton oxidation during treatment of real textile wastewater

Batch experiments of Fenton oxidation were carried out in glass beakers having 2 liters of operating capacity at room temperature. Fenton reagents and pH which were used for all the BBD experimental runs were based on factors and levels as shown in Table 3-6. Consequently, initially the pH of the sample was adjusted also according to Table 3-6 using 0.5 M H_2SO_4 . Subsequently, a catalyst $\text{FeSO}_4 \cdot 7\text{H}_2\text{O}$ was added and reaction proceeded with further addition of H_2O_2 . During reaction, the sample solution was continuously stirred using a magnetic stirrer at 150 rpm for 60 minutes. After 60 minutes, residual hydrogen peroxide was eliminated by addition of sodium sulfite. Consequently, pH of the solution increased beyond 7 with sodium hydroxide. Thus, settling of samples was carried out in Imhoff cone for 2 h. Finally, supernatant was analyzed.

3.3.4 Analytical procedures during treatment of real textile wastewater with conventional Fenton oxidation

The color of the samples was analyzed by measuring the absorbance of supernatant sample at wavelength corresponding to the maximum absorbance, i.e., 617 nm in Spectro UV-Vis UVD-3200 (USA). The COD concentration of the samples was measured using a COD digester -HI 839800 (Hungary) following standard methods[134]. The pH of the sample was determined using pH-meter.

3.3.5 Experimental design, analysis and statistical validation during degradation of real textile wastewater with conventional Fenton oxidation

Optimization of the process factors for both biological and chemical stages was carried out by response surface methodology (RSM). Moreover, BBD was particularly performed for the whole stages process optimization. The ranges of the investigated three independent process factors, namely, Fe^{2+} concentration (A), H_2O_2 (B) and pH (C) as shown in Table 3-6. Furthermore, these factors were designed based on 2^3 factorial design. The range and levels of these factors were selected based on preliminary experiments. Consequently, based on BBD, the total number of experiments which were conducted were 17. In addition, among these experiments 5 were center points and the designation of the values was according to [126].

Table 3-6 Coded level and independent variables used with BBD for real wastewater treatment

Factor	Unit	Coded values		
		low	medium	high
		-1	0	+1
Ferrous ion (Fe^{2+}) dose	mg/L	400.00	550.00	700.00
Hydrogen peroxide (H_2O_2) dose	mg/L	4200.00	6400.00	8600.00
pH	-	2.4	2.9	3.4

3.4 Sequencing batch reactor (SBR)

The setup of the laboratory scale SBR is shown in Figure 3-2. It is made of plexi glass with a total volume of 5.5L and working volume of 4L. Feeding of the wastewater and withdrawal of the decanted effluent was carried out using peristaltic pumps. Air was supplied with air diffuser. Mixing took place with mechanical stirrer at a speed of 150rpm. The reactor was seeded with biomass collected from the Kalti domestic wastewater treatment plant in Addis Ababa, Ethiopia.

In order to acclimatize the biomass, the SBR setup was left for 8 days with scheduled aeration at the rate of 8L/hr. Consequently, the reactor was filled with textile wastewater. The pH of the wastewater was fixed to 6.8 and its temperature was also maintained at 28 °C.

3.4.1 Experimental procedure of SBR

The potential process factors which were used in this study were : cycle period (12, 24 and 36h), air flow rate (8, 13 and 18 L/h) and SRT (12, 16 and 20d). The ranges and levels used for these process variables are shown in Table 3-7. The hydraulic retention time in the reactor was maintained at 4 days. These process factors were optimized with Box-Behnken design (BBD). The SBR was operated with five consecutive batch processes namely, feeding, aeration, sedimentation, draw step (decant) and idle step. During 0.5h raw textile wastewater was fed in to the reactor, aeration was carried out for 10h, sedimentation was carried out for 1h, the decanted effluent was taken for 0.38h and the system was closed in 0.13h. This process recycle used fresh textile wastewater as feed based on corresponding cycle periods. During the idle stage excess sludge was removed at the bottom of the reactor.

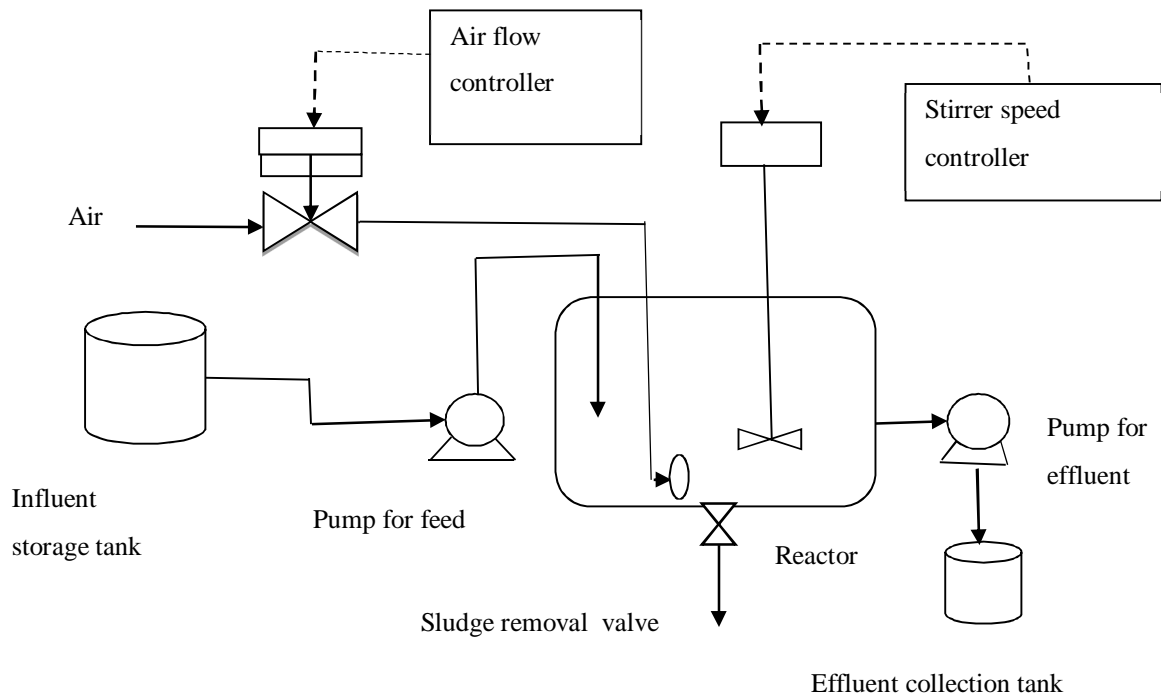


Figure 3-2 Schematic representation of the SBR system.

Table 3-7 Coded level and independent variables used in BBD by SBR biological system for KK textile wastewater.

Process factors	Code name of process factors	Units	Coded values		
			low	medium	high
			-1	0	+1
Cycle period	A	h	12	24	36
Air flow rate	B	L/h	8	13	18
Sludge retention time	C	d	12	16	20

Experiments were also conducted at optimized conditions at various organic loading rate (OLR) and hydraulic retention time (HRT) as shown in Table 3-8 using two distinct influent substrate concentrations obtained during dark shading and medium shading of the textile dyeing process. (1.25 and 1.96 g COD/L). COD removal, color removal, mixed liquor suspended solid (MLSS) and sludge volume index (SVI) were measured using standard analytical methods.

Table 3-8 Experimental conditions of SBR at optimized conditions for single SBR stage treatment.

Substrate concentration g COD/L	Days of operation (days)	HRT (days)	OLR (kg COD /m ³ d)
1.25	1-17	4	0.078
	18-23	3	0.104
	24-37	2	0.156
1.96	38-52	4	0.122
	53-61	3	0.163
	62-77	2	0.245

3.4.2 Experimental design, analysis and statistical validation during treatment of textile wastewater with SBR

Response surface methodology (RSM) was used for the optimization of experiments. In this research, BBD was used and RSM was employed for optimization of COD and color removal efficiencies. Here, a 2³ factorial design was used to identify the influence of 3 parameters including cycle period (A), air flow rate (B) and sludge retention time (C). These factors were chosen based on literature and preliminary experiments. From these preliminary experiments, the range of A, B and C was selected as shown in Table 3-7. A total of 17 experiments were conducted with 5 replicates at the central point, and the designation of values was according to Moghaddam et al. [126].

3.5 Integration of sequencing batch reactor with Fenton oxidation

3.5.1 Experimental procedure of SBR in the integrated system

The process variables were cycle period (24 h), air flow rate (15L/h) and SRT (16d). These values were obtained from optimization of the process factors using response surface methodology. The

hydraulic retention time in the reactor was 4d. The SBR operated with five consecutive batch process namely, feeding, aeration, sedimentation, draw step (decant) and idle step. During the 1h raw textile wastewater feed in to the reactor, aeration carried out for 20h, sedimentation carried out for 2h, the decanted effluent was taken for 0.76h and the system closed for 0.26h. Such process recycle using fresh textile wastewater based on corresponding cycle periods. During the complete mixed stage excess sludge was removed. The detail of optimization steps and related datas regarding SBR treatment stages were addressed in section 3.4.1 [135].

Experiments were also conducted at optimized conditions at various organic loading rate (OLR) and hydraulic retention time (HRT) as shown in Table 3-9. In addition, a substrate influent concentration obtained after dyeing process (1.25 gCOD) was used. COD removal and color removal were measured using standard method of analysis.

Table 3-9 Experimental conditions of SBR at optimized condition for integrated treatment system

Substrate concentration g COD/L	days	HRT(days)	OLR (Kg COD /m ³ d
1.25	1-19	4	0.078
	18-25	3	0.104
	24-39	2	0.156

3.5.2 Fenton oxidation after optimization for the combined process with SBR

Batch experiments of Fenton oxidation were carried out in glass beakers having 2 liters of operating capacity at room temperature. Optimum doses of Fenton reagents (Fe²⁺: 500.4 mg/L, H₂O₂: 5187.6 mg/L) was used and the reaction was carried out for 30 minutes. Consequently,

initially the pH of the sample was adjusted to 2.9 using 0.5 M H₂SO₄. Subsequently, a catalyst FeSO₄·7H₂O was added and reaction proceeded with further addition of H₂O₂. During reaction, the sample solution was continuously stirred using a magnetic stirrer at 150 rpm for 30 minutes. After 30 minutes, residual hydrogen peroxide was eliminated by addition of sodium sulfite. Consequently, pH of the solution was increased above 7 with sodium hydroxide. Consequently, settling of samples was carried out in Imhoff cone for 2 h. Finally, supernatant was analyzed.

3.5.3 Fenton oxidation before optimization in the integrated system

Batch experiments of Fenton oxidation were carried out in glass beakers having 2 liters of operating capacity at room temperature. Fenton reagents and pH which were used for all the BBD experimental runs were based on factors and levels as shown in Table 3-6. Consequently, initially the pH of the sample was adjusted according to Table 3-6 using 0.5 M H₂SO₄. Subsequently, a catalyst FeSO₄·7H₂O was added and reaction proceeded with further addition of H₂O₂. During reaction, the sample solution was continuously stirred using a magnetic stirrer at 150 rpm for 60 minutes. After 60 minutes, residual hydrogen peroxide was eliminated by addition of sodium sulfite. Consequently, pH of the solution was increased to the value greater than 7 with sodium hydroxide. Consequently, settling of samples was carried out in Imhoff cone for 2 h. Finally, supernatant was analyzed.

3.5.4 Fenton oxidation after optimization for the combined process with SBR

Batch experiments of Fenton oxidation were carried out in glass beakers having 2 liters of operating capacity at room temperature. Optimum doses of Fenton reagents (Fe²⁺: 500.4 mg/L, H₂O₂: 5187.6 mg/L) was used and the reaction was carried out for 30 minutes. Consequently, initially the pH of the sample was adjusted to 2.9 using 0.5 M H₂SO₄. Subsequently, a catalyst

FeSO₄.7H₂O was added and reaction proceeded with further addition of H₂O₂. During reaction, the sample solution was continuously stirred using a magnetic stirrer at 150 rpm for 30 minutes. After 30 minutes, residual hydrogen peroxide was eliminated by addition of sodium sulfite. Consequently, pH of the solution was increased above 7 with sodium hydroxide. Consequently, settling of samples was carried out in Imhoff cone for 2 h. Finally, supernatant was analyzed.

3.5.5 Fenton followed by SBR (Fenton stage+ SBR)

Initially the pH of the textile wastewater was adjusted to 2.9. Consequently, optimum Fenton reagent dose (Fe²⁺: 500.4 mg/L, H₂O₂: 5187.6 mg/L) were used. These effluents were further treated with optimum SBR process variable (cycle period (24h), air flow rate (15L/h) and SRT (16d)). Hence, COD removal and decolorization were measured using standard method of water and wastewater treatment [134].

3.5.6 SBR followed by Fenton (SBR stage +Fenton)

Initially in the SBR treatment stage, optimum SBR process factors with various organic loading rates (OLR) and hydraulic retention time (HRT) conditions were used. Furthermore, OLR was varied by altering the HRT (4, 3 and 2 days) while the influent wastewater concentration was kept constant (1.25 gCOD/L). The detail working situations SBR optimum conditions were given in Table 3-9. The total days of operation were 39 days. In these experiments, COD removal and decolorization were measured at the 19th, 25th, 39th days based on standard methods of water and wastewater treatment analysis. The pH of the effluent obtained from SBR treatment stage was fixed to 2.9. Treatment carried out with optimum Fenton reagent doses (Fe²⁺: 500.4 mg/L, H₂O₂: 5187.6 mg/L).

4 Results and Discussion

4.1 Mineralization of methyl orange dyes

4.1.1 RSM modelling in the mineralization of methyl orange dyes

The experimental and predicted values originating from the BBD are summarized below (Table 4-1). The ANOVA values were also summarized in Table 4-2. Optimal values for decolorization and TOC removal in the experimental runs can be determined by a second order polynomial as expressed by equations 4.1 and 4.2.

$$R_1 = 98.40 + 32.11B + 10.40AB - 7.88BC - 32.51B^2 \quad (4.1)$$

$$R_2 = 90.80 + 15.35A + 37.41B + 8.02AB - 15.70A^2 - 37.98B^2 \quad (4.2)$$

Where R_1 and R_2 are color and TOC removal respectively shows the regression coefficients and model performance indicators for the RSM model. In Equations 4.1 and 4.2, positive effect of a factor implies the response is improved when the factor level increases and a negative effect of the factor means that the response is not improved when the factor level increased [136]. In addition, In the case of color removal, it can be seen that B, AB, BC and B^2 were significant terms, and rest of the terms were not significant while for TOC removal, it was concluded that A, B, AB, A^2 and B^2 were only proved to be significant. In this regard, only coefficients of significant terms were included in the expressions of both equations.

The values for the adequate precision higher than 4 for both color removal and TOC removal, indicates that this model can be used to navigate the design space. Low values of C.V, i.e., 7.25 and 10.00 for color and TOC removal respectively indicated high accuracy and dependability of

experiments due to both these values are closer to 10%. Besides, the value of the predicted R^2 for color and TOC removal was 0.7160 and 0.7822 respectively, while the adjusted R^2 values were 0.9594 and 0.9689 respectively indicate a good agreement of the model due to the values between adjusted and predicted R^2 are closer to each other along with relatively high values of adjusted R^2 . Furthermore, Figure 4-1 shows how the predicted values fit well with the experimental values of TOC and color removal and it was also proved the appropriateness of the result which was obtained from both predicted and adjusted R^2 .

Table 4-1 Box–Behnken design matrix along with experimental and predicted values during treatment of methyl orange dyes with artificial solar Fenton oxidation

Run	A(mg/L) Dye doses	B(mg/L) Fe ²⁺	C(mg/L) H ₂ O ₂	R ₁ : Color removal (%)		R ₂ : TOC removal (%)	
				Experimental	Predicted	Experimental	Predicted
1	0	0	0	98.4	98.40	90.8	90.80
2	1	0	1	98.6	96.34	88.2	81.74
3	-1	1	0	96.9	92.16	51.2	51.16
4	-1	-1	0	53.8	48.74	0.2	-7.16
5	-1	0	1	94.4	101.94	63.5	64.89
6	0	-1	-1	18.1	20.90	2	3.35
7	0	0	0	98.4	98.40	90.8	90.80
8	0	1	-1	98.4	100.88	88	81.77
9	1	0	-1	94.2	86.66	88.5	87.11
10	0	1	1	93.8	91.00	88	86.65
11	0	0	0	98.4	98.40	90.8	90.80
12	1	-1	0	13.8	18.54	7	7.04
13	0	0	0	98.4	98.40	90.8	90.80
14	-1	0	-1	97.6	99.86	36.1	42.56
15	0	-1	1	45	42.52	9	15.42
16	0	0	0	98.4	98.40	90.8	90.80
17	1	1	0	98.5	103.56	90.1	97.91

Table 4-2 Regression coefficients and model performance indicators during treatment of Methyl orange dye with artificial solar Fenton oxidation

Source	Color removal		TOC reduction	
	F	P>F	F	P>F
Model	43.04	<0.0001	56.37	<0.0001
A	4.99	0.0606	44.63	0.0003
B	232.91	<0.0001	265.11	<0.0001
C	1.95	0.2054	3.40	0.1077
AB	12.21	0.0101	6.10	0.0429
AC	0.41	0.5435	4.54	0.0706
BC	7.00	0.0331	0.31	0.5969
A ²	2.247E-0.03	0.9635	24.57	0.0016
B ²	125.66	<0.0001	143.76	<0.0001
C ²	0.51	0.5000	3.62	0.0989
SD	5.95		6.50	
C.V. (%)	7.25		10.00	
R ²	0.9822		0.9864	
Adjusted R ²	0.9594		0.9689	
Predicted R ²	0.7160		0.7822	
Adeq.Precision	18.627		21.171	

Thus, statistical analysis showed that not all variables had a significant effect. It was further observed that the corresponding p-values of the Fisher test for color and TOC removal efficiencies were <0.0001 which indicated that the models were significant [121].

4.1.2 Assessment of the model adequacy for responses during mineralization of dye aqueous solution

Moreover, the difference between observed and predicted responses usually used to evaluate the adequacy of the models. In addition, residuals should have normal distribution [137]. Moreover,

the consistency of the prediction of the model can be evaluated by normal probability plot [122]. In this context, if this plots are scattered under usual condition along with keeping linearity with some reasonable irregularities of points, this indicates appropriate fitting of the model [138]. In addition, whether the model is properly fitted or not can be determined based on the pattern in which the points distributed above or under the line in this plot. Accordingly, if these points in the plot keeping their linearity and distributed along 45° with the straight line, then the model can be considered as properly fitted [139]. Accordingly, in this research assessment was made for both responses using normalized plot of residuals. Therefore, Figure 4-2 demonstrates about the adequacy of the model to predict mineralization of methyl orange dye aqueous solution with solar photo Fenton oxidation for both responses.

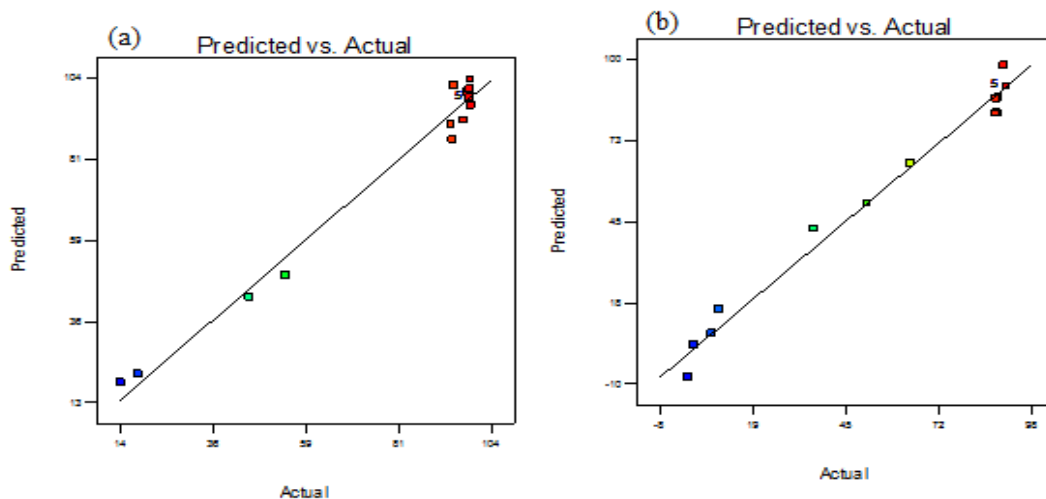


Figure 4-1 The variation between observed and predicted values for a. Color removal, b. TOC removal

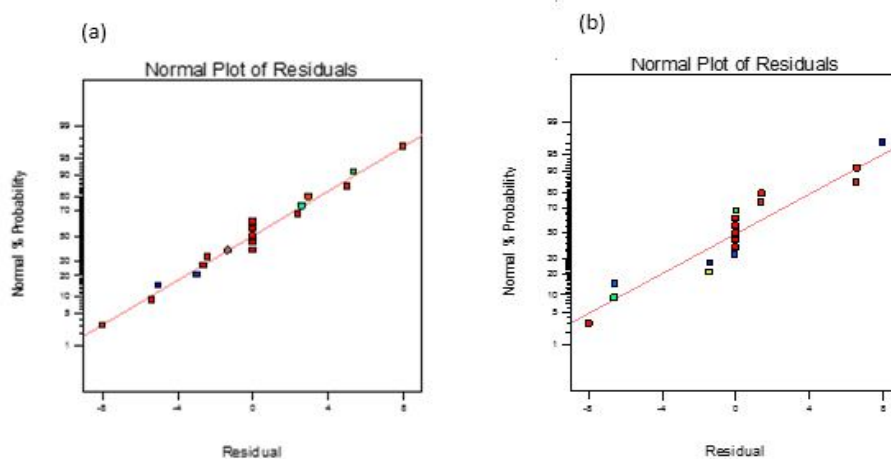


Figure 4-2 Normal probability plot of residual of linear model for **a** color removal , **b** TOC removal

4.1.3 Decolorization of methyl orange dye aqueous solution

Figure 4-3 shows the interaction of Fe^{2+} and dyestuff concentrations during artificial solar Fenton reaction on color removal at a constant H_2O_2 concentration of 1055 mg/L. The figure shows that, for a constant H_2O_2 concentration of 1055 mg/L, color removal was uniformly increase until Fe^{2+} concentrations increases to a maximum of 69 mg/L. However, the use of additional amount of Fe^{2+} above 69mg/L did not result in increasing the color removal efficiency. Furthermore, the optimal amount Fe^{2+} concentration requirement for a dye stuff below 99 mg/L was 55 mg/L while the requirement of Fe^{2+} dose for a dye stuff concentration greater than 99mg/L was 69 mg/L. Furthermore, at a constant H_2O_2 concentration of 1055 mg/L and dye dose of 135mg/L with various levels of Fe^{2+} doses (0 mg/L,69mg/Land 110 mg/L), color removal was found to be 34%, 99% and 98.5% respectively.

Therefore, this result showed that the concentrations of Fe^{2+} beyond 69 mg/L did not improve the removal of color. In this context, previous researcher also addressed similar trend of result about the requirement of proper amount of Fe^{2+} [118]. In addition, adverse effect in the use of excess

amount of Fe^{2+} were reported by [140]. Furthermore, in the absence of iron while using only artificial solar Fenton and H_2O_2 reagent the maximum color removal obtained was very low (34%). Hence, this result indicated the necessity of optimum amount of Fe^{2+} in the removal of color during artificial solar Fenton reaction.

Figure 4-4 shows the interaction of H_2O_2 and dyestuff concentrations during artificial solar Fenton reaction on color removal at a constant Fe^{2+} concentration of 60mg/L. Accordingly, in general, it was observed that percent color removal increased with the increase of H_2O_2 dose for all dye stuff ranges investigated. However, for dyestuff concentrations less than 65 mg /L, the addition of H_2O_2 concentrations above 1055 mg/L did not significantly increase efficiency of color removal. A possible reason for such trend could be due to the consumption of the hydroxyl radical by H_2O_2 . In this regard, similar trend of results in the requirement of proper amount of H_2O_2 were reported elsewhere [141, 142]. Other researchers also reported that color removal of organic compounds increased up to the addition of fixed amount of H_2O_2 and then decreased with the addition of further amount of H_2O_2 [140, 143]. Moreover, undesirable color removal effects were also observed when concentrations of H_2O_2 increased [144]. Furthermore, the possible reason for such phenomena was also addressed by previous researchers. The decrease in color removal when the concentrations of H_2O_2 increased is due to the scavenging of $\text{HO}\cdot$ by H_2O_2 and consequent formation of the less reactive radical $\text{HO}_2\cdot$ [145].

Furthermore, the effect of dye dose for all levels of initial dye used on percent color removal are indicated in Figure 4-3 and Figure 4-4. In this context, as the dose of dye increased, decolorization was decreased. Accordingly, in this research it was obtained that for a fixed H_2O_2 dose of 600mg/L and dye dose of 15mg/L, percent color removal was nearly 96% while for the highest dye dose level (255mg/L), the percent color removal efficiency was 77%. Moreover, for the lowest level

of dyestuff concentrations (15mg/L) , the requirement of optimal amount of Fe^{2+} / H_2O_2 /dyestuff ratio for complete removal of color was found to be 54/1794/15 mg/L, respectively. However, for the highest level of dyestuff dose of 255mg/L, complete color removal needs optimal amount of 67, 1862, 255 mg/L for Fe^{2+} , H_2O_2 , dyestuff concentrations used, respectively. Therefore, this result revealed that complete color removal at the highest level of dye stuff dose require greater amount of H_2O_2 and Fe^{2+} doses than dye dose of the least level.

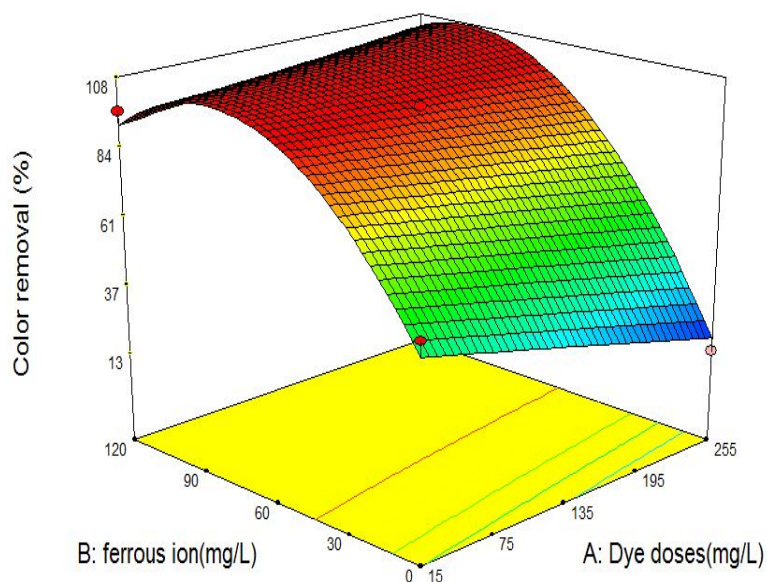


Figure 4-3 3D plot for the effect of ferrous ion and dye dose on color removal during artificial solar Fenton oxidation.

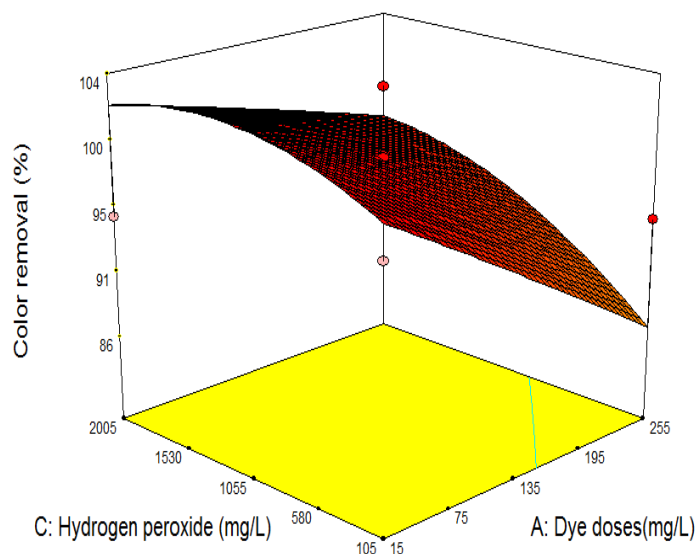


Figure 4-4 3D plots for the effect of hydrogen peroxide and dye dose on color removal during artificial solar Fenton oxidation.

4.1.4 Total organic carbon (TOC) removal of dye stuff

Based on responses measurement in the laboratory, the formation of colorless substances does not necessarily show the entire removal of TOC. Most of the time, colorless chemical species are usually formed faster than the degradation of dyestuffs. Furthermore, the colorless compounds formed before the completion of reaction are usually more toxic than the parent compounds. Therefore, it is important to recognize the extent of TOC removal during decolorization of dyes by the Fenton reaction. Accordingly, samples were analyzed for color and TOC removal at different intervals of time using experimental design center points (0,0,0). As seen in Figure 4-5, the highest color removal required 6 minutes while maximum mineralization needed 16 minutes. Moreover, the comparison about rate of color removal and mineralization at various intervals of time was summarized in Table 4-3. Similarly, achievement of color and TOC removal in 5 and 15 minutes, respectively, has been reported in a previous [123].

Table 4-3 Comparison between rate of mineralization and color removal.

Samples name	Time in minutes	Decolorization (%)	TOC removal (%)
C1	1	62	19.1
C2	2	65.5	37.4
C3	3	93.1	48.2
C6	6	98.2	67.4
C9	9	98.2	73.8
C12	12	98.2	82.4
C15	16	98.2	95.2

Figure 4-6 shows the interaction Fe^{2+} and dyestuff doses during Fenton reaction on TOC removal at a constant H_2O_2 concentrations of 1055 mg/L. Accordingly, TOC removal was mainly affected by the concentration of ferrous ion as indicated by the coefficient of this process factor in equation 4.2. Moreover, it was observed that for a constant dye concentration of 135mg/L and H_2O_2 doses of 1055 mg/L, percent TOC removal were 15, 90 and 91% respectively for Fe^{2+} doses of 0, 60 and 120mg/L respectively. Thus, this result shows that percent mineralization increased with the addition of Fe^{2+} doses up to 60 mg/L and then decreased with further increases in Fe^{2+} doses above 60 mg/L. Hence, the possible reason for such phenomena was due to excess $\text{OH}\cdot$ which was formed during the reaction consumed by Fe^{2+} during the reaction. Furthermore, previous study also revealed that when the concentrations of iron increases, the phenomena of self-scavenging effect takes place faster than the formation of hydroxyl radical leading to the decrease in TOC removal of the wastewater [146].

The pattern of TOC removal with various H_2O_2 doses consumed for different ranges of dyestuff concentrations (15–255 mg/L) at a constant Fe^{2+} concentration of 60 mg/L is illustrated in Figure 4-7. The figure shows that there was a uniform increase in TOC removal for a dye concentration lower than 105 mg/L by using minimum amount of H_2O_2 . However, for dye concentrations above 105mg/L, addition of extra amount of H_2O_2 beyond 1055 mg/L did not produce better removal of

TOC. Furthermore, previous research also showed that the degradation of organic compounds increased with the increase in the concentration of H_2O_2 up to definite amount then gradually decreased with the addition of extra amount of H_2O_2 [147]. Furthermore, there was a uniform increase in percent TOC removal until the concentration of dye was 205 mg/L. However, the decrease of mineralization was observed when the concentration of dye exceeded 205 mg/L, The decrease in percent TOC removal for a dye dose greater than 205 mg/L was probably due to lack of proportional amount of H_2O_2 and Fe^{2+} doses in order to react with that of the excess dye stuff that remained in the reaction.

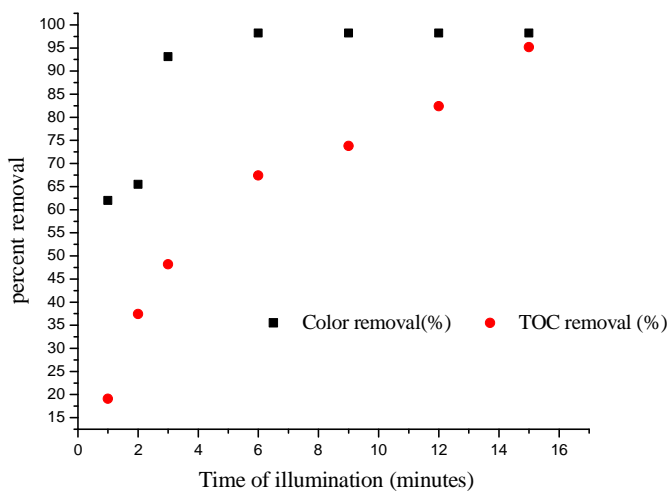


Figure 4-5 Difference between rate of decolorization and TOC removal.

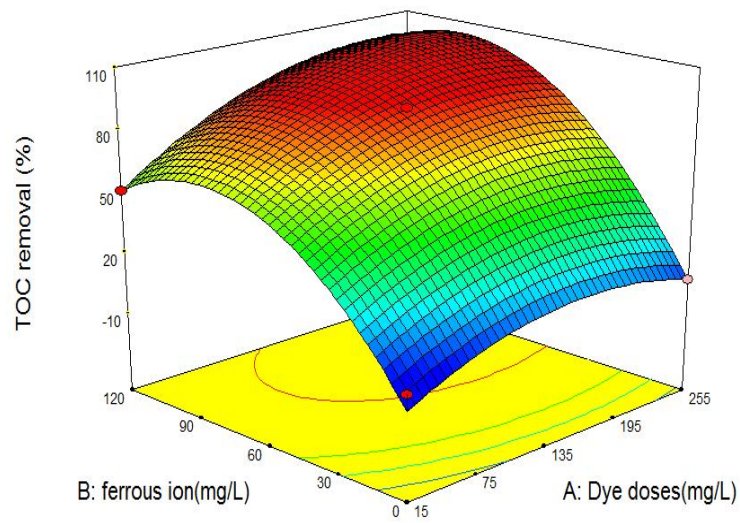


Figure 4-6 3D plot for the effect of ferrous ion and dye dose on TOC removal

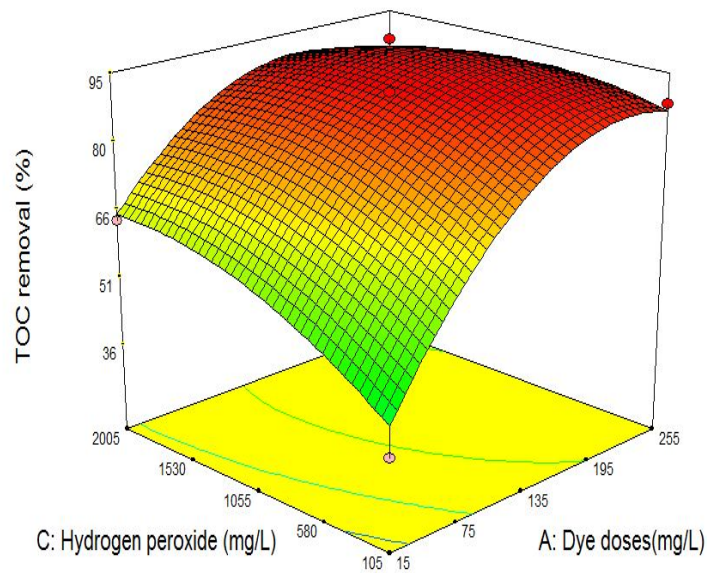


Figure 4-7 The effect of Hydrogen peroxide dose and dye dose on TOC removal

The optimal H_2O_2 and Fe^{2+} doses resulting in the highest removal of TOC and color by the artificial solar Fenton depends on the amount of dye used. In this research, it was observed that, for the lowest level of dyestuff dose of 15 mg/L, 23 percent TOC removal was achieved at an optimal process factor $\text{Fe}^{2+}/\text{H}_2\text{O}_2/\text{dyestuff}$ ratio of 33.6/154.2/15 mgL^{-1} respectively. On the contrary, at

the highest level of dye stuff concentrations (255 mg/L), 80% of TOC removal was obtained at optimal process factor $\text{Fe}^{2+}/\text{H}_2\text{O}_2/\text{dyestuff}$ ratio of 51.9/1798.1/255 (mg/L). Furthermore, the maximum efficiency of TOC removal obtained using both the highest and the least level of dye stuff concentrations shows that the requirement of H_2O_2 and Fe^{2+} increased proportionally with the increase of dye stuff dose used.

4.1.5 Perturbation plots during mineralization of methyl orange dye

In Figure 4-8, A, B and C, respectively represent dye dose, Ferrous ion, and hydrogen peroxide dose. It can be clearly seen from the figure that factor B is having the steepest slope as compared to factor A and C having relatively flat slopes for both color and TOC removal. A steeper slope shows that the response is more sensitive to that factor as compared to the other two factors taken in consideration. In plain terms, mineralization of dye and color removal are more influenced by ferrous ion dose than hydrogen peroxide and dye doses.

4.1.6 Optimization of Artificial Soar Fenton treated simulated dye aqueous solution for color and TOC removal

Based on equations 4.1 and 4.2, the color and TOC removal efficiencies were maximized by changing the process variables. In order to minimize operating costs, Fe^{2+} was varied between 0-120 mg/L and H_2O_2 was varied between 105-2005 mg/L while dye dose was chosen assuming a maximum dye concentration of 255 mg/L. The optimum values so obtained based on the selected criteria were: Dye dose: 255 mg/L, H_2O_2 :1386 mg/L and Fe^{2+} :72 mg/L with color and TOC removal of 100% and 96% respectively. The optimum result was checked by conducting an extra experiment at the optimal conditions. Thus, it was obtained that the values measured were in close relationship with the model values, i.e., color removal was 99.8% and TOC removal was 95.5% with a deviation from their mean with a value of 0.12% and 0.06%, respectively.

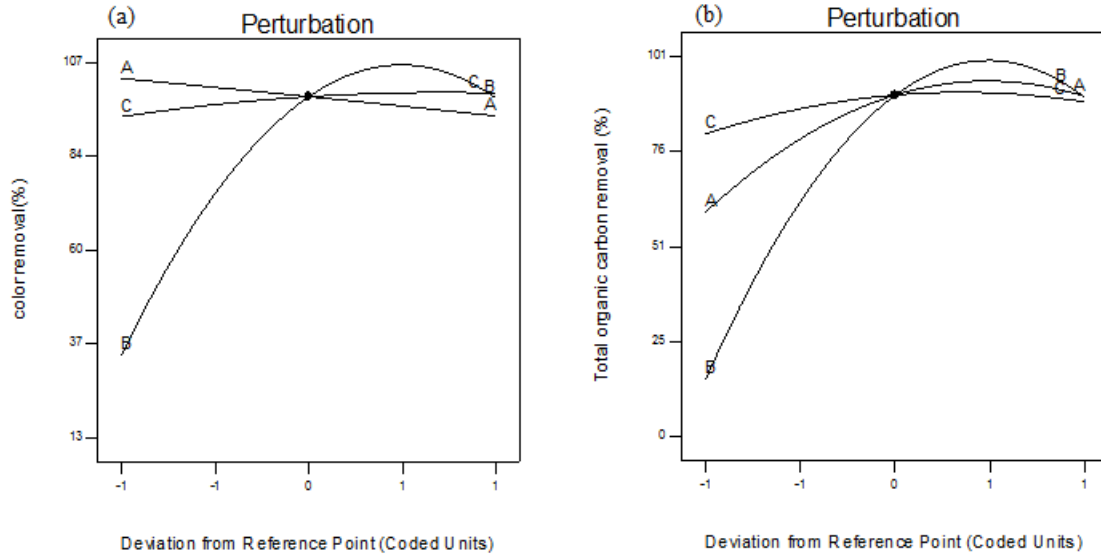


Figure 4-8 Perturbation plot for a, color removal, b TOC removal

4.2 Degradation of Basic blue 41 dye aqueous solution with conventional Fenton oxidation

4.2.1 Regression model and statistical testing in the degradation of a Basic Blue 41 dyes

The experimental and the predicted values for both percent color and COD removal are indicated in Table 4-4. In addition, optimal values for decolorization and COD removal are determined by a second- order polynomial as expressed by equations 4.3 and 4.4:

$$R_1 = 96.88 - 4.70A - 0.56B + 33.89C + 3.07AB + 13.32AC - 2.35BC - 2.07A^2 - 4.44B^2 - 32.83C^2 \quad (4.3)$$

$$R_2 = 88.43 + 11.32A - 3.05B + 29.14C + 6.77AB + 16.61AC - 19.25A^2 - 12.96B^2 - 34.37C^2 \quad (4.4)$$

Where R_1 and R_2 stand for color and COD removal respectively. In Equations 4.3 and 4.4, positive effect of a factor implies the response is improved when the factor level increases and a negative effect of the factor means that the response is not improved when the factor level increases.

Table 4-4 Box–Behnken design matrix along with experimental and predicted values during degradation of Basic Blue 41 dyes with conventional Fenton oxidation.

Runs	A(mg/L)	B(mg/L)	C(mg/L)	R ₁ :Color removal (%)		R ₂ : COD removal(%)	
	Dye doses	H ₂ O ₂	Fe ²⁺	Experimental	Predicted	Experimental	Predicted
1	-1	-1	0	96.9	98.71	56.2	54.72
2	0	0	0	96.8	96.88	84.7	88.43
3	0	-1	1	97.3	96.41	72.8	73.51
4	0	1	-1	26.6	27.51	9.8	9.13
5	0	-1	-1	18.1	23.93	14.0	14.78
6	-1	0	1	88.1	87.25	35.2	36.02
7	-1	1	0	84.8	91.44	35.1	35.09
8	0	0	0	97.2	96.88	91.7	68.43
9	0	0	0	96.8	96.88	89.3	88.43
10	1	0	-1	9.2	10.07	1.1	0.37
11	-1	0	-1	53.6	49.10	10.3	10.96
12	0	1	1	96.4	90.59	67.8	66.96
13	0	0	0	96.8	96.88	87.6	88.43
14	1	0	1	96.9	104.79	92.5	91.88
15	1	1	0	90.0	88.19	69.7	71.26
16	0	0	0	96.8	96.88	88.8	88.43
17	1	-1	0	89.8	83.16	63.8	63.82

Therefore, in the case of color removal, it can be seen that C, AC and C² were significant terms, while for COD removal, it was obtained that A, B, C, AB, AC, A², B² and C² were proved to be significant. Furthermore, Table 4-5 clearly shows that the corresponding F values for color and COD removal efficiencies were 41.57 and 371.39 along with very low probability value (p value <0.0001). Therefore, the F values for both color and COD removal indicate that both models were reasonably significant and adequate.

Table 4-5 Regression coefficients and model performance indicators for RSM modeling of color removal and COD reduction when treating Basic-Blue 41 dyes with Fenton oxidation.

Source	Color removal		COD reduction	
	F	P>F	F	P>F
Model	41.57	<0.0001	371.39	<0.0001
A	4.44	0.0732	200.28	<0.0001
B	0.064	0.8083	14.51	0.0066
C	230058	<0.0001	1327.64	<0.0001
AB	0.95	0.3624	35.81	0.0006
AC	17.80	0.0039	215.76	<0.0001
BC	0.55	0.4808	0.040	0.8480
A ²	0.45	0.5231	304.82	<0.0001
B ²	2.08	0.1926	138.19	<0.0001
C ²	113.90	<0.0001	972.35	<0.0001
St.dev.	6.31		2.26	
C.V.(%)	8.06		3.96	
R ²	0.9816		0.9979	
Adjusted R ²	0.9580		0.9952	
Predicted R ²	0.7062		0.9893	
Adeq.Precision	19.501		52.745	

Besides, R² values for color and COD removal were 0.9816 and 0.9979 respectively which indicated that the predicted values entirely fit with the experimental ones. Furthermore, the values of predicted R² for color and COD and removal were 0.7062 and 0.9893 respectively, while their corresponding values of adjusted R² were 0.9580 and 0.9952. In addition, the difference between predicted and adjusted R² was less for both models. Therefore, both values of predicted and adjusted R² showed the models were adequate. Moreover, Figure 4-9 suggests that the predicted values match well with the experimental values of COD and color removal and confirmed the result obtained from both predicted and adjusted R². Furthermore, the values of adequate precision for Color removal and for COD removal were 19.5 and 52.7 respectively. Therefore, this result indicated that the model can be used to navigate the design space. Moreover, low values of C.V, i.e., 8.06 and 3.96 for color and COD removal respectively indicated that the experiments were accurate and reliable.

4.2.2 Evaluation of the model adequacy for responses during degradation of Basic Blue 41 dye aqueous solution

The difference between observed and predicted responses usually used to evaluate the adequacy of the models. In addition, residuals should have normal distribution [137]. Furthermore, the consistency of the prediction of the model can be evaluated by normal probability plot [122]. In this context, if this plots are scattered under usual condition along with keeping linearity with some reasonable irregularities of points, this indicates appropriate fitting of the model [138]. Besides, whether the model is properly fitted or not can be determined based on the pattern in which the points distributed above or under the line in this plot. Accordingly, if these points in the plot keeping their linearity and distributed along 45° with the straight line, then the model can be considered as properly fitted [139]. Consequently, in this study an evaluation was made for both responses using normalized plot of residuals. Hence, Figure 4-10 illustrates about the adequacy of the model to predict degradation of Basic Blue dye aqueous solution with Fenton oxidation for both responses.

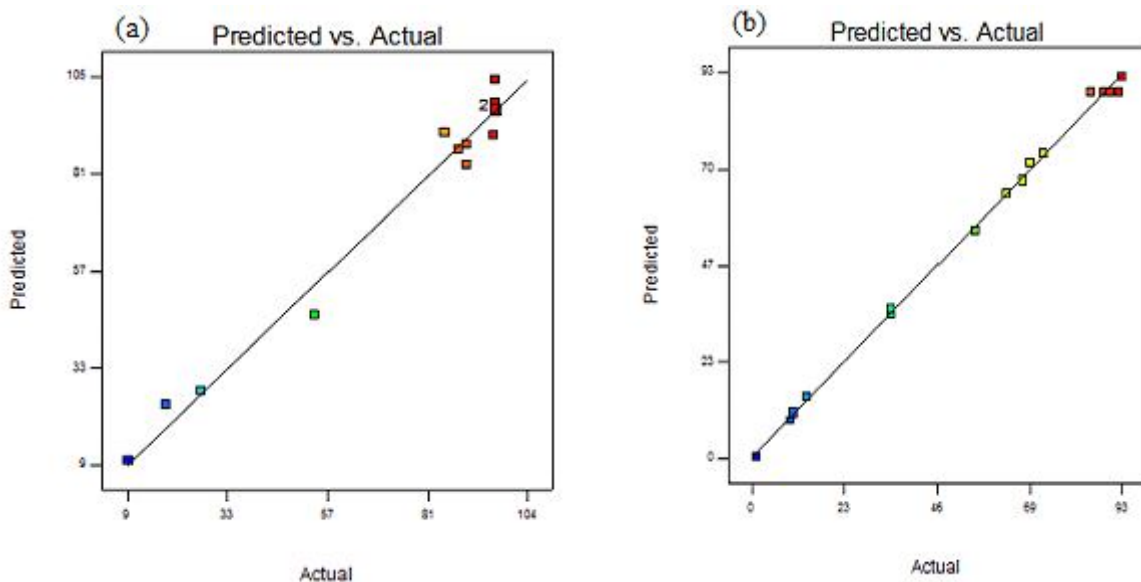


Figure 4-9 Predicted versus actual plot for **a** Color removal , **b** COD removal during treatment of Basic Blue 41 dyes with conventional Fenton oxidation

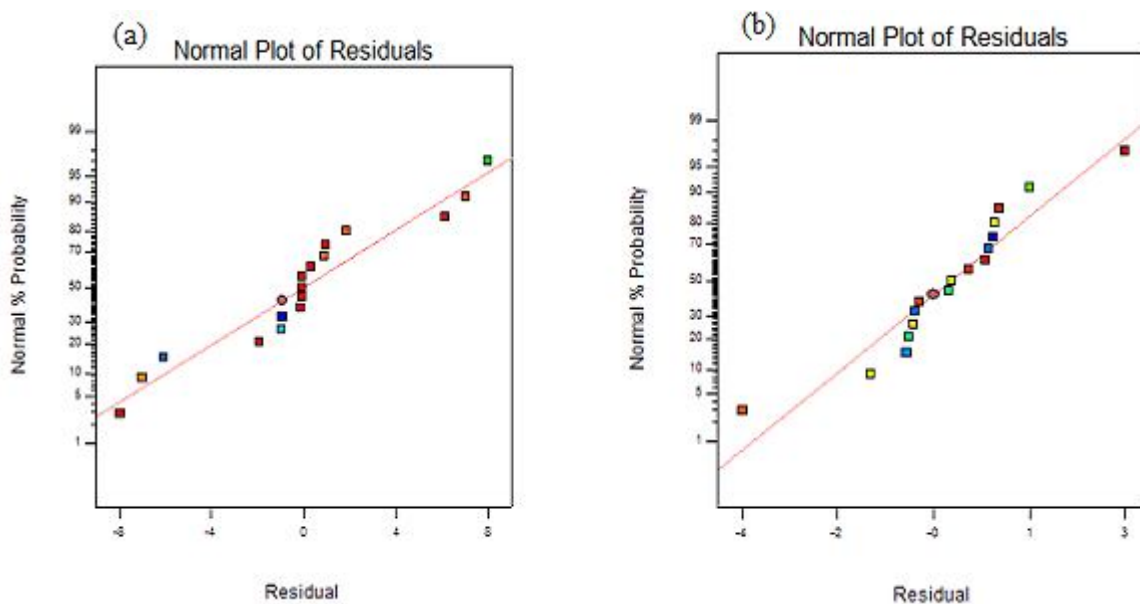


Figure 4-10 Normal probability plot of residual of linear model for **a** color removal , **b** COD removal during treatment of Basic Blue 41 dyes with conventional Fenton oxidation

4.2.3 Color removal in for Basic Blue 41 dyes

Figure 4-11 shows the interaction between H_2O_2 and dyestuff concentrations during Fenton reaction on percent color removal with a constant Fe^{2+} concentration of 60mg/L. Accordingly, for dyestuff concentrations less than 165 mg /L , the addition of H_2O_2 concentrations above 1530 mg/L was not able to increase the efficiency of color removal. In addition, the possible reason for such trend could be due to the consumption of the hydroxyl radical formed during the process by H_2O_2 . Such phenomena were also reported by previous researchers. The color removal of organic compounds increased up to the addition of fixed amount of H_2O_2 and then decreased with further addition of H_2O_2 [148, 149]. Undesirable color removal effects were also observed when concentrations of H_2O_2 increased [144, 150]. A possible reason for such phenomena was also addressed by previous researchers [144, 150]. . In addition, the decrease in color removal with further increase in H_2O_2 concentration was due to the scavenging effect of $HO\cdot$ by H_2O_2 and consequent formation of the less reactive radical $HO_2\cdot$.

Furthermore, the ratio of optimal doses of process factors for complete color removal with the least level of dye dose of (15mg/L) was found to be 105/62/15 mg/L for (H_2O_2 / Fe^{2+} /dyestuff) respectively. On the other hand, the ratio of optimal doses of process factors for complete color removal with the highest level of dye dose of (255mg/L) was found to be 408/82/255 mg/L for (H_2O_2 / Fe^{2+} /dyestuff) respectively. Therefore, this result revealed that complete color removal at the highest level of dye stuff dose require greater amount of H_2O_2 and Fe^{2+} doses than dye dose of the least level.

Figure 4-12 shows the interaction between Fe^{2+} and dyestuff concentrations during Fenton reaction for percent color removal efficiencies with a constant H_2O_2 concentration of 1055 mg/L and using various ranges of Fe^{2+} concentrations. Consequently, color removal was uniformly increased during Fenton reaction using a constant concentration H_2O_2 1055 mg/ and with the variation of Fe^{2+} concentrations between 70 and 90mg/L. However, further addition of Fe^{2+} above 90mg/L did not result in the increase of percent color removal. Therefore, the optimal amount Fe^{2+} concentration which was required for the highest color removal for a dye stuff dose below 105 mg/L was found to be 64 mg. On the other hand, the optimal dose of Fe^{2+} concentration which was required for the highest color removal for a dye stuff greater than 105 mg/L was found to be 70 mg/L. Hence, this trend of this result showed that the concentrations of Fe^{2+} beyond 70 mg/L was not able to improve the efficiency of color removal.

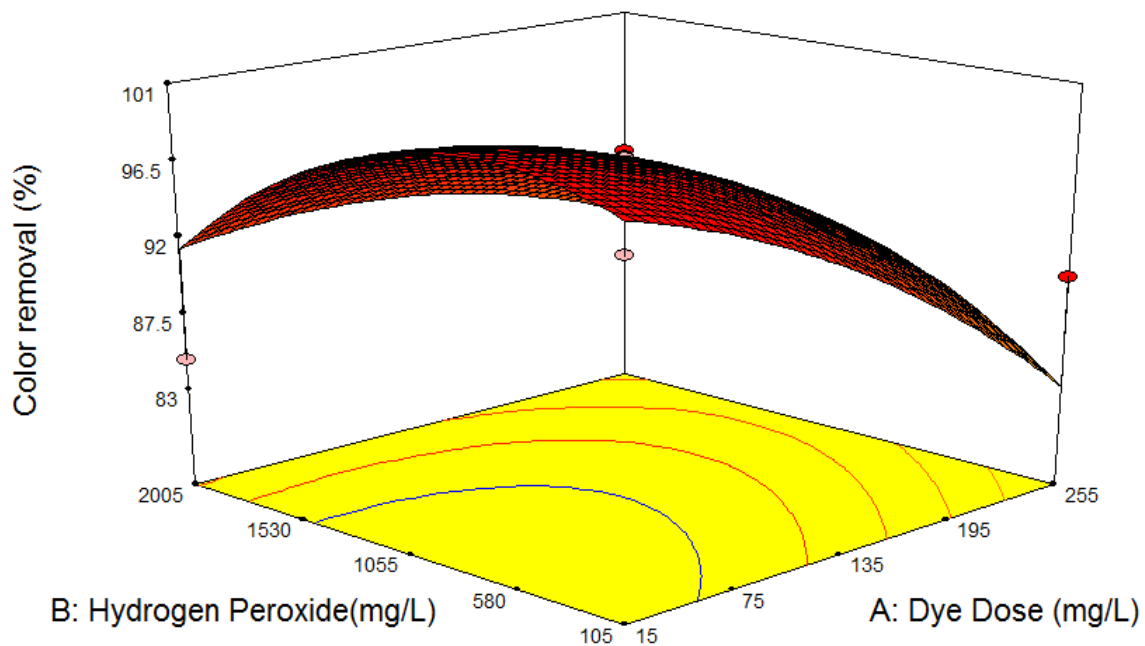


Figure 4-11 3D plot for the effect of hydrogen peroxide and dye dose on color removal during treatment of Basic Blue 41 dyes with conventional Fenton oxidation

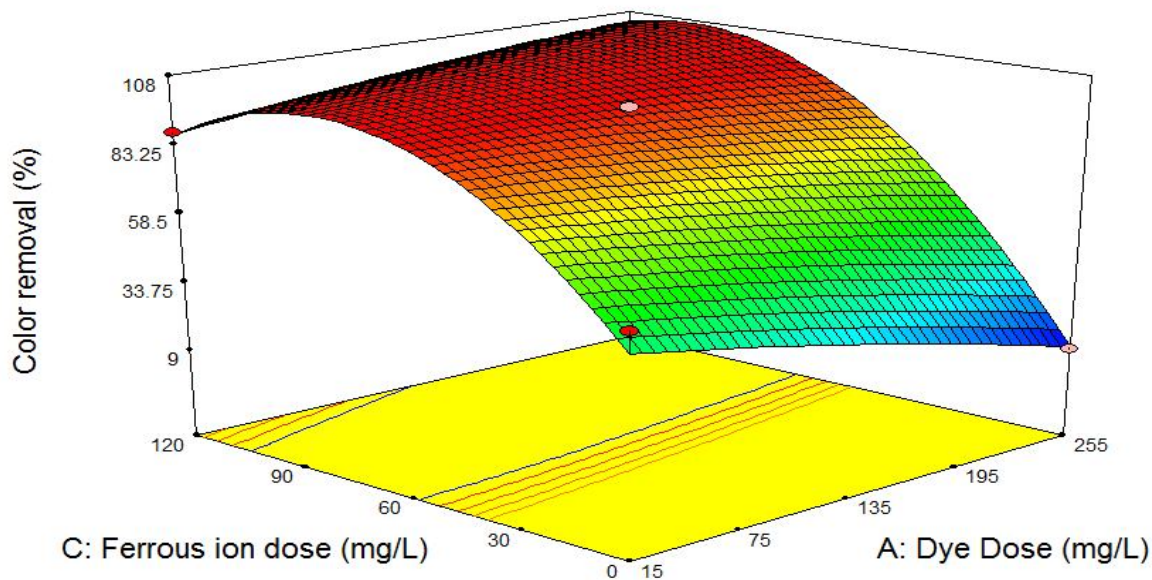


Figure 4-12 The effect of iron and dye dose on color removal during treatment of Basic Blue 41 dyes with conventional Fenton oxidation

4.2.4 Chemical oxygen demand (COD) removal of Basic Blue 41 dye stuff

The pattern of COD removal with various H_2O_2 doses at different dyestuff concentrations (15–255 mg/L) using a constant Fe^{2+} concentration of 60 mg/L is illustrated in Figure 4-13. The figure shows that there was an increase in COD removal using a maximum of H_2O_2 concentrations 1055 mg/L. However, further addition of H_2O_2 concentration above 1055 mg/L was not able to improve percent COD removal. Other research works have also shown similar pattern of results. Accordingly, degradation of organic compounds increase with the increase of concentrations of H_2O_2 up to definite amount of H_2O_2 and then gradually decreased with the addition of extra amount of H_2O_2 [147].

During responses measurement, various intermediate compounds were formed at various stages of the Fenton reaction. In addition, the formation of colorless substances did not necessarily show the entire removal of COD. Accordingly, colorless chemical species are usually formed faster than the degradation of dyestuffs. Consequently, the colorless compounds which were formed before the completion of reaction might be more toxic than the parent compounds [123]. Therefore, it is important to recognize the extent of COD removal during decolorization of dyes by the Fenton reaction.

The decrease in COD removal for dyestuff concentrations above 135 mg/L can be caused by lack of required amount of H_2O_2 and Fe^{2+} to effectively degrade the highest level of this dye stuff. In this context, the ratio of process factors for the purpose of 91% COD removal at a dye stuff dose of 135 mg/L was obtained to be 1055/66/135mg/L for $\text{H}_2\text{O}_2/\text{Fe}^{2+}/\text{dye}$ stuff, respectively. Previous research also reported that in the case of treatment with the highest level dye stuff concentration for complete COD removal, high doses of H_2O_2 and Fe^{2+} should be used [145]. From the above

it is possible to conclude that the initial dyestuff concentration was one of the key parameters affecting the COD removal by Fenton treatment.

Figure 4-14 shows the interaction between Fe^{2+} and dyestuff doses during Fenton reaction for percent COD removal with a constant H_2O_2 concentrations of 1055 mg/L. Accordingly, the degradation of dye stuff steadily increased until the concentrations of Fe^{2+} reached to 90 mg/L. However, further increases of Fe^{2+} greater 90 mg/L was not able to improve the percent COD removal. Thus, the reason for the decrease in percent COD removal with further increase of Fe^{2+} was due to the excess $\text{OH}\cdot$ formed during the reaction was gradually consumed by Fe^{2+} instead of the COD removal of dyes. Moreover, previous study also reported similar phenomenon [146]. Accordingly, Arslan-alaton et al. 2009 [146] reported that, when the concentrations of iron increases, the phenomena of self-scavenging effect takes place faster than the formation of hydroxyl radical leading to the decrease in COD removal rate of pollutants.

The highest COD removal (60%) using the lowest level dyestuff dose of 15mg/L was achieved by using optimal factor ratio of 692/71/15 mg/L for the process factors($\text{H}_2\text{O}_2/ \text{Fe}^{2+}/\text{dyestuff}$) respectively. On the other hand, the highest COD removal (91%) with the highest level dye dose of 255 mg/L was obtained using the optimal process factor ratio of 1151/75/255 mg/L for process factors ($\text{H}_2\text{O}_2/ \text{Fe}^{2+}/ \text{dyestuff}$) respectively. Therefore, the maximum efficiency of COD removal using both the highest and least level of dye stuff concentrations showed that the requirement of H_2O_2 and Fe^{2+} dose increased proportionally with the increase in the dye stuff dose.

Furthermore, a comparison regarding the requirement in the doses of Fenton reagents for both color and COD removal with the highest level of dye dose was analyzed. Accordingly, for the highest level of dyestuff concentration 255 mg/L, only 130 mg/L H_2O_2 dose was required for

complete decolorization. Likewise, for the highest level dyestuff concentration of 255 mg/L, complete COD removal required 1202 mg/L H₂O₂ dose. On the contrary, for the highest level of a dyestuff concentration 255 mg/L, the requirement of Fe²⁺ was 90 mg/L for both color and COD removal. Therefore, this result indicated that for the highest level of a dyestuff concentration of 255 mg/L, the removal of COD required considerable amount of H₂O₂ than the removal of color. However, the requirement of Fe²⁺ doses for the highest level of a dyestuff concentration was found to be the same for both color and COD removal.

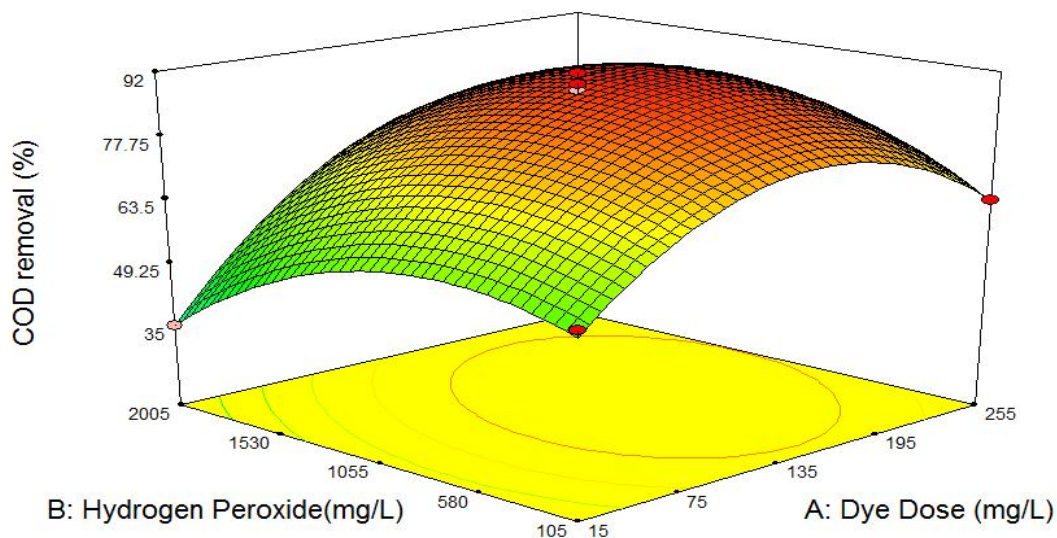


Figure 4-13 3D plot for the effect of Hydrogen peroxide and dye dose on COD removal during treatment of Basic Blue 41 dyes with conventional Fenton oxidation

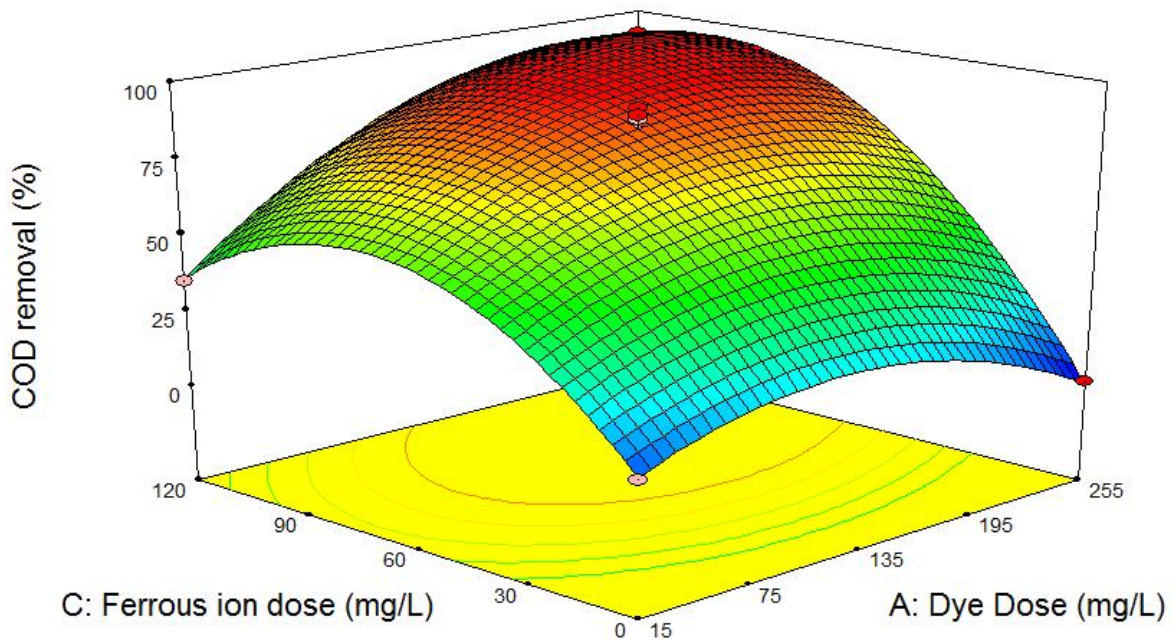


Figure 4-14 3D plot for the effect of ferrous ion and dye dose on COD removal during treatment of Basic Blue 41 dyes with conventional Fenton oxidation

4.2.5 Perturbation plots during degradation of Basic Blue 41 dye aqueous solution

Figure 4-15 is demonstrating the comparison among process factors in the extent of influencing the responses. Accordingly, A represents dye dose, B represents hydrogen peroxide dose and C represents Ferrous ion dose. Furthermore, it can be clearly seen from the graph that factor C was shown the steepest slope as compared to factor A and B which were shown relatively flat slopes for both color and COD removal.

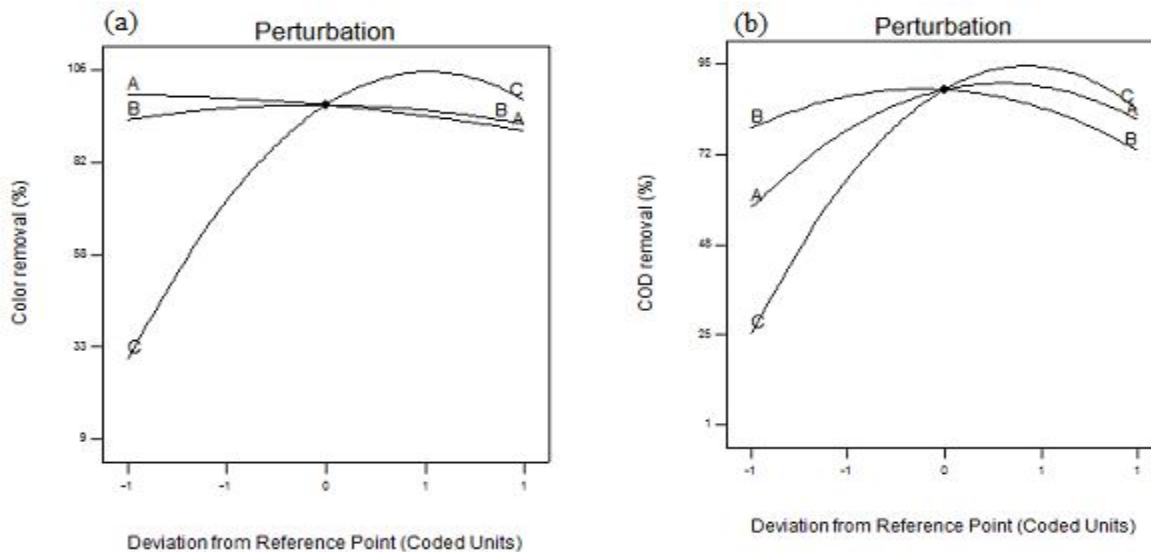


Figure 4-15 Perturbation plot for **a** color removal , **b** COD removal during treatment of Basic Blue 41 dyes with conventional Fenton oxidation

In this sense, factor A which has a steeper slope shows that the responses were more sensitive to this factor as compared to the other two factors (B and C). Hence, it can be said that COD and color removal efficiencies were highly influenced by Ferrous ion dose as compared to hydrogen peroxide dose and dye dose.

4.2.6 Optimization of Fenton treated Basic blue 41 dye solution for color and COD removal

Design-Expert® version 7.0.0 (Stat-Ease, Inc.) software was used for optimization. The purpose of optimization was to maximize both color and COD removal efficiencies. In this regard, reasonable process factors criteria were selected. Accordingly, in order to minimize operating costs of Fenton reagents, Fe^{2+} was varied between 0-120mg/L and H_2O_2 was also varied between 105-2005mg/L. In addition, dye dose was chosen by assuming a maximum dye concentration of 255 mg/l. Finally, optimum working conditions and percent removal efficiencies' were obtained. Therefore, the optimum values obtained base on the selected criteria were: Dye dose: 255 mg/L, H_2O_2 :1195 mg/L and Fe^{2+} :90 mg/L with color and COD removal of 100% and 95% respectively.

The optimum result was also checked by conducting an extra experiment at the optimal conditions. The values measured were in close relationship with the model values, i.e., color removal was 99.7% and COD removal was 94.5% with a deviation from their mean with a value of 0.15% and 0.08% respectively.

4.3 Degradation of real textile wastewater with conventional Fenton oxidation

4.3.1 RSM modeling for Fenton oxidation stage in the degradation of real textile wastewater

The experimental outcomes obtained from the BBD are summarized in Table 4-6. Besides, the model values obtained using the RSM model are summarized in Table 4-7. Optimal values for decolorization and COD removal in the experimental runs can be determined by a second-order polynomial using equations 4.5 and 4.6.

$$R_1 = 92.06 - 6.89A + 2.78B + 1.29C - 3.43AB - 29.83A^2 - 6.41B^2 - 7.18C^2 \quad (4.5)$$

$$R_2 = 85.04 - 3.82A + 2.49B + 2.06C - 24.93A^2 - 8.86B^2 - 10.56C^2 \quad (4.6)$$

Where R_1 and R_2 represents percent color and COD removal respectively. Table 4-7 indicated the regression coefficients and model representations for the RSM approach.

Table 4-6 Box–Behnken Design matrix along with experimental and predicted values during real wastewater treatment with conventional Fenton oxidation.

Runs	A(mg/L) Fe ²⁺	B(mg/L) H ₂ O ₂	C pH	R ₁ : Color removal (%)		R ₂ : COD removal (%)	
				Experimental	Predicted	Experimental	Predicted
1	1	-1	0	50.2	49.59	44.4	46.84
2	-1	0	1	63.6	63.17	57.4	58.19
3	0	0	0	93.2	92.06	86.4	85.04
4	0	1	-1	79.5	80.09	62.7	63.97
5	0	-1	1	77.7	77.11	64.4	63.12
6	0	0	0	93.6	92.06	87.4	85.04
7	0	0	0	89.4	92.06	83.1	85.04
8	-1	-1	0	55.5	56.51	50.2	50.69
9	1	0	1	48.3	49.50	46.2	45.04
10	1	0	-1	46.4	46.82	47.2	46.41
11	0	0	0	92.4	92.06	83.9	85.04
12	-1	0	-1	61.9	60.70	47.4	48.56
13	0	-1	-1	74.1	74.29	64.8	63.15
14	0	0	0	91.7	92.06	84.4	85.04
15	0	1	1	82.6	82.41	70.6	72.25
16	1	1	0	49.3	48.29	48.5	48.01
17	-1	1	0	68.3	68.91	61.9	59.46

Table 4-7 Model performance indicators for color removal and COD reduction during treatment of real wastewater with conventional Fenton oxidation

Source	Color removal		COD reduction	
	F	P>F	F	P>F
Model	4874.46	<0.0001	3971.43	<0.0001
A	379.50	<0.0001	117.04	0.002
B	61.61	0.017	49.50	0.0163
C	13.26	<0.0563	34.03	0.045
AB	46.92	0.0036	14.44	0.1464
AC	0.010	0.9517	30.25	0.0500
BC	0.063	0.8796	17.22	0.1176
A ²	3746.65	<0.0001	2617.39	<0.0001
B ²	172.73	<0.0001	330.34	0.0001
C ²	217.06	<0.0001	469.1	<0.0001
SD	1.59		2.23	
C.V. (%)	2.23		3.63	
R ²	0.9964		0.9905	
Adjusted R ²	0.9917		0.9784	
Predicted R ²	0.9742		0.8952	
Adeq.Precision	36.992		22.416	

Furthermore, according to equations 4.5 and 4.6, the relative values of perfection for the responses with factor levels can be determined based on the sign of the effect of the factor. Accordingly, positive effect of a factor indicated the perfection of the response while negative effect showed lack of perfection of the response [136]. The extent of model representation can be described by ranges of values between predicted R² and adjusted R². In this sense, if the values are nearer to each other, it indicates good agreement of the model.

Hence, the values of predicted R^2 for color and COD removal were 0.9742 and 0.8952 respectively and the values of the adjusted R^2 for color and COD were also 0.9917 and 0.9784 respectively. Therefore, these values indicated good agreement of the model. Whenever the values of coefficient of variation (C.V) less than 10%, it indicated high accuracy and reliability of the experiments. Hence, the values of C.V. for both responses were 2.23% and 3.63% for color and COD removal respectively.

4.3.2 Effect of iron doses on color and COD removal for real wastewater treatment with Fenton oxidation

The effect of Fe^{2+} on color removal at a fixed dose of H_2O_2 (4200mg/L) was shown in Figure 4-16 using 3D plot. Based on this plot, the maximum color removal was observed when the doses of Fe^{2+} was in the range of 400-500mg/L. In addition, in this Fe^{2+} dose range, color removal increased from 63% to 85%. However, as the dose of Fe^{2+} increased to 700mg/L, color removal gradually decreased to 56%. The result is also supported by previous researcher that when the doses of iron increased self-scavenging effect takes place faster than the formation of hydroxyl radical and cause for the decrease in color removal efficiency. Furthermore, this phenomena is explained using equation 4.7 [146].



The effect of Fe^{2+} on COD removal at a fixed dose of H_2O_2 (4200mg/L) is shown in Figure 4-17. Based on this plot, as the dose of iron increased from 400-550mg/L, the removal of COD increased from 53% to 79%. On the other hand, when the dose of Fe^{2+} further increased to 587-700mg/L, COD removal decreased from 73% to 63%. Similar results were also reported by Mansoorian et al. [151] about COD removal using lower and higher doses of iron and they obtained that, at higher concentration of iron, decomposition of hydrogen peroxide leads to the

formation of per-hydroxyl radicals (HO₂·), while at lower iron concentration, its reaction with hydrogen peroxide leads to the formation of hydroxyl radicals(OH·), which are more reactive than per-hydroxyl radicals. Wang et al. [152] also reported that when the doses of iron increased by an amount of 0.33mM while the COD removal decreased from 43% to 19%.

4.3.3 Effect of hydrogen peroxide doses on color and COD removal in the Fenton oxidation stage

The effect of H₂O₂ dose on both color and COD removal efficiency at a fixed Fe²⁺ dose of 400mg/L are given in Figure 4-16 and Figure 4-17 respectively. Accordingly, when the dose of H₂O₂ was 7500mg/L, color removal efficiency was increased up to 59%. However, as the dose of H₂O₂ increased further to 8600mg/L, color removal decreased to 56%. Furthermore, when the dose of H₂O₂ dose was in the range of 4200–6400 mg/L, COD removal efficiency increased to 63%. However, as the dose of H₂O₂ increased to 8600mg/L, COD decreased to 58%. This result was also supported by previous researchers and they explained that degradation of organic compounds increased with the increase of H₂O₂ dose up to a certain values until critical limit was reached and such phenomenon was further supported by the following equations (Eqns.4.8,4. 9 and 4. 10) [153].



According to Mansoorian et al. [151] by increasing the doses of H₂O₂ from 2mM-5mM, COD removal efficiency was improved, while further increasing of H₂O₂ to 5mM caused the decrease in COD removal efficiency. Zhang et al. [154] was also observed that, removal of organic materials in the leachate effluent was decreased with the increase in the Fe²⁺ and H₂O₂ doses.

4.3.4 Effect of pH on color and COD removal Efficiency in the Fenton oxidation stage

The effect of pH on both color and COD removal efficiency are illustrated in Figure 4-18 and Figure 4-19 respectively. Accordingly, using a constant Fe^{2+} doses of 400mg/L , the highest removal of COD and color removal was observed when the pH range was in between 2.9 - 3.1. In addition, when the range of pH was between 2.4 and 2.9, color removal efficiency was increased from 62% to 64%. On the other hand, further increasing of pH to 3.5 result in the decrease of color removal to 56%. Similarly, when the range of pH was 2.4 -2.9, COD removal efficiency increased from 47% to 61%. However, a further increasing the pH to 3.4 was caused for the decrease of COD to fifty six percent.

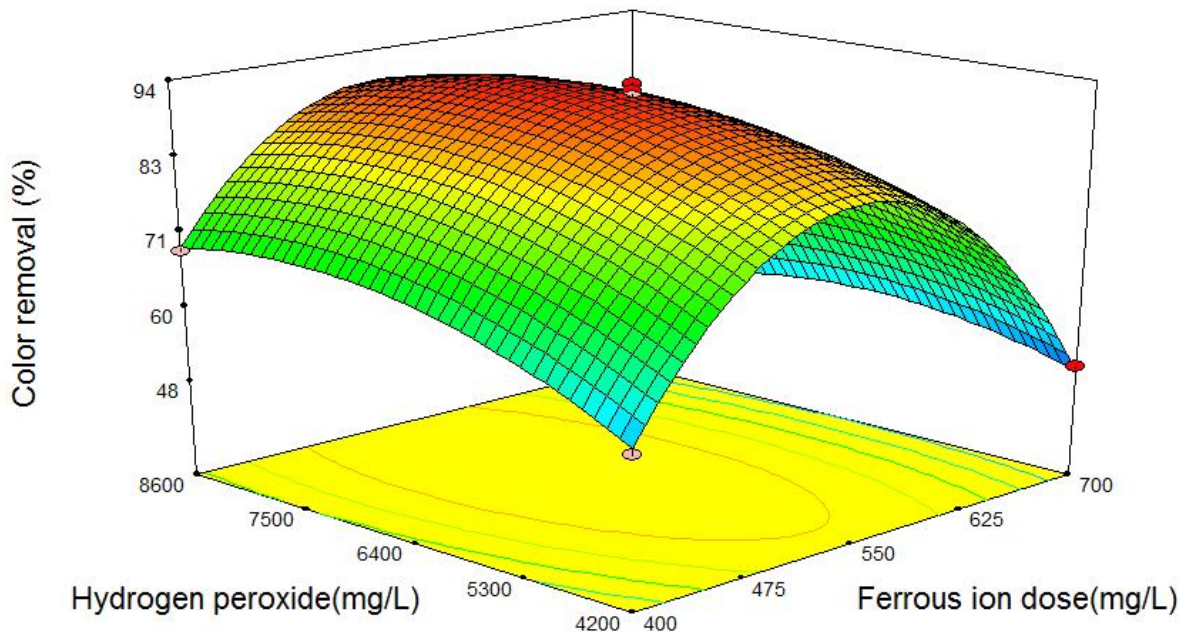


Figure 4-16 3D plot that shows effect of iron and hydrogen peroxide doses on color removal during treatment of real wastewater with conventional Fenton oxidation

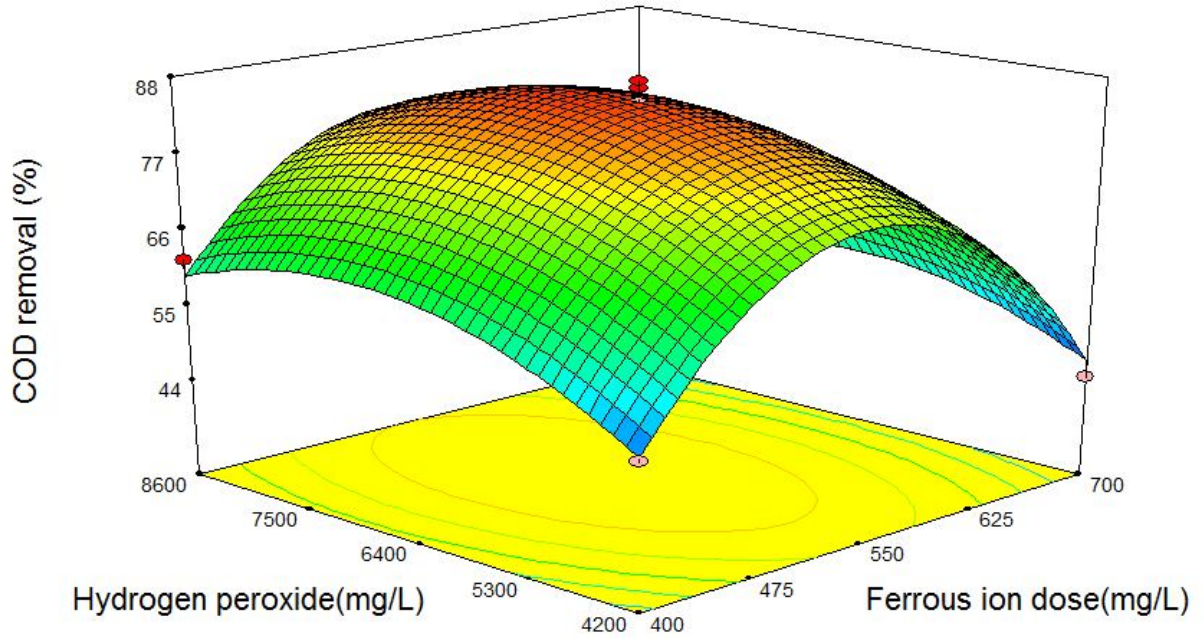


Figure 4-17 3D plot that shows effect of iron and hydrogen peroxide doses on color removal COD removal during treatment of real wastewater with conventional Fenton oxidation

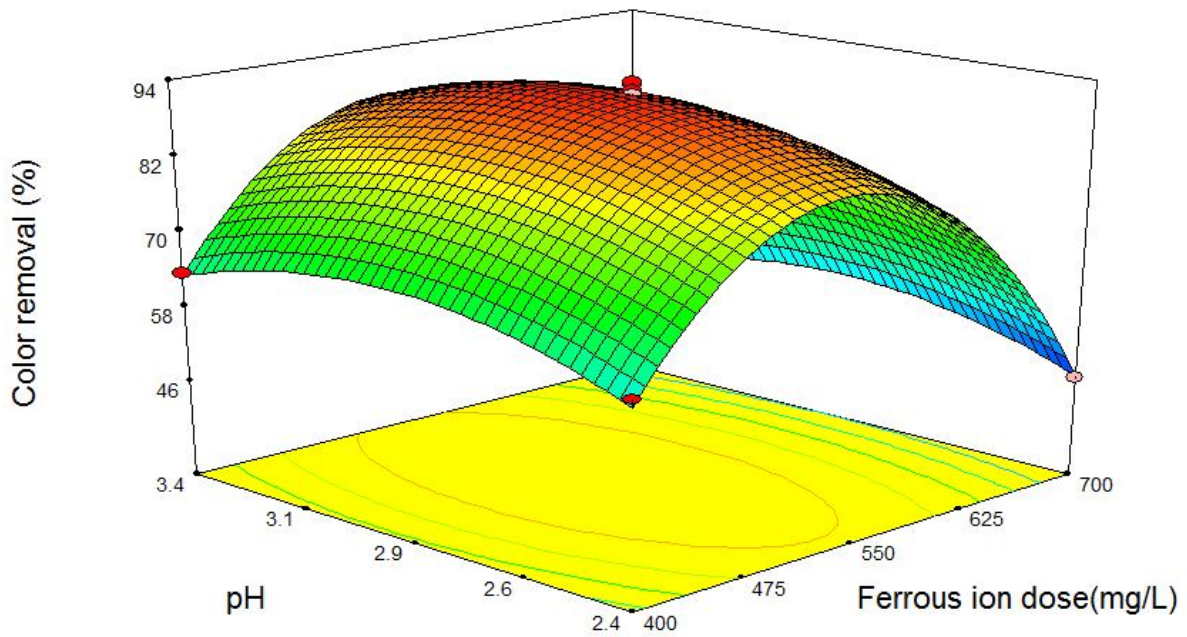


Figure 4-18 3D plot that shows effect of pH on color removal

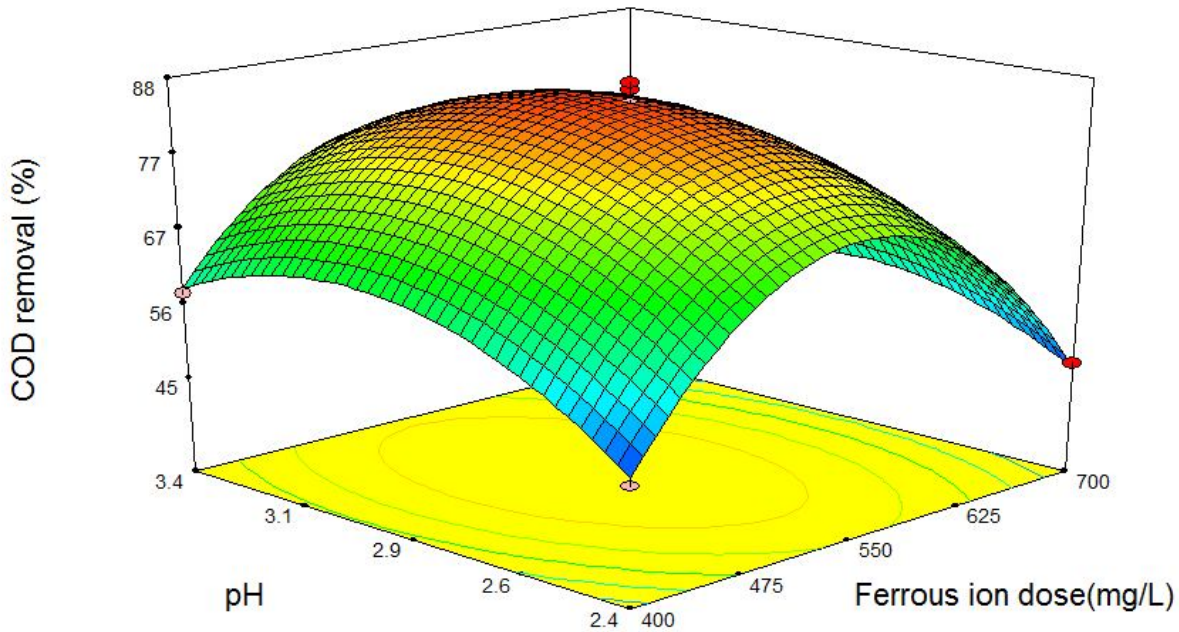


Figure 4-19 3D plot that shows effect of pH on COD removal

Similar results have also been reported by several researchers. Lucas [89] reported decolorization of dyes at a pH of 3, Kaptan [91] showed that 99% of color removal was achieved at a pH range of 3-3.5. When a pH decreased to 2.9, there would be a formation of more stable compound than H_2O_2 , oxonium ion (H_3O_2^+), could be formed by the reaction between H_2O_2 and hydrogen ion. Furthermore, (H_3O_2^+) usually less reacts with Fe^{2+} towards the production of $\text{HO}\cdot$ [155, 156]. The possible reason for the reduction of $\text{HO}\cdot$ during the formation of (H_3O_2^+) is due to the decrease in the amount of Fe^{3+} and this species would be in equilibrium with other iron species such as with $\text{Fe}(\text{OH})_2$ and $\text{Fe}(\text{OH})^{+2}$ [89].

4.3.5 Perturbation plots during degradation of real wastewater with conventional Fenton oxidation

In Figure 4-20, A represents ferrous ion, B represents hydrogen peroxide dose and C represents pH. It can be clearly seen from the following graph that, factor A is having the steepest slope as compared to factor B and C having relatively flat slopes for both color and COD removal. A steeper

slope is showing that the response is more sensitive to that factor as compared to the other two factors taken for consideration. Therefore, COD and color removal were highly influenced by Ferrous ion dose as compared to hydrogen peroxide dose and pH.

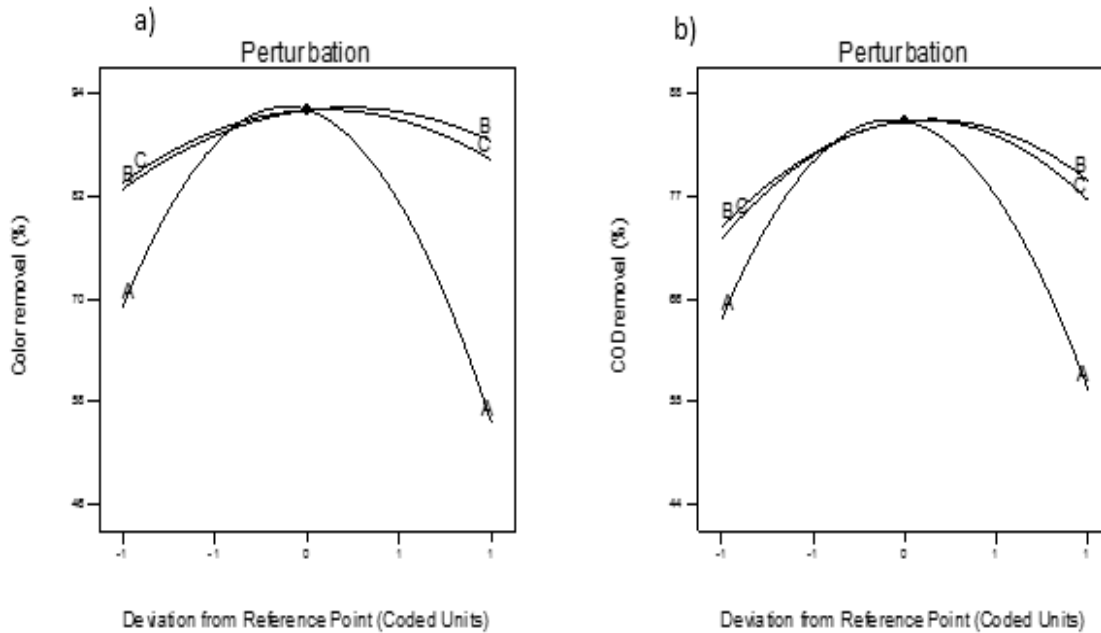


Figure 4-20 Perturbation plot for a) color removal and b) COD removal during treatment of real wastewater with conventional Fenton oxidation

4.3.6 Optimization during treatment of real textile wastewater with conventional Fenton oxidation

Based on equations 4.5 and 4.6 the color and COD removal efficiencies were maximized by changing the process variables. In order to minimize operating costs of the treatment used in this study, Fe^{2+} and H_2O_2 were chosen to be minimize while pH chosen in the range. Hence, optimum working conditions and percent removal efficiencies were obtained. The optimum values obtained base on the selected criteria were: Fe^{2+} : 500.4 mg/L, H_2O_2 : 5187.6 mg/L and pH:2.9 with color and COD removal of 87% and 79% respectively. The optimum values were confirmed by conducting additional experiment at the optimal conditions. Finally, It was found that the values measured were approximately closer to the model values, i.e., color removal was 86.7% and COD

removal was 78.5% with a deviation from their mean with a value of 0.18% and 0.05% respectively.

4.4 Treatment of textile wastewater with SBR

4.4.1 Regression model and statistical testing for degradation of textile wastewater with SBR

The experimental results originating from the BBD are summarized in Table 4-8, and the resulting model values obtained by using the RSM model are shown in Table 4-9 -Table 4-11. Optimal values for color and COD removal and measurement of sludge volume index in the experimental runs could be determined by second- order polynomials as expressed by equations 4.11, 4.12 and 4.13.

$$\begin{aligned} & \text{COD removal}(R_1) & (4.11) \\ & = 56.60 + 1.43A + 2.66B + 0.66C + 0.050AB - 0.40AC \\ & - 1.82BC + 1.21A^2 - 7.01B^2 - 5.41C^2 \end{aligned}$$

$$\begin{aligned} & \text{Color removal}(R_2) & (4.12) \\ & = 53.58 + 0.45A + 2.45B + 0.85C + 0.000AB - 0.75AC \\ & - 1.85BC + 0.61A^2 - 7.39B^2 - 4.14C^2 \end{aligned}$$

$$\begin{aligned} \text{SVI}(R_3) = & 80.00 + 7.88A - 5.755B - 4.88C + 0.75AB - 5.00AC + 4.25BC & (4.13) \\ & + 5.50A^2 + 13.25B^2 + 9.00C^2 \end{aligned}$$

Where R_1 for color removal, R_2 stands for COD removal and R_3 accounts for SVI respectively shows the regression coefficients and model performance indicators for the RSM model. In Equations 4.11, 4.12 and 4.13, positive effect of a factor implies the response is improved when the factor level increases and a negative effect of the factor means that the response is not improved when the factor level increases [136]. Values of probability < 0.05 show that model terms are significant and values > 0.1000 point out that model terms are not significant [121].

In the case of both COD and color removal, it can be seen that A, B, C, BC, A², B² and C² were significant terms. In addition, for SVI it was concluded that A, B, C, AC, BC, A², B² and C² proved to be significant. Thus, statistical analysis showed that not all variables had a significant effect.

The relationship between each factors and the role of each process factor can be described using Fisher test. The smaller P>f value and the greater F value usually indicate the adequacy of the model [157]. It was further observed that the corresponding p-values of the Fisher test for COD removal ,color removal and SVI were <0.0001 which indicated the regression itself was significant and adequate [121].

The value of the predicted R² for all the three responses were found to be > 0.97. This implies the prediction of experimental data was satisfactory. Low values of coefficient of variation (C.V) indicated high accuracy and dependability of experiments as the values are <10%. In this case all the three responses have a C.V value of <10%. The contour figures were drawn to indicate the interaction between two independent factors. Moreover, the value of one variable kept constant to clearly see the interaction among two independent process factors. The contour plots clearly illustrate the behavior of the system in the experimental design. These plots were indicated in Figure 4-21 - Figure 4-23. The behavior of the response surface plot usually indicates the relationship between the process factors. The nature of the response surface curves shows the interaction between the variables.

The elliptical shape of the curve indicates good interaction between the two variables and circular shape indicates no interaction between the variables. From the figures, it is observed that the elliptical nature of the contour in all the graphs depicts the mutual interactions of all the variables. There was a relative significant interaction between every two variables, and there was a maximum

predicted decolorization and COD reduction as indicated by the surface confined in the smallest ellipse in the contour diagrams. Hence, in these plots, there were significant interaction between process factors and there was the highest predicted COD and color removal which is shown by the surface confined in the smallest ellipse in the counter plots.

Table 4-8 Experimental and predicted values for COD removal, color removal and SVI during single stage SBR stage treatment.

Runs	Process factors in terms of their codes			R ₁ : COD removal (%)		R ₂ : Color removal (%)		R ₃ : SVI (mL/g)	
	A(h)	B(L/h)	C(d)	Expt.	Predicted	Expt.	Predicted	Expt	Predicted
1	0	-1	-1	38.2	39.03	36.7	36.90	115	117.13
2	1	0	1	53.7	54.09	50.5	50.60	90	92.50
3	-1	1	0	51.2	51.99	49	48.80	85	84.38
4	1	0	-1	53.6	53.56	50.8	50.40	115	112.25
5	0	-1	1	43.6	44.00	42.6	42.30	102	98.88
6	0	0	0	56.7	56.60	53.5	53.58	80	80.00
7	0	0	0	56.5	56.60	53.7	53.50	80	80.00
8	1	-1	0	50.3	49.51	44.6	44.80	111	111.63
9	0	0	0	56.5	56.60	53.6	53.60	80	80.00
10	-1	-1	0	47.2	46.76	44	43.90	97	97.37
11	-1	0	-1	50.3	49.91	48.1	48.00	89	86.50
12	1	1	0	54.5	54.94	49.6	49.70	102	101.62
13	0	0	0	56.8	56.60	53.5	53.58	80	80.00
14	-1	0	1	52	52.04	50.8	51.20	84	86.75
15	0	0	0	56.5	56.60	53.6	53.58	80	80.00
16	0	1	1	46.5	45.68	43.7	43.50	98	95.88
17	0	1	-1	48.4	48.00	45.2	45.50	94	97.13

4.4.2 Effect of process variables on treatment of textile wastewater in SBR

Figure 4-21 shows the effect of air flow rate and SRT on COD removal. From this figure it can be seen that an initial increase in air flow rate causes increase in removal of COD. However, further increase of air flow rate above 13.8 L/h cause a decrease in COD removal efficiency. The possible reason for the increase in COD removal at low value of air flowrate was due to better interaction between air and microorganisms. On the contrary, the decrease in COD removal at high air flow rate is due to the decrease in the retention time of air. Moreover, the decrease in the retention time of air can lead to the decrease in the interaction between microorganisms and air molecules. Figure 4-21 also shows that the increase of SRT up to 16 days lead to the increase of COD removal efficiency.

The effect of air flow rate and SRT on decolorization (Figure 4-22) were in similar pattern with that of COD removal observed in Figure 4-21. While cycle period has no effect for both COD and color removal. Similar results were reported elsewhere [158].

Table 4-9 Response surface quadratic model for color removal during single SBR treatment stage.

Source	Coefficient factors	Sum of square	Degree of freedom	Mean square	F value	P value prob >F
Model	53.58	387.91	9	43.10	414.44	<0.0001
A	0.45	1.62	1	1.62	15.58	0.0056
B	2.45	48.02	1	48.02	461.73	<0.0001
C	0.85	5.78	1	5.78	55.58	0.0001
AB	0.000	0.000	1	0.000	0.000	1.0000
AC	-0.75	2.25	1	2.25	21.63	0.0023
BC	-1.85	13.69	1	13.69	131.63	<0.0001
A ²	0.61	1.57	1	1.57	15.06	0.0060
B ²	-7.39	229.95	1	229.95	2211.02	<0.0001
C ²	-4.14	72.17	1	72.17	693.91	<0.0001
SD	0.32				0.32	
C.V. (%)	0.67					
R ²	0.9981					
Adjusted R ²	0.9957					
Predicted R ²	0.9711					
Adeq.Precision	67.438					
Residual		0.73	7	0.10		
Lack of fit		0.70	3	0.23	33.33	0.0027
Pure error		0.020	4	7.000E-0.03		
Total (corr)		388.84	16			

Table 4-10 Response surface quadratic model for COD reduction during single SBR treatment stage.

Source	Coefficient factors	Sum of square	Degree of freedom	Mean square	F value	P value prob >F
Model	56.60	439.78	9	48.86	92.76	<0.0001
A	1.43	16.25	1	16.25	30.84	0.0009
B	2.66	56.71	1	56.71	107.66	<0.0001
C	0.66	3.51	1	3.51	6.67	0.0364
AB	0.050	1.000E-0.02	1	1.000E-0.02	0.019	0.8943
AC	-0.40	0.64	1	0.64	1.21	0.3068
BC	-1.82	13.32	1	13.32	25.29	0.0015
A ²	1.21	6.19	1	6.19	11.75	0.0.0110
B ²	-7.01	207.05	1	207.05	393.05	<0.0001
C ²	-5.41	123.35	1	123.35	234.15	<0.0001
SD	0.73					
C.V. (%)	1.41					
R ²	0.9917					
Adjusted R ²	0.9810					
Predicted R ²	0.8696					
Adeq.Precision	0.73					
Residual		3.69	7	0.53		
Lack of fit		3.61	3	1.20	60.12	0.0009
Pure error		0.080	4	0.020		
Total (corr)		443.47	16			

Table 4-11 Response surface quadratic model for SVI during single SBR treatment stage.

Source	Coefficient factors	Sum of square	Degree of freedom	Mean square	F value	P value prob >F
Model	80.00	2453.69	9	272.63	33.33	<0.0001
A	7.88	496.13	1	496.13	60.66	0.0005
B	-5.75	264.50	1	264.50	32.34	0.0007
C	-4.88	190.13	1	190.1	23.25	0.0019
AB	0.75	2.25	1	2.25	0.20	0.6161
AC	-5.00	100.00	1	100.00	12.23	0.0100
BC	4.25	72.25	1	72.25	8.89	0.0207
A ²	5.50	127.37	1	127.37	15.57	0.0056
B ²	13.25	739.21	1	739.21	90.38	<0.0001
C ²	9.00	341.05	1	341.05	41.70	0.0003
SD	2.86					
C.V. (%)	3.07					
R ²	0.9722					
Adjusted R ²	0.9479					
Predicted R ²	0.6352					
Adeq.Precision	16.926					
Residual		57.25	7	8.18		
Lack of fit		57.25	3	19.08		
Pure error		0.000	4	0.000		
Total (corr)		2510.94	16			

The effect of air flow rate on SVI is shown on Figure 4-23, initially it was observed that the value of air flowrate increase from 8-16 L/hr. while the value of SVI was decreased. However, further increase of air flowrate lead to the increase in the value of SVI. This phenomena can occur due to the breakdown of sludge's at higher air flow rate. Furthermore, the figures also illustrated that, air flowrate beyond 16L/hr. improve the value of SVI. In

addition, the effect of SRT on SVI is shown in Figure 4-23. The figure shows the increase of SRT from 10-16 days cause to decrease in the value of SVI. However, at the maximum level of SRT (20d) SVI values was proportionally increased.

In Figure 4-23 cycle period is seen to have no effect on the value of SVI. SVI was the best indicator of sludge settling properties. The value of SVI obtained experimentally in this research was (80-115mL/g). The value of SVI can be in the range of (30-400 mL/g). If the value of SVI is less than 150mL/g, It usually shows better settling properties of the sludge. On the other hand, if the value of SVI greater is than 150mL/g, it usually indicates bulking of the sludge [159]. In this sense, the value of SVI which was experimentally measured in this research was (80-115 mL/g). This result was relatively lower than the results which was reported by previous researchers [160, 161].

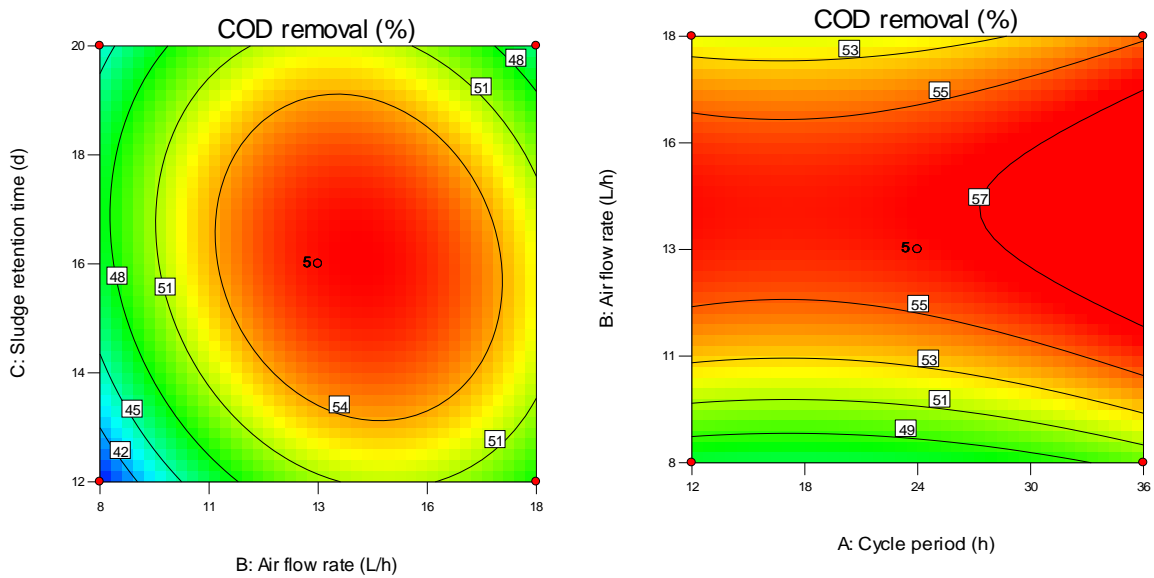


Figure 4-21 Effect of air flowrate, sludge retention time and cycle period on COD removal.

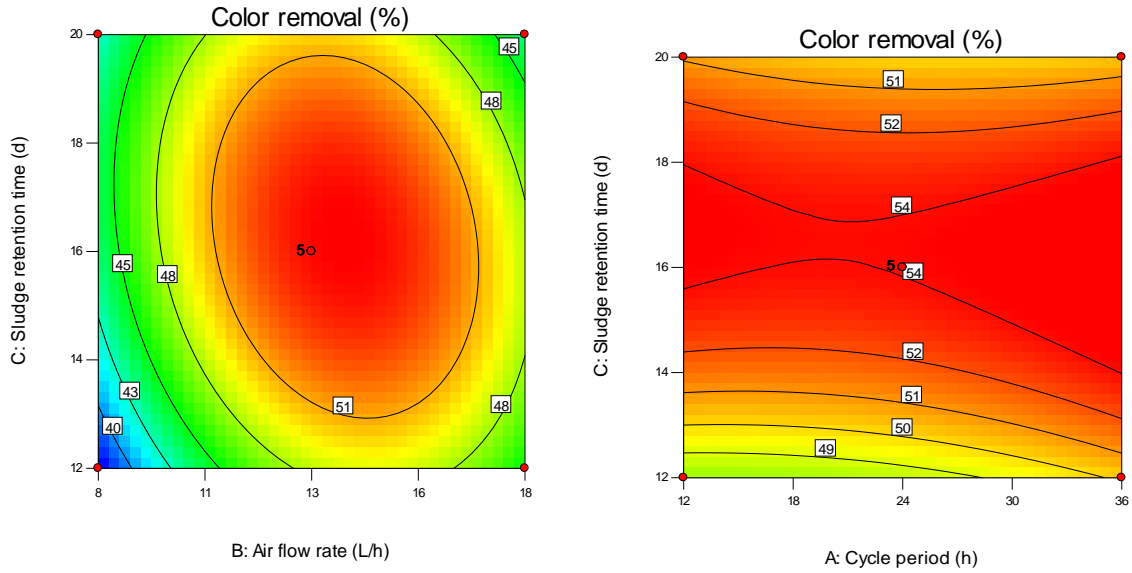


Figure 4-22 Effect of air flowrate, sludge retention time and cycle period on color removal.

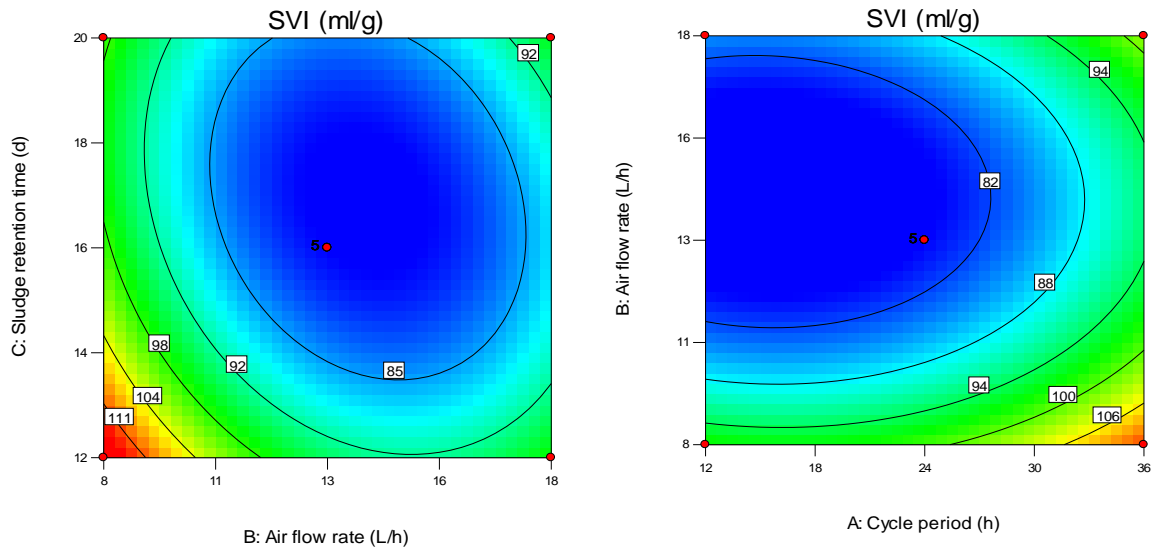


Figure 4-23 Effect of air flowrate, sludge retention time and cycle period on SVI.

4.4.3 Optimization of process factors of SBR treated textile waste water for color and COD removal

Optimization was carried out using statistical software package Design-Expert® version 7.0.0 (Stat-Ease, Inc.) with BBD. Optimal values of the three responses were based on equations 4.11,

4.12 and 4.13. Furthermore, the main purpose of optimization was to achieve maximum efficiency of the SBR wastewater treatment process. In addition, optimization was done based on preferred selected criteria. In this sense, COD and color removal efficiency were selected to be maximized, cycle period, air flow rate and SRT were selected in range while SVI was selected to be minimized. Based on this selection criteria, optimum working conditions and percent removal efficiencies were obtained. The optimum values obtained from BBD based on the selected criteria were: cycle period: 25 h, air flow rate: 15 L/h and SRT:16 d with COD and color removal efficiency of 57% and 54% respectively.

4.4.4 Optimum condition Performance of SBR at various OLR

Further experiments were conducted based on optimum conditions of the process factors by varying influent substrate concentrations (1.25 and 1.96 g COD/L) and HRT (4, 3 and 2d). Moreover, the value of OLR varies based on the duration of these HRT and quantities of influent substrate concentrations. The detail working conditions are given in Table 3-8. The total days of operation was seventy seven days. In these reactor continuous working days, COD removal, decolorization and value of SVI were investigated based on standard methods of water and wastewater treatment analysis [134].

In the beginning of the reactor performance, the influent substrate concentration was 1.25g COD/L and HRT was four days while the OLR was 0.078 Kg COD/m³d. In this process condition, the removal of both COD and color was minimum as the microorganisms required longer time for adaptation of the reactor environment. However, gradually within 17 days (1-17 days) of the reactor continuous operation the system reached to steady state condition. At this stage, a maximum of 73% COD and 65.8% color removal efficiency were achieved. Likewise, on the 18th day the OLR was increased to 0.104 kg COD/m³d by decreasing the

HRT to three days while the influent wastewater concentration was kept constant. In these process conditions, (18-23 days) the reactor reached another steady state conditions within six days. At this stage, a maximum of 71.6 % COD and 63.7% color removal was obtained. Similarly, on the 24th day the OLR was increased to 0.156 kg COD/m³d by decreasing the HRT to two days while keeping the influent concentration constant. In this process condition, the reactor reached steady state within fourteen days of continuous operation (24-37 days). At this stage, a maximum of 64.5% COD and 58% color removal was obtained.

After thirty seven days of reactor operation (on the 38th day), the inlet substrate concentration was increased to 1.96g COD/L, the HRT was 4 days and the corresponding OLR was 0.122 Kg COD/m³d. In this process condition, after fifteen days of continuous reactor operation (38-52 days), the system reached to steady state condition. At this stage, a maximum of 56.1% COD reduction and 51.6% color removal was achieved. In addition, on the 53th day the OLR was increased to 0.163 Kg COD/m³d by decreasing the HRT to three days while keeping the influent substrate concentration constant. In these process conditions, (53-61 days) reactor operation steady state conditions was achieved within nine days. At this stage, a maximum of 55.6 % COD and 50.5% color removal was obtained. Finally, on the 62th day the OLR was increased to 0.245Kg COD/m³d by decreasing the HRT to two days while keeping the influent concentration constant. In this process condition, the reactor reached steady state within sixteen days continuous operation (62-77 days). At this stage, a maximum of 48.7% COD and 42.5% color removal was obtained.

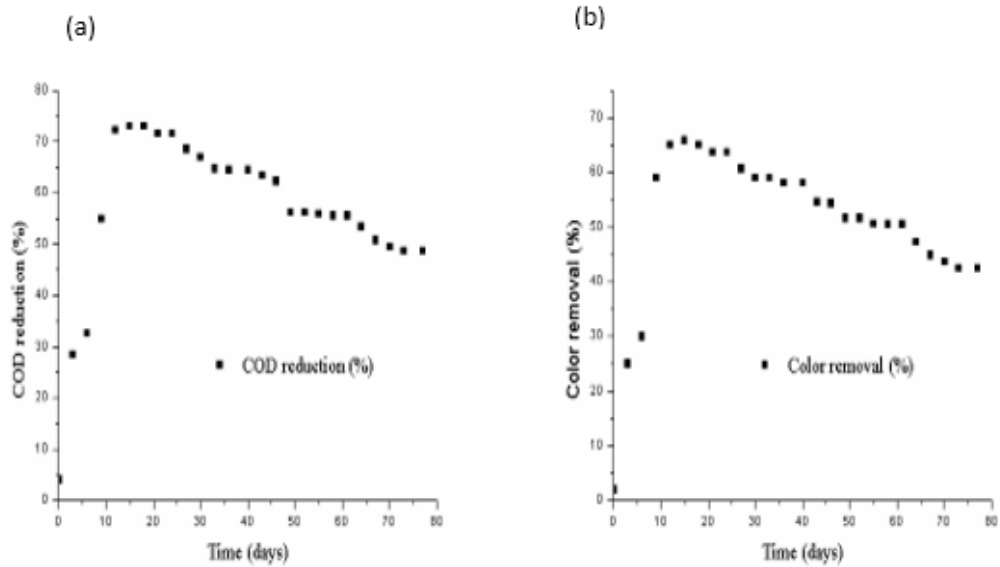


Figure 4-24 (a) COD removal and (b) decolorization of textile wastewater at optimum conditions using various OLR and HRT.

Table 4-12 COD removal and decolorization of textile wastewater at optimum conditions at various OLR and HRT.

Substrate concentration g COD/L	days	HRT (days)	OLR (Kg COD /m ³ d)	COD removal (%)	Color removal (%)
1.25	1-17	4	0.078	73	65.8
	18-23	3	0.104	71.6	63.7
	24-37	2	0.156	64.5	58
1.96	38-52	4	0.122	56.1	51.6
	53-61	3	0.163	55.6	50.5
	62-77	2	0.245	48.7	42.5

The percent of COD removal and decolorization using various OLR and HRT for a total of 77 continuous days at steady state conditions are summarized in Table 4-12. In addition, the trends of COD and color removal using various HRT and OLR are also clearly illustrated in Figure 4-24. In this sense, whenever HRT decreased the OLR increased and usually such

condition always result in the decrease of both percent removal efficiency of COD and color. This outcome also indicated how SBR resist the variation of OLR. Similar trend was also observed by previous researchers by increasing OLR and using various inlet concentrations. Kapdan and Oztekin did experiments on SBR performance on simulated dye wastewater using different HRT and they reported that whenever HRT decreased, COD removal and decolorization also decreased [162].

The trend of measured SVI in SBR is clearly illustrated on Figure 4-25. Initially the value of SVI in the reactor was 180mg/L. However, after 17 days of reactor operation the value of SVI dramatically changed. Gradually, the SVI started to decrease, At the end of the reactor operation the value of SVI decreased to 90mL/g. The measured SVI at optimum condition was mainly in the range of 90-92mL/g. The value of SVI obtained in this study was small and in agreement with previous studies. Previous researchers obtained the value of SVI in the range of 30-60mL/g [163] and also in the range of 65-105mL/g [164].

During the initial stage of SBR operation, MLSS decreased from 1495-1290 mg/L. The possible reason for the decrease in MLSS at this stage could be due to discharge of smaller sludge. On the other hand, after the SBR ran continuously for several days, the MLSS started to increase from 1780-5993 mg/L. However, gradually the amount of sludge started to slightly decrease due to gradual formation of large size granules. It is known that the formation of large size granules inhibit the availability of dissolved oxygen and nutrients to the microorganisms. This phenomenon also inhibits the growth of microorganisms in the system. Similar results are reported elsewhere [165–169].

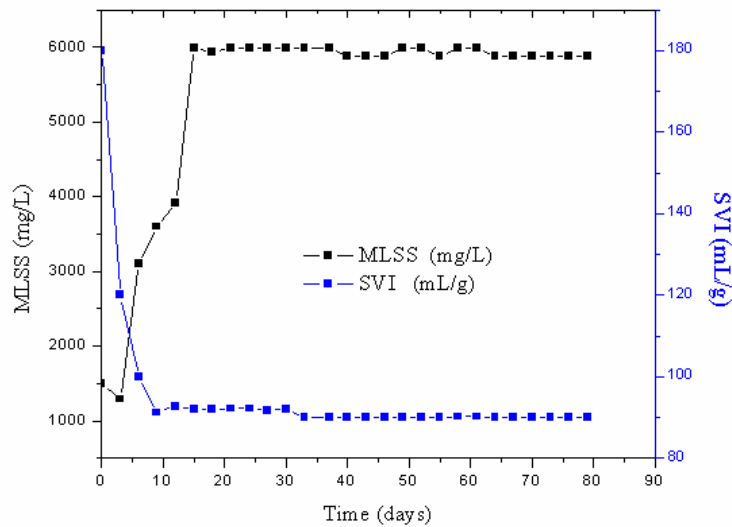


Figure 4-25 MLSS and SVI of textile wastewater at optimum conditions using various OLR and HRT.

4.4.5 Kinetic study in SBR

The kinetic study was carried out for the treatment of textile wastewater at various level of substrate concentration and hydraulic retention time. The microorganisms usually used the available substrate concentrations in wastewater. The biodegradation process usually expressed by first order kinetic model. By integrating in between defined limits, such a first order model can be expressed as:

$$\ln\left(\frac{C_s}{C_{s0}}\right) = -K_1 t \quad (4.14)$$

Where C_{s0} is the initial substrate concentrations (g COD/L), C_s is the substrate concentration (g COD/L), t is the degradation time (d), K_1 is the first order rate constant (d^{-1}). Figure 4-26 shows how the experimental data fitted with first order model at different substrate

concentrations and various hydraulic retention times. The first order rate constant(K_1) was calculated from the slope of the line by least square fit in the Figure 4-26.

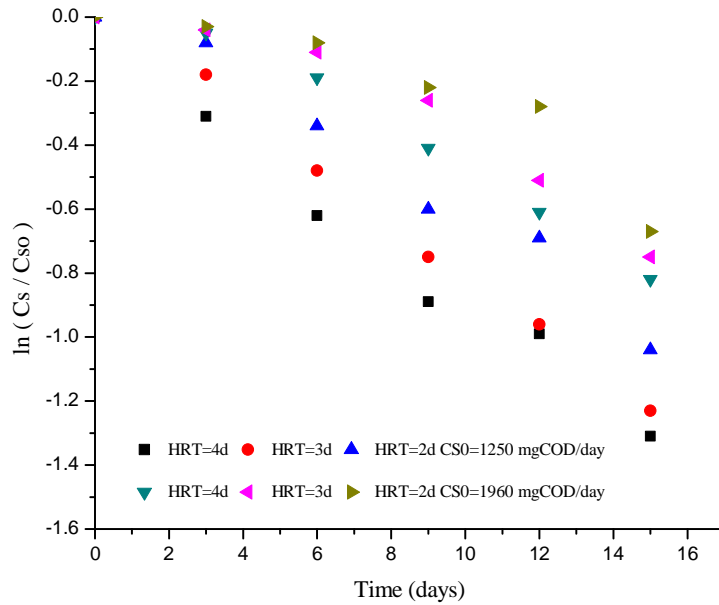


Figure 4-26 Kinetic plot for the treatment of textile wastewater in SBR.

Table 4-13 Values of rate constant (K) and the determination coefficient (R^2) at various OLR and HRT.

Substrate concentration g COD/L	days	HRT (days)	OLR (Kg COD/m ³ d)	COD removal (%)	Color removal (%)	K (1/d)	R ²
1.25	1-17	4	0.078	73	65.8	0.0844	0.9839
	18-23	3	0.104	71.6	63.7	0.0817	0.9925
	24-37	2	0.156	64.5	58	0.0694	0.9742
1.96	38-52	4	0.122	56.1	51.6	0.0571	0.9701
	53-61	3	0.163	55.6	50.5	0.0506	0.9174
	62-77	2	0.245	48.7	42.5	0.0404	0.8286

The value of R^2 and K are shown in Table 4-13. The values of R^2 indicate the ability of the model to represent first order used in this kinetic model. K values for 4d and 3d are nearer to each other, the smallest K values in the SBR is observed at the highest organic loading rate (0.245 kg COD/m³d). A possible reason for this might be inhibitory effect of the substrate on the microbial activity.

4.5 Treatment of textile wastewater with the integration Fenton with SBR

4.5.1 Single Fenton oxidation stage at optimum conditions at various reaction time

Single Fenton oxidation was carried out using optimal Fenton process factors (Fe^{2+} : 500.4 mg/L, H_2O_2 : 5187.6 mg/L , pH:2.9 and 60 minutes reaction time) where 87 and 79% color and COD removal were obtained, respectively. However, during the integrated treatment stage, similar reaction conditions were used while the duration of reaction was decreased to 30 minutes. The reaction time was decreased for the purpose of analyzing the contribution of biological oxidation stage on the integrated treatment scheme. Accordingly, the COD and color removal efficiency decreased to 67 and 86 %, respectively. Color removal efficiency was almost equal for both reaction times while there was significant difference in the COD removal efficiency. The possible reason for significant reduction in the percent COD removal than color during short reaction time might be that the azo bonds were breaking faster than total degradation processes [123].

Other researchers also reported about removal efficiency of single Fenton oxidation stage during treatment of textile wastewater using the integration of Fenton with SBR. However, their results were lower than the results of the present study. Fongsatitkul et al. [14] obtained 30% color removal using 25–200 mg/L range Fenton's reagent, pH=3, and 30 minutes reaction time. Blanco et al. [8] also reported 70% COD removal efficiency using the best Fenton reagent conditions:

216mg/L Fe^{2+} , 1650 mg/L H_2O_2 at room temperature. Mandal et al. [170] reported 60 % COD removal efficiency using 44 g/L H_2O_2 , 6gm Fe^{2+} and 30 minutes reaction time.

4.5.2 Single SBR stage treatment for integrated system

Based on optimum condition of SBR process variables (24 h, air flow rate: 15 L/h and SRT: 16days), further experiments were conducted to analyze the performance of SBR at various organic loading rate (OLR) and hydraulic retention time (HRT) conditions. OLR was varied by altering the HRT (4, 3 and 2 days). The optimal working situations for SBR stage treatment was given in Table 3-9. In addition, the total days of operation were 39 days. In these days, COD removal and decolorization were investigated based on standard methods of water and wastewater treatment analysis [134].

In the beginning of SBR operations, the influent substrate concentration was 1.25g COD/L and HRT was four days while the OLR was 0.078 Kg COD/m³d. In this process condition, the removals of both COD and color were minimum due to the microorganism required longer time for adaptation of the reactor environment. However, gradually within 19 days (1-19 days) of the reactor continuous operation the system reached to steady state condition. At this stage, a maximum of 74.1% COD and 64.6% color removal efficiency was achieved. Likewise, on the 20th day the OLR was increased to 0.104 Kg COD/m³d by decreasing the HRT to three days while the influent wastewater concentration was kept constant. In these process conditions, the reactor within six days (20-25 days) another steady state conditions was achieved. At this stage, a maximum of 72.7 % COD and 62.5% color removal was obtained. Table 4-14 shows the operating conditions of SBR at various OLR and HRT.

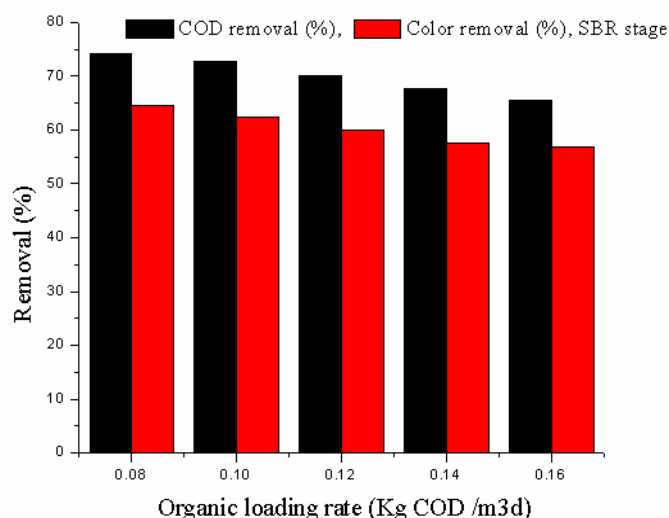


Figure 4-27 Treatment of textile wastewater using SBR

Similarly, on the 26th day the OLR was increased to 0.156 Kg COD/m³d by decreasing the HRT to two days while keeping the influent concentration constant. In this process condition, the reactor reached steady state within fourteen days of continuous operation (26-39 days). At this stage, a maximum of 65.6% COD and 56.8% color removal were obtained. The treatment efficiency comparison with various OLR and HRT in the SBR treatment stage was illustrated in Figure 4-27.

Table 4-14 COD removal and decolorization of textile wastewater using SBR at optimum conditions at various OLR and HRT

Substrate concentration g COD/L	Time of SBR operation (days)	HRT(day)	OLR (Kg COD /m ³ d)	COD removal (%)	Color removal (%)
1.25	1-19	4	0.078	74.1	64.6
	18-25	3	0.104	72.7	62.5
	24-39	2	0.156	65.6	56.8

Various previous researchers have also reported about the removal efficiency of a single SBR treatment method during treatment of textile effluent with the integration of SBR with Fenton oxidation. Accordingly, these results were relatively lower than the removal efficiency of the

present study. In this regard, the better removal at SBR treatment stage in this research was due to the optimization of SBR process factors during biological oxidation stage. Carmen et al. [8] studied about the integration of Fenton with SBR on the study of biodegradability improvement of Fenton pre oxidation on textile wastewater treatment. SBR single stage treatment with a solids retention time (SRT) of 10 days at steady stage gave a maximum color removal of 63.9%. Mandal et al. [170] also using biological single treatment with *T. ferrooxidans* obtained 17% COD and 56% COD removal in one day and seven days treatment, respectively.

4.5.3 Fenton followed by SBR (Fenton + SBR)

Initially the pH of raw textile wastewater was fixed to 2.9. In addition, optimum doses of Fenton reagents (Fe^{2+} : 500.4 mg/L, H_2O_2 : 5187.6 mg/L) were used and the reaction was carried out for 30 minutes. Unusually, the total time of the first Fenton oxidation was smaller as compared to the usual recommended duration of Fenton reaction. In this process conditions, the efficiency of color and COD removal were found to be 86% and 67% respectively. Moreover, the biodegradability of Fenton stage oxidized effluent was usually checked for all runs using a ratio of BOD:COD and also residual hydrogen peroxide was also eliminated by addition of sodium sulfite for the purpose of removing the toxicity effect of H_2O_2 during Fenton treatment stage to the microorganisms in the next SBR stage. Subsequently, the decanted effluent from the Fenton stage was feed to SBR reactor.

The bioreactor was run for a total of 23 days using optimum conditions of SBR (cycle period :24 h , air flow rate: 15 L/h and SRT 16 days) and also using effluent from Fenton treatment stage as a feed to the second SBR stage treatment as shown in Table 4-15. The effluent obtained from Fenton reagent treatment stage was fed to the first steady state treatment stage of SBR. Within 11 days the first steady state was achieved. In this first steady state condition, COD and color

removal efficiency were measured using Fenton +SBR. The values of COD and color removal efficiency obtained were 86.3% and 84%, respectively. Gradually, as shown on Table 4-15, OLR was increased from 0.078 Kg COD /m³d to 0.104 Kg COD /m³d by reducing the HRT from 4 to 3 days.

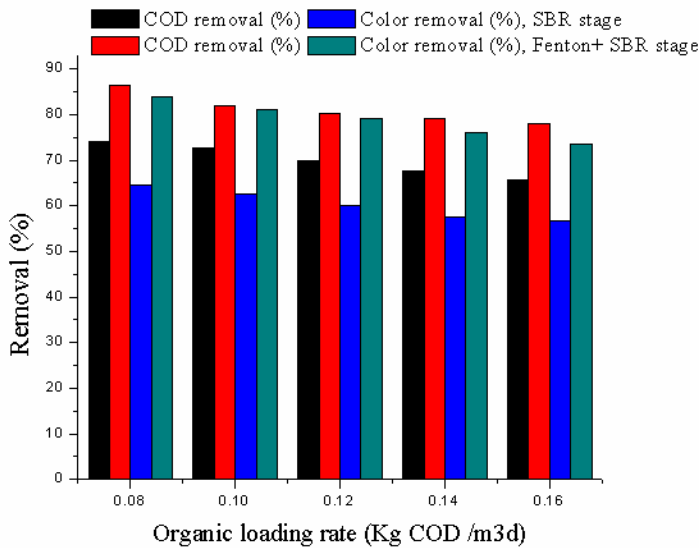


Figure 4-28 Treatment of textile wastewater using Fenton followed by SBR

Subsequently, after the fourth day (15th day) the reactor achieved the second steady state condition. At this stage, COD removal and color were measured and obtained to be 82% and 81% respectively. Likewise, OLR was increased from 0.104 Kg COD /m³d to 0.156 Kg COD /m³d by decreasing HRT from 3 to 2 days. After 8 days of the reactor operation (23rd day) reached to steady condition. In this stage the maximum efficiency of COD and color removal where as measured and obtained to be 78.1% and 73.6% respectively. Furthermore, a comparison of textile wastewater treatment between SBR alone and treatment using Fenton +SBR for COD and color removal efficiency was illustrated in Figure 4-28. Previous researchers were also reported similar trend of percent COD and color removal efficiency but relatively lower values as compared to this study [90, 117].

Table 4-15 Treatment of textile wastewater using Fenton followed by SBR

Treatment conditions				SBR stage		Fenton +SBR	
Substrate concentration g COD/L	Time of SBR operation (days)	HRT (days)	OLR (KgCOD/ m ³ d)	COD removal (%)	Color removal (%)	COD removal (%)	Color removal (%)
1.25	1-11	4	0.078	74.1	64.6	86.3	84
	12-15	3	0.104	72.7	62.5	82	81
	16-23	2	0.156	65.6	56.8	78.1	73.6

Previous researchers also reported different comparative removal efficiency between SBR and the integrated system of Fenton oxidation followed by SBR on textile wastewater treatment. Carmen et al. [12] in the study of pre oxidation improvement on biodegradability improvement reported that, the integrated process SBR showed 33.4 % color removal improvement than single SBR stage. Fongsatitkul et al. [14] also reported that the COD removal efficiency of integrated treatment showed 7.8% better removal efficiency than single SBR treatment technology. In addition, Mandal et al. [170] during treatment of combined industrial wastewater using the combination of AOP'S followed by bio treatment, reported that the integrated treatment scheme enhanced the percent COD reduction by 20% than single biological stage. Carmen et al. [13] also reported regarding removal efficiency of AOP's followed by SBR using various types of textile waste waters (acrylic, cotton and polyester dyeing industries). Accordingly, the variation in percent removal efficiency were dependent on the constituents of these raw textile waste waters.

4.5.4 SBR followed by Fenton (SBR stage +Fenton)

Initially, the textile wastewater was treated using SBR treatment scheme., COD removal and decolorization were measured when the system achieved steady state at 19th , 25th and 39th days.

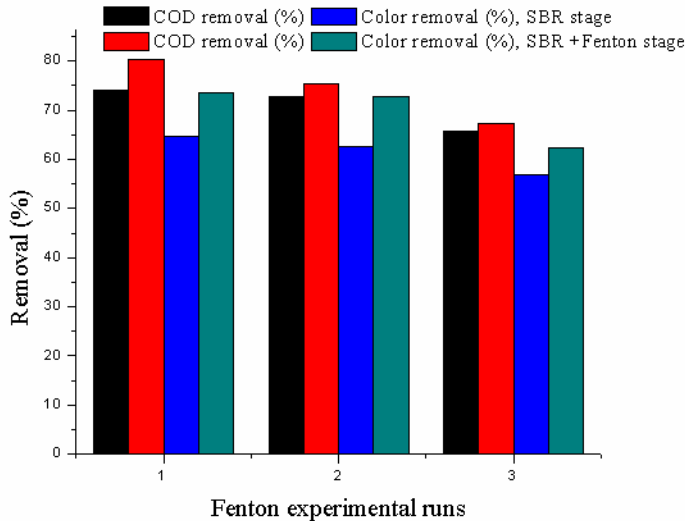


Figure 4-29 Treatment of textile wastewater using SBR followed by Fenton

The effluent obtained from SBR at a steady state conditions at 19th , 25th and 39th days was further treated by Fenton oxidation using optimum Fenton reagent concentration. Initially, the effluent obtained at the 19th day SBR operation was used as a feed to the Fenton oxidation. In this first experiment COD and color removal efficiency was found to be 80.2% and 73.8% respectively.

Secondly, the effluent obtained from SBR at the 25th day was used as a feed to the second Fenton experimental run. At this stage, COD and color removal efficiency were found to be 75.3% and 72.7% respectively. Likewise, the effluent obtained from SBR at 39th day was used as a feed to the third Fenton experimental run. In this stage, percent COD and color removal efficiency was obtained to be 64.3% and 62.4% respectively. The summary of the

comparison SBR with Fenton for three Fenton oxidation experimental runs was summarized in Table 4-16. Furthermore, the comparison of SBR and SBR+ Fenton was shown on Figure 4-29.

Table 4-16 Treatment of textile wastewater using SBR followed by Fenton (SBR +Fenton)

Runs	Process factors (optimum Fenton process factors)			SBR +Fenton (%)	
	A(mg/L) Fe ²⁺	B(mg/L) H ₂ O ₂	C pH	COD removal (%)	Color removal (%)
1	500.4	5187.6	2.9	80.2	73.6
2	500.4	5187.6	2.9	75.3	72.7
3	500.4	5187.6	2.9	64.3	62.4

Previous researchers reported about the removal efficiency of the integrated system (SBR followed by Fenton oxidation). Accordingly, Blanco et al. [8] reported that during the integrated process 11% COD removal efficiency were obtained than single SBR treatment stage and Fongsatitkul et al. [14] also reported that the COD removal efficiency of the integrated processes showed 3.6% better removal efficiency than single SBR treatment stage.

4.5.5 Comparison of treatment efficiencies of single Fenton stage, single SBR stage, Fenton+ SBR and SBR+ Fenton

Single SBR treatment stage could give significant COD removal efficiency than color removal while single Fenton oxidation could give significant color removal than COD removal. Previous authors also reported similar results. Accordingly, Hayat et al. [15] reported on the comparative study of percent COD and color removal efficiency between anaerobic IC bioreactor and Fenton oxidation with 25%,50%,75% and 100% diluted textile wastewater samples. Accordingly, the maximum color removal was achieved with Fenton oxidation at pH 3 than anaerobic IC bioreactor. On the other hand, maximum percent COD removal were obtained by means of anaerobic IC bioreactor than Fenton oxidation. Similarly, Fongsatitkul et al. [14] also reported that, better percent COD removal efficiency was obtained with single SBR stage than with single Fenton

oxidation treatment stage while better color removal efficiency was achieved with single Fenton oxidation stage than single SBR stage treatment. Table 4-17 shows summary of treatment efficiencies of SBR, Fenton + SBR and SBR + Fenton. Accordingly, among the three treatment options, Fenton oxidation followed by SBR result in an overall better quality of effluent than both SBR and SBR followed by Fenton oxidation. In addition, both scheme of integrated treatment alternatives (Fenton + SBR and SBR + Fenton) significantly enhanced color removal than COD removal. Fongsatitkul et al. [14] also reported similar results regarding comparison of efficiency between Fenton + SBR and SBR + Fenton.

Table 4-17 Summary of treatment of textile waste water by different treatment schemes

S. No.	SBR (stage 1)		Fenton+ SBR (stage 2)		SBR+ Fenton (stage 3)	
	COD (%)	Color (%)	COD (%)	Color (%)	COD (%)	Color (%)
1.	74.1	64.6	86.3	84	80.2	73.6
2.	72.7	62.5	82	81	75.3	72.7
3.	65.6	56.8	78.1	73.6	64.3	62.4

5 Conclusions and Recommendations

5.1 Conclusions

The total time of irradiation used in the case of artificial solar Fenton oxidation was the smallest as compared to the total time required for conventional Fenton oxidation processes while the removal efficiency of solar Fenton was better than conventional Fenton due to additional hydroxyl radical production during solar photo Fenton processes. At constant dye stuff dose color, TOC and COD removal increased with increasing H_2O_2 and Fe^{2+} concentrations up to a certain level. High concentrations of H_2O_2 and Fe^{2+} for a constant dye stuff dose did not result in better removal of color, TOC and COD due to hydroxyl radical was gradually consumed by both oxidant and catalyst. Percent color removal was higher than TOC removal indicating the production of colorless intermediate compounds. Mineralization requires a lot of reagents and longer irradiation time than color removal due to mineralization require complete oxidation while color removal needs only the breaking of azo bonds. Besides, conventional Fenton oxidation using optimum Fenton reagents at a pH of 2.9 is effective for the treatment of acrylic fiber dyeing processing textile wastewater.

Real textile wastewater was taken and treated with SBR using a biomass taken from domestic wastewater treatment plant. Process factors such as cycle period, air flowrate and sludge retention time (SRT) were optimized using RSM. The optimum ratio of cycle period/ air flowrate/HRT which gives a 57% COD removal and 54% color removal was found to be 25h / 15L/h /16 d. Using two range of influent substrate concentrations and HRT at optimized condition COD removal, color removal, SVI and MLSS were measured. The maximum removal of 73% COD and 65.8% color were obtained at an organic loading rate of 0.078Kg COD/m³d. It is also possible to conclude that as HRT decreases, there was a decrease in the percent COD and color removal. Significant

reduction in percent COD and color removal was observed between HRT 3 and 2 days. Small value of SVI usually indicated good performance of SBR. First order model was best to represent degradation of textile wastewater using SBR. It is possible to conclude that SBR can be applied in the treatment of textile wastewater.

Furthermore, SBR has better efficiency in the removal of COD but lower efficiency in the removal of color. However, it was possible to increase its treatment efficiency by combining with chemical treatment using optimum chemical reagents concentrations and optimum SBR process factors. It was possible to increase the biodegradability and also decrease the toxicity of chemical oxidant upon the next biological stage by using optimum quantity of chemical reagents. Among the three treatment schemes, the effluent obtained from SBR followed by Fenton (SBR+ Fenton) for three runs showed a maximum COD and color removal efficiency of 80.2% and 73.6 % respectively.

From the overall result of this study, it is possible to conclude that the use of advanced oxidation process based on Fenton reagent is effective for the removal of dye containing wastewater. Besides, artificial solar Fenton reaction is effective for the removal of dye containing wastewater in a short period of time. Moreover, conventional Fenton oxidation using optimum Fenton reagents and at pH of 2.9 and biological process with sequencing batch bio reactor were effective for the degradation of wastewater which was obtained from acrylic fiber dyeing process industry. In general, from the present study, It is possible to conclude, chemical treatment before biological process (Fenton+ SBR) was the best option and can be effectively applied in the treatment of textile wastewater.

5.2 Recommendation

From the present study, it was obtained that the integrated system of chemical followed by biological processes can be effectively treated textile wastewater. However, the following points which were not addressed in this research should be considered in the future to check its real application at large scale.

- ✓ Identification of various intermediate compounds which are formed during single Fenton oxidation process during the treatment of dye aqueous solution.
- ✓ Detail toxicity investigation of chemically pre oxidized real textile effluent to check its effect on the microorganisms during the subsequent biological process stage treatment.
- ✓ Characterization of the effluent obtained from the integrated system in order to check its potential use for various activities such as for the purpose of reuse and irrigation purposes.
- ✓ Detail study on economic analysis of each single stage and the integrated system to check its real application at the level of pilot plant and industrial scale.

6 References

1. Oller I, Malato S, Sánchez-Pérez JA (2011) Combination of Advanced Oxidation Processes and biological treatments for wastewater decontamination-A review. *Sci Total Environ* 409:4141–4166. <https://doi.org/10.1016/j.scitotenv.2010.08.061>
2. Holkar CR, Jadhav AJ, Pinjari D V., et al (2016) A critical review on textile wastewater treatments: Possible approaches. *J Environ Manage* 182:351–366. <https://doi.org/10.1016/j.jenvman.2016.07.090>
3. Khurana K (2018) An overview of textile and apparel bussiness advances in Ethiopia. *Res J Text Appar* 22:212–223. <https://doi.org/https://doi.org/10.1108/>
4. Dadi D (2011) Environmental and Health Impacts of Effluents from Textile Industries in Ethiopia: The Case of Gelan and Dukem, Oromia Regional State Diriba Dadi , Till Stellmacher. 32:
5. Blanco J, Torrades F, De M, García-montaña J (2012) Fenton and biological-Fenton coupled processes for textile wastewater treatment and reuse. *Desalination* 286:394–399. <https://doi.org/10.1016/j.desal.2011.11.055>
6. Paździor K, Bilińska L, Ledakowicz S (2019) A review of the existing and emerging technologies in the combination of AOPs and biological processes in industrial textile wastewater treatment. *Chem Eng J* 376:.. <https://doi.org/10.1016/j.cej.2018.12.057>
7. Mantzavinos D, Psillakis E (2004) Enhancement of biodegradability of industrial wastewaters by chemical oxidation pre-treatment. *J Chem Technol Biotechnol* 79:431–454. <https://doi.org/10.1002/jctb.1020>
8. Blanco J, Torrades F, De la Varga M, García-Montaña J (2012) Fenton and biological-Fenton coupled processes for textile wastewater treatment and reuse. *Desalination* 286:394–399. <https://doi.org/10.1016/j.desal.2011.11.055>
9. Kapoor SSS (2017) Effect of Fenton process on treatment of simulated textile wastewater : optimization using response surface methodology. *Int J Environ Sci Technol*. <https://doi.org/10.1007/s13762-017-1253-y>
10. Nidheesh PV, Gandhimathi R (2013) Degradation of dyes from aqueous solution by Fenton processes : a review. *Env Sci Pollut Res* 20:2099–2132.

<https://doi.org/10.1007/s11356-012-1385-z>

11. Guieysse B, Norvill ZN (2014) Sequential chemical-biological processes for the treatment of industrial wastewaters: Review of recent progresses and critical assessment. *J Hazard Mater* 267:142–152. <https://doi.org/10.1016/j.jhazmat.2013.12.016>
12. Rodrigues CSD, Madeira LM, Boaventura RAR (2009) Treatment of textile effluent by chemical (Fenton ' s Reagent) and biological (sequencing batch reactor) oxidation. *J Hazard Mater* 172:1551–1559. <https://doi.org/10.1016/j.jhazmat.2009.08.027>
13. Rodrigues CSD, Madeira LM, Boaventura RAR (2014) Synthetic textile dyeing wastewater treatment by integration of advanced oxidation and biological processes – Performance analysis with costs reduction. *J Environ Chem Eng* 2:1027–1039
14. Fongsatitkul P, Elefsiniotis P, Yamasmit A, Yamasmit N (2004) Use of sequencing batch reactors and Fenton ' s reagent to treat a wastewater from a textile industry. *Biochem Eng J* 21:213–220. <https://doi.org/10.1016/j.bej.2004.06.009>
15. Hayat H, Mahmood Q, Pervez A, et al (2015) Comparative decolorization of dyes in textile wastewater using biological and chemical treatment. *Sep Purif Technol* 154:149–153. <https://doi.org/10.1016/j.seppur.2015.09.025>
16. Santos B, Cervantes FJ, Lier JB Van (2007) Review paper on current technologies for decolourisation of textile wastewaters : Perspectives for anaerobic biotechnology. *Bioresour Technol* 98:2369–2385. <https://doi.org/10.1016/j.biortech.2006.11.013>
17. Sharma P, Kaur H, Sharma M, Sahore V (2011) A review on applicability of naturally available adsorbents for the removal of hazardous dyes from aqueous waste. *Env Monit Assess* 183:151–195. <https://doi.org/10.1007/s10661-011-1914-0>
18. Pearce CI, Lloyd JR, Guthrie JT (2003) The removal of colour from textile wastewater using whole bacterial cells: A review. *Dye Pigment* 58:179–196. [https://doi.org/10.1016/S0143-7208\(03\)00064-0](https://doi.org/10.1016/S0143-7208(03)00064-0)
19. Demirbas A (2009) Agricultural based activated carbons for the removal of dyes from aqueous solutions: A review. *J Hazard Mater* 167:1–9. <https://doi.org/10.1016/j.jhazmat.2008.12.114>
20. Hai FI, Yamamoto K, Fukushi K (2007) Hybrid treatment systems for dye wastewater. *Crit Rev Environ Sci Technol* 37:315–377. <https://doi.org/10.1080/10643380601174723>
21. Fu K li, Lu D nian (2014) Reaction kinetics study of α -amylase in the hydrolysis of starch

- size on cotton fabrics. *J Text Inst* 105:203–208.
<https://doi.org/10.1080/00405000.2013.834574>
22. Magdum SS, Minde GP, Kalyanraman V (2013) Rapid determination of indirect cod and polyvinyl alcohol from textile desizing wastewater. *Pollut Res* 32:515–519
 23. Sarayu K, Sandhya S (2012) Current technologies for biological treatment of textile wastewater-A review. *Appl Biochem Biotechnol* 167:645–661.
<https://doi.org/10.1007/s12010-012-9716-6>
 24. Liang T, Wang L (2015) An environmentally safe and nondestructive process for bleaching birch veneer with peracetic acid. *J Clean Prod* 92:37–43.
<https://doi.org/10.1016/j.jclepro.2014.12.087>
 25. Stephenson R.L. BJB (1998) Study on trend of biodegradability of phenolic compounds during photo-fenton advanced oxidation process. Lewis publishers, New York, USA
 26. Rathore JS, Choudhary V, Sharma S (2014) Implications of Textile Dyeing and Printing Effluents on Groundwater Quality for Irrigation Purpose Pali, Rajasthan. *Eur Chem Bull* 3:805–808. <https://doi.org/10.17628/ECB.2014.3.805>
 27. Clark M (2011) Principles, processes and types of dyes, 1st ed. Woodhead Publishing Limited, Cambridge CB22 3HJ, UK
 28. Kant R (2012) Textile dyeing and printing industry: An environmental hazard. *Nat Sci* 4:22–26
 29. Bisschops I, Spanjers H (2003) Literature review on textile wastewater characterisation. *Environ Technol (United Kingdom)* 24:1399–1411.
<https://doi.org/10.1080/09593330309385684>
 30. Aslam MM, Baig MA, Hassan I, et al (2004) Textile wastewater characterization and reduction of its rCOD & BOD by oxidation. *Electron J Environ Agric Food Chem* 804–811
 31. Bisschops I, Spanjers H (2003) literature review on textile wastewater characterization. *Environ Technol* 37–41. <https://doi.org/http://dx.doi.org/10.1080/09593330309385684>
 32. Aye T, Mehrvar M, Anderson WA (2004) Effects of Photocatalysis on the Biodegradability of Cibacron Brilliant Yellow 3G-P (Reactive Yellow 2). *J Environ Sci Heal - Part A Toxic/Hazardous Subst Environ Eng* 39:113–126.
<https://doi.org/10.1081/ESE-120027372>

33. Renou S, Givaudan JG, Poulain S, et al (2008) Landfill leachate treatment: Review and opportunity. *J Hazard Mater* 150:468–493. <https://doi.org/10.1016/j.jhazmat.2007.09.077>
34. Banat F, Al-Asheh S, Al-Makhadmeh L (2003) Evaluation of the use of raw and activated date pits as potential adsorbents for dye containing waters. *Process Biochem* 39:193–202. [https://doi.org/10.1016/S0032-9592\(03\)00065-7](https://doi.org/10.1016/S0032-9592(03)00065-7)
35. Gupta VK, Jain R, Varshney S (2007) Electrochemical removal of the hazardous dye Reactofix Red 3 BFN from industrial effluents. *J Colloid Interface Sci* 312:292–296. <https://doi.org/10.1016/j.jcis.2007.03.054>
36. Cristóvão RO, Tavares APM, Iraidy A, et al (2011) *Journal of Molecular Catalysis B : Enzymatic Immobilization of commercial laccase onto green coconut fiber by adsorption and its application for reactive textile dyes degradation.* 72:6–12. <https://doi.org/10.1016/j.molcatb.2011.04.014>
37. Sun Q, Yang L (2003) The adsorption of basic dyes from aqueous solution on modified peat-resin particle. *Water Res* 37:1535–1544. [https://doi.org/10.1016/S0043-1354\(02\)00520-1](https://doi.org/10.1016/S0043-1354(02)00520-1)
38. R Ananthashankar AG (2013) Production, Characterization and Treatment of Textile Effluents: A Critical Review. *J Chem Eng Process Technol* 05:1–18. <https://doi.org/10.4172/2157-7048.1000182>
39. EPA (2004) Draft environmental regulations and standards. Addis Ababa city government., Addis Ababa
40. Vasanth Kumar K, Sivanesan S, Ramamurthi V (2005) Adsorption of malachite green onto *Pithophora* sp., a fresh water algae: Equilibrium and kinetic modelling. *Process Biochem* 40:2865–2872. <https://doi.org/10.1016/j.procbio.2005.01.007>
41. Yeap KL, Teng TT, Poh BT, et al (2014) Preparation and characterization of coagulation/flocculation behavior of a novel inorganic-organic hybrid polymer for reactive and disperse dyes removal. *Chem Eng J* 243:305–314. <https://doi.org/10.1016/j.cej.2014.01.004>
42. Jadhav AJ, Srivastava VC (2013) Adsorbed solution theory based modeling of binary adsorption of nitrobenzene, aniline and phenol onto granulated activated carbon. *Chem Eng J* 229:450–459. <https://doi.org/10.1016/j.cej.2013.06.021>
43. Gal an, J., Rodríguez, A., Gomez J. (2013) Reactive dye adsorption onto a novel

- mesoporous carbon. *Chem Eng J* 219:62–68
44. Gupta VK, Gupta B, Rastogi A, et al (2011) A comparative investigation on adsorption performances of mesoporous activated carbon prepared from waste rubber tire and activated carbon for a hazardous azo dye-Acid Blue 113. *J Hazard Mater* 186:891–901. <https://doi.org/10.1016/j.jhazmat.2010.11.091>
 45. Chollom MN, Rathilal S, Pillay VL, Alfa D (2015) The applicability of nanofiltration for the treatment and reuse of textile reactive dye effluent. *Water SA* 41:398–405. <https://doi.org/10.4314/wsa.v41i3.12>
 46. Hoek EMV, Tarabara V V., Koyuncu I, Güney K (2013) Membrane-Based Treatment of Textile Industry Wastewaters. *Encycl Membr Sci Technol*. <https://doi.org/10.1002/9781118522318.emst127>
 47. Alinsafi A, Evenou F, Abdulkarim EM, et al (2007) Treatment of textile industry wastewater by supported photocatalysis. 74:. <https://doi.org/10.1016/j.dyepig.2006.02.024>
 48. Yadav A, Mukherji S, Garg A (2013) Removal of Chemical Oxygen Demand and Color from Simulated Textile Wastewater Using a Combination of Chemical / Physicochemical Processes
 49. Sevimli MF, Sarikaya HZ (2002) Ozone treatment of textile effluents and dyes : effect of applied ozone dose , pH and dye concentration. 850:. <https://doi.org/10.1002/jctb.644>
 50. Tünay O, Kabdasli I, Eremektar G, Orhon D (1996) Color removal from textile wastewaters. *Water Sci Technol* 34:9–16. [https://doi.org/10.1016/S0273-1223\(96\)00815-3](https://doi.org/10.1016/S0273-1223(96)00815-3)
 51. Babuponnusami A, Muthukumar K (2013) Journal of Environmental Chemical Engineering A review on Fenton and improvements to the Fenton process for wastewater treatment. *Biochem Pharmacol*. <https://doi.org/10.1016/j.jece.2013.10.011>
 52. Malato S, Blanco J, Vidal A, Richter C (2002) Photocatalysis with solar energy at a pilot-plant scale: An overview. *Appl Catal B Environ* 37:1–15. [https://doi.org/10.1016/S0926-3373\(01\)00315-0](https://doi.org/10.1016/S0926-3373(01)00315-0)
 53. Levec J, Pintar A (2007) Catalytic wet-air oxidation processes: A review. *Catal Today* 124:172–184. <https://doi.org/10.1016/j.cattod.2007.03.035>
 54. Glaze WH, Kang JW, Chapin DH (1987) The chemistry of water treatment processes involving ozone, hydrogen peroxide and ultraviolet radiation. *Ozone Sci Eng* 9:335–352. <https://doi.org/10.1080/01919518708552148>

55. Hoigné J (1997) Inter-calibration of OH radical sources and water quality parameters. *Water Sci Technol* 35:1–8. [https://doi.org/10.1016/S0273-1223\(97\)00002-4](https://doi.org/10.1016/S0273-1223(97)00002-4)
56. Klavarioti M, Mantzavinos D, Kassinos D (2009) Removal of residual pharmaceuticals from aqueous systems by advanced oxidation processes. *Environ Int* 35:402–417. <https://doi.org/10.1016/j.envint.2008.07.009>
57. Rosenfeldt EJ, Chen PJ, Kullman S, Linden KG (2007) Destruction of estrogenic activity in water using UV advanced oxidation. *Sci Total Environ* 377:105–113. <https://doi.org/10.1016/j.scitotenv.2007.01.096>
58. Arantes V, Milagres AMF (2007) The effect of a catecholate chelator as a redox agent in Fenton-based reactions on degradation of lignin-model substrates and on COD removal from effluent of an ECF kraft pulp mill. *J Hazard Mater* 141:273–279. <https://doi.org/10.1016/j.jhazmat.2006.06.134>
59. Mohajerani M, Mehrvar M EF (2009) An overview of the integration of advanced oxidation technologies and other processes for water and wastewater treatment. *Int J Eng* 3(2):120–146
60. Barbusinski K MJ (2018) Discoloration of azo dye acid red 18 by Fenton reagent in the presence of iron powder. *Pol J Env Stud* 12:151–155
61. Hsing HJ, Chiang PC, Chang EE, Chen MY (2007) The decolorization and mineralization of Acid Orange 6 azo dye in aqueous solution by advanced oxidation processes: A comparative study. *J Hazard Mater* 141:8–16. <https://doi.org/10.1016/j.jhazmat.2006.05.122>
62. Meriç S, Kaptan D, Ölmez T (2004) Color and COD removal from wastewater containing Reactive Black 5 using Fenton's oxidation process. *Chemosphere* 54:435–441. <https://doi.org/10.1016/j.chemosphere.2003.08.010>
63. Kochany J, Lipczynska-Kochany E (2009) Utilization of landfill leachate parameters for pretreatment by Fenton reaction and struvite precipitation-A comparative study. *J Hazard Mater* 166:248–254. <https://doi.org/10.1016/j.jhazmat.2008.11.017>
64. Kang N, Lee DS, Yoon J (2002) Kinetic modeling of Fenton oxidation of phenol and monochlorophenols. *Chemosphere* 47:915–924. [https://doi.org/10.1016/S0045-6535\(02\)00067-X](https://doi.org/10.1016/S0045-6535(02)00067-X)
65. Hassan H HB (2011) Decolorization of Acid Red 1 by heterogeneous Fenton-like reaction

- using Fe-ball clay catalyst. *Desalination International Conf Environ Sci Eng IPCBEE IACSIT Press Singapore* 269:291–293. <https://doi.org/10.1016/j.desal.2010.11.016>
66. Gu L, Nie JY, Zhu N wen, et al (2012) Enhanced Fenton's degradation of real naphthalene dye intermediate wastewater containing 6-nitro-1-diazo-2-naphthol-4-sulfonic acid: A pilot scale study. *Chem Eng J* 189–190:108–116. <https://doi.org/10.1016/j.cej.2012.02.038>
 67. Bishop DF, Stern G, Fleischman M, Marshall LS (1968) Hydrogen peroxide catalytic oxidation of refractory organics in municipal waste waters. *Ind Eng Chem Process Des Dev* 7:110–117. <https://doi.org/10.1021/i260025a022>
 68. Kiwi J, Pulgarin C, Peringer P, Grätzel M (1993) Beneficial effects of homogeneous photo-Fenton pretreatment upon the biodegradation of anthraquinone sulfonate in waste water treatment. *Appl Catal B, Environ* 3:85–99. [https://doi.org/10.1016/0926-3373\(93\)80070-T](https://doi.org/10.1016/0926-3373(93)80070-T)
 69. Deng N, Luo F, Wu F, et al (2000) Discoloration of aqueous reactive dye solutions in the UV/Fe₀ system. *Water Res* 34:2408–2411. [https://doi.org/10.1016/S0043-1354\(00\)00099-3](https://doi.org/10.1016/S0043-1354(00)00099-3)
 70. Fu F, Wang Q, Tang B (2010) Effective degradation of C.I. Acid Red 73 by advanced Fenton process. *J Hazard Mater* 174:17–22. <https://doi.org/10.1016/j.jhazmat.2009.09.009>
 71. Pagano M, Volpe A, Lopez A, et al (2011) Degradation of chlorobenzene by Fenton-like processes using zero-valent iron in the presence of Fe³⁺ and Cu²⁺. *Environ Technol* 32:155–165. <https://doi.org/10.1080/09593330.2010.490855>
 72. Bali U, Karagözoğlu B (2007) Performance comparison of Fenton process, ferric coagulation and H₂O₂/pyridine/Cu(II) system for decolorization of Remazol Turquoise Blue G-133. *Dye Pigment* 74:73–80. <https://doi.org/10.1016/j.dyepig.2006.01.013>
 73. Pecci L, Montefoschi G, Cavallini D (1997) Some new details of the copper-hydrogen peroxide interaction. *Biochem Biophys Res Commun* 235:264–267. <https://doi.org/10.1006/bbrc.1997.6756>
 74. Walling C (1975) Fenton's Reagent Revisited. *Acc Chem Res* 8:125–131. <https://doi.org/10.1021/ar50088a003>
 75. Kang SF, Liao CH, Chen MC (2002) Pre-oxidation and coagulation of textile wastewater by the Fenton process. *Chemosphere* 46:923–928. [https://doi.org/10.1016/S0045-6535\(01\)00159-X](https://doi.org/10.1016/S0045-6535(01)00159-X)

76. Buxton G V., Greenstock CL, Helman WP, Ross AB (1988) Critical Review of rate constants for reactions of hydrated electrons, hydrogen atoms and hydroxyl radicals ($\cdot\text{OH}/\cdot\text{O}^-$ in Aqueous Solution. *J Phys Chem Ref Data* 17:513–886.
<https://doi.org/10.1063/1.555805>
77. Bielski BHJ, Cabelli DE, Arudi RL, Ross AB (1985) Reactivity of HO_2/O_2^- Radicals in Aqueous Solution. *J Phys Chem Ref Data* 14:1041–1100.
<https://doi.org/10.1063/1.555739>
78. Kang SF, Liao CH, Po ST (2000) Decolorization of textile wastewater by photo-fenton oxidation technology. *Chemosphere* 41:1287–1294. [https://doi.org/10.1016/S0045-6535\(99\)00524-X](https://doi.org/10.1016/S0045-6535(99)00524-X)
79. Poyatos JM, Muñio MM, Almecija MC, et al (2010) Advanced oxidation processes for wastewater treatment: State of the art. *Water Air Soil Pollut* 205:187–204.
<https://doi.org/10.1007/s11270-009-0065-1>
80. Bandala ER, Peláez MA, García-López AJ, et al (2008) Photocatalytic decolourisation of synthetic and real textile wastewater containing benzidine-based azo dyes. *Chem Eng Process Process Intensif* 47:169–176. <https://doi.org/10.1016/j.cep.2007.02.010>
81. Gogate PR, Pandit AB (2004) A review of imperative technologies for wastewater treatment II: Hybrid methods. *Adv Environ Res* 8:553–597.
[https://doi.org/10.1016/S1093-0191\(03\)00031-5](https://doi.org/10.1016/S1093-0191(03)00031-5)
82. Petrovic M, Radjenovic J BD (2011) Advanced oxidation processes (AOPs) applied for wastewater and drinking water treatment elimination of pharmaceuticals. *Holist Appr Env* 2:63–74
83. Tamimi M, Qourzal S, Barka N, et al (2008) Methomyl degradation in aqueous solutions by Fenton's reagent and the photo-Fenton system. *Sep Purif Technol* 61:103–108.
<https://doi.org/10.1016/j.seppur.2007.09.017>
84. Will IBS, Moraes JEF, Teixeira ACSC, et al (2004) Photo-Fenton degradation of wastewater containing organic compounds in solar reactors. *Sep Purif Technol* 34:51–57.
[https://doi.org/10.1016/S1383-5866\(03\)00174-6](https://doi.org/10.1016/S1383-5866(03)00174-6)
85. Muruganandham M, Swaminathan M (2004) Decolourisation of Reactive Orange 4 by Fenton and photo-Fenton oxidation technology. *Dye Pigment* 63:315–321.
<https://doi.org/10.1016/j.dyepig.2004.03.004>

86. Sagawe G, Lehnard A, Lübber M, Bahnemann D (2001) The insulated solar fenton hybrid process: Fundamental investigations. *Helv Chim Acta* 84:3742–3759.
[https://doi.org/10.1002/1522-2675\(20011219\)84:12<3742::AID-HLCA3742>3.0.CO;2-Q](https://doi.org/10.1002/1522-2675(20011219)84:12<3742::AID-HLCA3742>3.0.CO;2-Q)
87. Hatchard CG PC (1956) A new sensitive chemical actinometer - II. Potassium ferrioxalate as a standard chemical actinometer. *Proc R Soc London Ser A Math Phys Sci* 235:518–536. <https://doi.org/10.1098/rspa.1956.0102>
88. Carneiro PA, Nogueira RFP, Zanoni MVB (2007) Homogeneous photodegradation of C . I . Reactive Blue 4 using a photo-Fenton process under artificial and solar irradiation. 74:.
<https://doi.org/10.1016/j.dyepig.2006.01.022>
89. Lucas MS (2006) Decolorization of the azo dye Reactive Black 5 by Fenton and photo-Fenton oxidation. *Dye Pigm* 71:236–244. <https://doi.org/10.1016/j.dyepig.2005.07.007>
90. Fongsatitkul P, Elefsiniotis P, Yamasmit A, Yamasmit N (2004) Use of sequencing batch reactors and Fenton’s reagent to treat a wastewater from a textile industry. *Biochem Eng J* 21:213–220. <https://doi.org/10.1016/j.bej.2004.06.009>
91. Kaptan D (2004) Color and COD removal from wastewater containing Reactive Black 5 using Fenton ’ s oxidation process S u. *Chemosphere* 54:435–441.
<https://doi.org/10.1016/j.chemosphere.2003.08.010>
92. Sun J, Sun S, Sun J, et al (2007) Degradation of azo dye Acid black 1 using low concentration iron of Fenton process facilitated by ultrasonic irradiation. *Ultrason Sonochem* 14:761–766. <https://doi.org/10.1016/j.ultsonch.2006.12.010>
93. Salvadori P, Cuzzola A BM (2002) A preliminary study on iron species as heterogeneous catalysts for the degradation of linear alkylbenzene sulphonic acids by H 2 O 2 ”. *Appl Catal* 36:231–237
94. Muñoz I, Rieradevall J, Torrades F, et al (2005) Environmental assessment of different solar driven advanced oxidation processes. *Sol Energy* 79:369–375.
<https://doi.org/10.1016/j.solener.2005.02.014>
95. Metcalf & Eddy (2014) *Wastewater engineering. Treatment, disposal and reuse.*, 5th Ed. Mc. Graw-Hill, Inc, New York, USA.
96. Grady C.P.L., Daigger G.T. LHC (1999) *Biological wastewater treatment*, 2nd Ed. Marcel Dekker, Inc, ., ., New York, USA.
97. Arden E. LW. (33AD) *Experiments on the oxidation of sewage without the aid of filters.* .

Soc Chem Ind, 523-539.:

98. Singh M, Srivastava RK (2011) Sequencing batch reactor technology for biological wastewater treatment: a review. *Asia-pacJ.chemEng.m* 199–203.
<https://doi.org/10.1002/apj>
99. Wilderer P.A., Irvine R.L. GMC (2001) Sequencing batch reactor technology. IWA publishing, , London, UK.
100. Mace S. M-AJ (2002) Review of SBR Technology for Wastewater Treatment. *Ind Eng Chem Res*, 41,:5539-5553. <https://doi.org/10.1002/apj>
101. Oliveira RP, Ghilardi JA, Ratusznei SM, et al (2008) Anaerobic sequencing batch biofilm reactor applied to automobile industry wastewater treatment: Volumetric loading rate and feed strategy effects. *Chem Eng Process Process Intensif* 47:1374–1383.
<https://doi.org/10.1016/j.cep.2007.06.014>
102. Mohan SV, Rao NC, Prasad KK, et al (2005) Treatment of complex chemical wastewater in a sequencing batch reactor (SBR) with an aerobic suspended growth configuration. *Process Biochem* 40:1501–1508. <https://doi.org/10.1016/j.procbio.2003.02.001>
103. Tsang YF, Hua FL, Chua H, et al (2007) Optimization of biological treatment of paper mill effluent in a sequencing batch reactor. *Biochem Eng J* 34:193–199.
<https://doi.org/10.1016/j.bej.2006.12.004>
104. Ng WJ, Sim TS, Ong SL, et al (1993) Efficiency of sequencing batch reactor (SBR) in the removal of selected microorganisms from domestic sewage. *Water Res* 27:1591–1600.
[https://doi.org/10.1016/0043-1354\(93\)90105-Q](https://doi.org/10.1016/0043-1354(93)90105-Q)
105. Metcalf &Eddy (2003) wastewater Engineering: Treatment and reuse, Fourth Edi. McGraw Hill, New York
106. Poole AJ (2004) Treatment of biorefractory organic compounds in wool scour effluent by hydroxyl radical oxidation. *Water Res* 38:3458–3464.
<https://doi.org/10.1016/j.watres.2004.06.001>
107. EPA (1998) Preliminary industry characterization: fabric printing, coating, and dyeing. USA
108. Crini G (2006) Non-conventional low-cost adsorbents for dye removal: A review. *Bioresour Technol* 97:1061–1085. <https://doi.org/10.1016/j.biortech.2005.05.001>
109. Mohan D, Pittman CU (2007) Arsenic removal from water/wastewater using adsorbents-A

- critical review. *J Hazard Mater* 142:1–53. <https://doi.org/10.1016/j.jhazmat.2007.01.006>
110. Bouberka Z, Kacha S, Kameche M, et al (2005) Sorption study of an acid dye from an aqueous solutions using modified clays. *J Hazard Mater* 119:117–124. <https://doi.org/10.1016/j.jhazmat.2004.11.026>
 111. Ireland N (1984) e r g a m o n A D S O R P T I O N OF ACID DYES O N T O G R A N U L A R
 112. Yin CY, Aroua MK, Daud WMAW (2007) Review of modifications of activated carbon for enhancing contaminant uptakes from aqueous solutions. *Sep Purif Technol* 52:403–415. <https://doi.org/10.1016/j.seppur.2006.06.009>
 113. Wingenfelder U, Nowack B, Furrer G, Schulin R (2005) Adsorption of Pb and Cd by amine-modified zeolite. *Water Res* 39:3287–3297. <https://doi.org/10.1016/j.watres.2005.05.017>
 114. Mamma D, Gerontas S, Philippopoulos CJ, et al (2004) Combined Photo-Assisted and Biological Treatment of Industrial Oily Wastewater. *J Environ Sci Heal - Part A Toxic/Hazardous Subst Environ Eng* 39:729–740. <https://doi.org/10.1081/ESE-120027738>
 115. A. Marco, S. Esplugas and GS (1997) How and why combine chemical and biological processes for wastewater treatment”. *Water Sci Technol* 35 (4):321–327
 116. Al-Kdasi A, Idris A, Saed K, Guan CT (2004) Treatment of textile wastewater by advanced oxidation processes– A review. *Glob Nest J* 6:222–230. <https://doi.org/10.30955/gnj.000288>
 117. Rodrigues CSD, Madeira LM, Boaventura RAR (2009) Treatment of textile effluent by chemical (Fenton’s Reagent) and biological (sequencing batch reactor) oxidation. *J Hazard Mater* 172:1551–9. <https://doi.org/10.1016/j.jhazmat.2009.08.027>
 118. Lodha B, Chaudhari S (2007) Optimization of Fenton-biological treatment scheme for the treatment of aqueous dye solutions. *J Hazard Mater* 148:459–466. <https://doi.org/10.1016/j.jhazmat.2007.02.061>
 119. Tantak NP, Chaudhari S (2006) Degradation of azo dyes by sequential Fenton’s oxidation and aerobic biological treatment. *J Hazard Mater* 136:698–705. <https://doi.org/10.1016/j.jhazmat.2005.12.049>
 120. Bas D (2007) Modeling and optimization I : Usability of response surface methodology. *J Food Eng* 78:836–845. <https://doi.org/10.1016/j.jfoodeng.2005.11.024>

121. Rosales E, Sanromán MA, Pazos M (2012) Application of central composite face-centered design and response surface methodology for the optimization of electro-Fenton decolorization of Azure B dye. *Env Sci Pollut Res* 19:1738–1746.
<https://doi.org/10.1007/s11356-011-0668-0>
122. Nair AT, Makwana AR, Ahammed MM (2014) The use of response surface methodology for modelling and analysis of water and wastewater treatment processes : a review. *Water Sci Technol* 69(3):464–478. <https://doi.org/10.2166/wst.2013.733>
123. Ay F, Catalkaya EC, Kargi F (2009) A statistical experiment design approach for advanced oxidation of Direct Red azo-dye by photo-Fenton treatment. *J Hazard Mater* 162:230–236. <https://doi.org/10.1016/j.jhazmat.2008.05.027>
124. Al-Musawi TJ, Kamani H, Bazrafshan E, et al (2019) Optimization the Effects of Physicochemical Parameters on the Degradation of Cephalexin in Sono-Fenton Reactor by Using Box-Behnken Response Surface Methodology. *Catal Letters* 149:1186–1196.
<https://doi.org/10.1007/s10562-019-02713-x>
125. López N, Plaza S, Afkhami A, et al (2017) Treatment of Diphenhydramine with different AOPs including photo-Fenton at circumneutral pH. *Chem Eng J* 318:112–120.
<https://doi.org/10.1016/j.cej.2016.05.127>
126. Moghaddam SS, Moghaddam MRA, Arami M (2010) Coagulation / flocculation process for dye removal using sludge from water treatment plant : Optimization through response surface methodology. *J Hazard Mater* 175:651–657.
<https://doi.org/10.1016/j.jhazmat.2009.10.058>
127. Zhu X, Tian J, Liu R, Chen L (2011) Optimization of Fenton and electro-Fenton oxidation of biologically treated coking wastewater using response surface methodology. *Sep Purif Technol* 81:444–450. <https://doi.org/10.1016/j.seppur.2011.08.023>
128. Xu H, Qi S, Li Y, Zhao Y (2013) Heterogeneous Fenton-like discoloration of Rhodamine B using natural schorl as catalyst : optimization by response surface methodology. *Env Sci Pollut Res* 20:5764–5772. <https://doi.org/10.1007/s11356-013-1578-0>
129. Gilpavas E, Dobroz-Gomez I G-GM (2012) Decolorization and mineralization of Diarylide Yellow 12 (PY12) by photo-Fenton process : the Response Surface Methodology as the optimization tool Edison GilPavas , Izabela Dobrosz-Gómez and Miguel Ángel Gómez-García. *water sci technol* 65:1795–1801.

- <https://doi.org/10.2166/wst.2012.078>
130. Fathinia M, Khataee AR, Zarei M, Aber S (2010) A : Chemical Comparative photocatalytic degradation of two dyes on immobilized TiO₂ nanoparticles : Effect of dye molecular structure and response surface approach. *J Mol Catal AChemical* 333:73–84. <https://doi.org/10.1016/j.molcata.2010.09.018>
 131. Kapoor, S Sharma S, S. Sharma RAC (2017) Effect of Fenton process on treatment of simulated textile wastewater : optimization using response surface methodology. *Int J Environ Sci Technol*. <https://doi.org/10.1007/s13762-017-1253-y>
 132. Mason R, Gunst R HJ (2003) *Statistical Design and Analysis of Experiments With Applications to Engineering and Science*, 2nd edn. Wiley, Newyork
 133. Souâd Bouafia-Chergui , Nihal Oturan HK& MAO (2010) Parametric study on the effect of the ratios [H₂O₂]/[Fe³⁺] and [H₂O]/[substrate] on the photo-Fenton degradation of cationic azo dye Basic Blue 41., *J Environ Sci Heal Part A Toxic/Hazardous Subst Environ Eng* 45:5:622–629. <https://doi.org/10.1080/10934521003595746>
 134. APHA (2005) *Standard Methods for the Examination of Water and Wastewater*, 21th edn. American Public Health Association (APHA):, Washington, DC, USA
 135. Solomon D, Kiflie Z, Hulle S Van (2019) Kinetic investigation and optimization of a sequencing batch reactor for the treatment of textile wastewater. *Nanotechnol Environ Eng* 4:15. <https://doi.org/https://doi.org/10.1007/s41204-019-0062-6>
 136. Saldana-Robels A, Gerra-Sanchez R, Maldonado-Rubio M P-HJ (2014) Optimization of the operating parameters using RSM for the Fenton oxidation process and adsorption on vegetal carbon of MO solutions. *J Ind Eng Chem* 20:848–857. <https://doi.org/10.1016/j.jiec.2013.06.015>
 137. Khataee A, Safarpour M, Naseri A ZM (2012) photoelectro-Fenton/nanophotocatalysis decolorization of three textile dyes mixture: response surface modeling and multivariate calibration procedure for simultaneous determination. *Electroanal Chem* 672:53–62
 138. Carlson R, Carlson J (2005) *Design and optimization in organic synthesis*, 1st edn. Elsevier, Amsterdam
 139. Anderson M, Whitcomb P (2007) *DOE simplified: practical tools for effective experimentation*, 3rd edn. CRC Press, Newyork
 140. Xu X, Li X, Li X, Li H (2009) Degradation of melatonin by UV , UV / H₂O₂ , Fe²⁺ /

- H₂O₂ and. 68:261–266. <https://doi.org/10.1016/j.seppur.2009.05.013>
141. Pupo Nogueira R (2002) Photodegradation of dichloroacetic acid and 2,4-dichlorophenol by ferrioxalate/H₂O₂ system. *Water Res* 34:895–901. [https://doi.org/10.1016/s0043-1354\(99\)00193-1](https://doi.org/10.1016/s0043-1354(99)00193-1)
 142. Emilio CA, Jardim WF, Litter MI, Mansilla HD (2002) EDTA destruction using the solar ferrioxalate advanced oxidation technology (AOT). *J Photochem Photobiol A Chem* 151:121–127. [https://doi.org/10.1016/s1010-6030\(02\)00173-9](https://doi.org/10.1016/s1010-6030(02)00173-9)
 143. Torrades F, Pérez M, Mansilla HD, Peral J (2003) Experimental design of Fenton and photo-Fenton reactions for the treatment of cellulose bleaching effluents. *Chemosphere* 53:1211–1220. [https://doi.org/10.1016/S0045-6535\(03\)00579-4](https://doi.org/10.1016/S0045-6535(03)00579-4)
 144. Ghaly MY, Ha G, Mayer R, Haseneder R (2001) Photochemical oxidation of p - chlorophenol by UV / H₂O₂ and photo-Fenton process . A comparative study. *Waste Manag* 21:41–47
 145. Ay F, Catalkaya EC, Kargi F (2008) Advanced Oxidation of Direct Red (DR 28) by Fenton Treatment. *Environ Eng Sci* 25:1445–1462. <https://doi.org/10.1089/ees.2007.0218>
 146. Arslan-alaton I, Tureli G, Olmez-hanci T (2009) Treatment of azo dye production wastewaters using Photo-Fenton-like advanced oxidation processes : Optimization by response surface methodology. *J Photochem Photobiol A* 202:142–153. <https://doi.org/10.1016/j.jphotochem.2008.11.019>
 147. Hsueh CL, Huang YH, Wang CC, Chen CY (2005) Degradation of azo dyes using low iron concentration of Fenton and Fenton-like system. 58:1409–1414. <https://doi.org/10.1016/j.chemosphere.2004.09.091>
 148. Emilio CA, Jardim WF, Litter MI, Mansilla HD (2002) EDTA destruction using the solar ferrioxalate advanced oxidation technology (AOT) Comparison with solar photo-Fenton treatment. *J Photochem Photobiol* 151:121–127
 149. Nogueira RFP, Guimaraes J. (2000) Photo degradation of dichloro acetic acid and 2 , 4- dichlorophenol by ferric oxalate / H₂O₂ system. *WatRes* 34:895–901
 150. Torrades F, Perez, M, Mansilla, M.D, And Peral J (2003) Experimental design of Fenton and photo-Fenton reactions for the treatment of cellulose bleaching effluents. *Chemosphere* 53:1211–1220. [https://doi.org/10.1016/S0045-6535\(03\)00579-4](https://doi.org/10.1016/S0045-6535(03)00579-4)
 151. Mansoorian HJ, Bazrafshan E, Yari A AM (2014) Removal of Azo dyes from aqueous

- solution using Fenton and modified Fenton processes. *Heal Scope* 3:e15507
152. Wang CT, Chou WL, Chung MH, Kuo YM (2010) COD removal from real dyeing wastewater by electro-Fenton technology using an activated carbon fiber cathode. *Desalination* 253:129–134. <https://doi.org/10.1016/j.desal.2009.11.020>
 153. Lodha B, Chaudhari S (2007) Optimization of Fenton-biological treatment scheme for the treatment of aqueous dye solutions. *J Hazard Mater* 148:459–466. <https://doi.org/10.1016/j.jhazmat.2007.02.061>
 154. Zhang H, Heung JC, Huang CP (2005) Optimization of Fenton process for the treatment of landfill leachate. *J Hazard Mater* 125:166–174. <https://doi.org/10.1016/j.jhazmat.2005.05.025>
 155. Kavitha V, Palanivelu K (2005) Destruction of cresols by Fenton oxidation process. *Water Res* 39:3062–3072. <https://doi.org/10.1016/j.watres.2005.05.011>
 156. Kwon BG, Lee DS, Kang N, Yoon J (1999) Characteristics of p-chlorophenol oxidation by Fenton's reagent. *Water Res* 33:2110–2118. [https://doi.org/10.1016/S0043-1354\(98\)00428-X](https://doi.org/10.1016/S0043-1354(98)00428-X)
 157. Montgomery D. (2010) *Design and analysis of experimenters*, 7 th edn. Wiley India Pvt Ltd, New Delhi
 158. Novais JM, Pinheiro HM (2001) Effect of some operational parameters on textile dye biodegradation in a sequential batch reactor. *J Biotechnol* 89:163–174
 159. Palm JC, Jenkins D, Parker DS (1980) Relationship between organic oxygen sludge dissolved loading , and concentration in the completely settleability mixed activated process sludge. *J WPCF* 52:2484–06
 160. Zinatizadeh AAL, Mansouri Y, Akhbari A, Pashaei S (2011) , Biological treatment of a synthetic dairy wastewater in a sequencing batch biofilm reactor: statistical modeling using optimization using response surface methodology. *Chem Ind Chem Eng Q* 17:485–495. <https://doi.org/10.2298/CICEQ110524034Z>
 161. Janczukowicz W, Szewczyk M, Krzemieniewski M, Pesta J (2001) Settling Properties of Activated Sludge from a Sequencing Batch Reactor (SBR)z. *Polish J Environ Stud* 10:15–20
 162. Kapdan IK, Oztekin R (2006) The effect of hydraulic residence time and initial COD concentration on color and COD removal performance of the anaerobic-aerobic SBR

- system. *J Hazard Mater* 136:896–901. <https://doi.org/10.1016/j.jhazmat.2006.01.034>
163. Janczukowicz W, Szewczyk M, Krzemieniewski M, Pesta J (2001) Settling Properties of Activated Sludge from a Sequencing Batch Reactor (SBR). *Polish J Environ Stud* 10:15–20
164. Zinatizadeh AAL, Mansouri Y, Akhbari A, Pashaei S (2011) Biological treatment of a synthetic dairy wastewater in a sequencing batch biofilm reactor. *Chem Ind Chem Eng Q* 17:485–495. <https://doi.org/10.2298/CICEQ110524034Z>
165. Ong SA, Toorisaka E, Hirata M, Hano T (2005) Treatment of azo dye Orange II in aerobic and anaerobic-SBR systems. *Process Biochem* 40:2907–2914. <https://doi.org/10.1016/j.procbio.2005.01.009>
166. Zheng YM, Yu HQ, Sheng GP (2005) Physical and chemical characteristics of granular activated sludge from a sequencing batch airlift reactor. *Process Biochem* 40:645–650. <https://doi.org/10.1016/j.procbio.2004.01.056>
167. Arrojo B, Mosquera-Corral A, Garrido JM, Méndez R (2004) Aerobic granulation with industrial wastewater in sequencing batch reactors. *Water Res* 38:3389–3399. <https://doi.org/10.1016/j.watres.2004.05.002>
168. J-H T, Q-S L, Y L (2001) Microscopic observation of aerobic granulation in sequential aerobic sludge blanket reactor. *J Appl Microbiol* 91:168–175. <https://doi.org/10.1046/j.1365-2672.2001.01374.x>
169. J.-H. T, Q.-S. L, Y. L (2002) The effects of shear force on the formation, structure and metabolism of aerobic granules. *Appl Microbiol Biotechnol* 57:227–233. <https://doi.org/10.1007/s002530100766>
170. Mandal T, Maity S, Dasgupta D, Datta S (2010) Advanced oxidation process and biotreatment: Their roles in combined industrial wastewater treatment. *Desalination* 250:87–94. <https://doi.org/10.1016/j.desal.2009.04.012>